An extended dual weighted residual error estimator for discontinuous solutions of transport problems

submitted by Susanne Beckers
2016 in Hamburg

Day of oral defense: May 10th, 2017

The following evaluators recommend
the admission of the dissertation

Prof. Dr. Jörn Behrens
Department of Mathematics,
Universität Hamburg
Hamburg, Germany
email: joern.behrens@uni-hamburg.de

Prof. Dr. Winnifried Wollner
Department of Mathematics,
Technische Universität Darmstadt
Darmstadt, Germany
email: wollner@mathematik.tu-darmstadt.de

Declaration on Oath

I hereby declare on oath, that I have written the present dissertation on my own and have not used other than the acknowledged resources and aids.

. . . .
Date and place   Signature

Acknowledgements

I like to express my deepest gratitude to my supervisor Prof. Dr. Jörn Behrens. Through all the time of my Ph.D. research his door was always open for me. With patience and kindness he discussed scientific topics with me as well as coding issues. Additionally to his continuous support, I highly appreciate his support of my attendance at several international conferences.

Deep gratitude is also due to Prof. Dr. Winnifried Wollner. As my second supervisor he showed much patience in scientific discussions, in person and on several different media. I like to thank him very much for his constructive advice and motivating support.

As chair of my advisory panel, Prof. Dr. Thomas Rung was very active and involved. For his effort and commitment a big thank-you.

In this context, I also like to acknowledge the support of the Lothar Collatz Graduate School for Computing in Science.

I am grateful for the buzzing life in our working group and the regular communication we had. This is especially true for Anja Jeschke. Time in our office would not have been the same without you!

I am in dept to my esteemed colleagues Dr. Stefan Vater and Dr. Konrad Simon for proofreading.

I also like to thank my parents, Josef and Ursula, for supporting me with love and encouragement throughout all my life. You are wonderful parents!

Besides all my friends, who did not see me for quite some time, but still supported me and cheered me up whenever necessary, I also like to thank my best friend and my soon-to-be husband, Daniel. You are my complement set; with you, I can reach any point in space.

Contents

List of Figures

List of Tables

0.1 Abstract

In the dual-weighted residual method for goal-oriented error estimation residuals have to be evaluated which include the computation of derivatives. For hyperbolic problems in general the residuals are computed in the standard weak form. Potential discontinuities of the solution prohibit direct (weak) derivatives, therefore all derivatives are taken on the test function by means of partial integration. The same holds true for the dual problem. In the dual-weighted residual method, the test function of the primal residual contains the dual solution and the test function of the dual residual contains the primal solution. Therefore computation of residuals and weights is not well defined in the situation of coinciding discontinuities.

In this thesis the problem of coinciding discontinuities in primal and dual solution is avoided by adding artificial viscosity to the dual equation, while leaving the primal problem unchanged. This procedure causes an additional residual term in the error estimator, accounting for the inconsistency between primal and dual problem.

The effectivity of the extended error estimator, assessing the global error by a suitable functional of interest, is tested numerically in 1D and 2D. Used as an indicator to control grid refinement, the proposed extended and an unmodified error estimator perform similarly. However, only the proposed modified method provides an efficient error estimator in 1D.

In 2D, with the tested parameters and approximation of weights, the effectivity index does not converge to one. However, the efficiency of the modified error estimator is better than the unmodified one.

0.2 Kurzfassung

Die dual-gewichtete Residuen (DWR) Methode für ziel-orientierte Fehlerschätzung nutzt die Auswertung von gewichteten Residuen zur Bestimmung von Fehlerschätzern. Dabei müssen auch Ableitungen berechnet werden. Bei hyperbolischen Problemen in der schwachen Form werden die Ableitungen durch partielle Integration auf die Testfunktionen angewendet, da mögliche Unstetigkeiten der Lösung selbst eine schwache Ableitung der Lösung nicht zulassen. Da dieser Sachverhalt auch für das duale Problem gilt, ist die Berechnung von Residuen und Gewichten im DWR Kontext für den Fall von aufeinandertreffenden Unstetigkeiten nicht definiert.

In dieser Arbeit wird das Problem der aufeinandertreffenden Unstetigkeiten umgangen, in dem in der dualen Gleichung eine künstliche Viskosität hinzugefügt wird. Dabei wird das primale Problem nicht verändert. Für dieses inkonsistente primale-duale Problem wird in dieser Arbeit ein Fehlerschätzer entwickelt, der im Vergleich zu dem klassischen DWR Fehlerschätzer ein zusätzliches duales Residuum beinhaltet, das der Inkonsistenz Rechnung trägt.

Die Effizienz des erweiterten Fehlerschätzers wurde in einem 1D Testfall untersucht, bei dem die analytische Lösung bekannt ist. Dabei zeigte sich, dass sowohl der erweiterte, wie auch der klassische Fehlerschätzer als Fehlerindikator geeignet ist, jedoch nur die erweiterte Version effizient ist.

Des Weiteren wurde der Fehlerschätzer in 2D getestet, ohne eine gegebene analytische Lösung, sodass eine Approximation der Gewichte durchgeführt wurde. Der Effektivitätsindex des modifizierten Fehlerschätzers konvergierte mit den getesteten Parametern nicht gegen Eins. Jedoch ist die Effizienz des in diser Arbeit vorgeschlagenen Fehlerschätzers besser, als die des klassischen DWR Fehlerschätzers.

0.3 Nomenclature

Real and natural numbers:

$b \in \mathbb{R}^+$	Jump penalty term
$C \in \mathbb{R}^+$	Constant for estimation
$c \in \mathbb{R}^+$	Constant for estimation
$\tilde{c} \in \{-1, 1\}$	Stabilization coefficient for DG
$\bar{c} \in \mathbb{R}$	Coefficient for transport equation
$c_1, \ldots, c_4 \in \mathbb{R}$	Constants for estimation
$d \in \mathbb{N}$	Degrees of freedom/
	dimension of finite dimensional space
$\text{eff} \in \mathbb{R}^+$	Effectivity of the error estimator
$h \in \mathbb{R}^+$	Spatial step/ element size
$h_{\text{ref}} \in \mathbb{R}^+$	Spatial step/ element size of refined mesh
$k \in \mathbb{R}^+$	Time step size
$K \in \mathbb{N}$	Order of continuous differentiability
$m \in \mathbb{N}$	Number of elements
$M \in \mathbb{N}$	Number of quadrature points per element
$N \in \mathbb{N}$	$N + 1$ time steps
$n \in \mathbb{R}$	Spatial dimension
$p \in \mathbb{N}$	Polynomial order
$P \in \mathbb{N}$	Order of integrability
$P_h \in \mathbb{R}^+$	Peclet number
$R \in \mathbb{R}$	Remainder of goal error estimation
$\tilde{R} \in \mathbb{R}$	Remainder of goal error estimation
$T \in \mathbb{R}^+$	Final time
$t \in \mathbb{R}_0^+$	Time variable
$t_j \in \mathbb{R}_0^+, j = 0, \ldots, N$	Steps for time discretization
$\tilde{t} \in \mathbb{R}_0^+$	Fixed time
$TOL \in \mathbb{R}^+$	Error tolerance
$s \in [0, 1]$	Integration parameter
$v \in \mathbb{R}$	Advection velocity
$w_i \in \mathbb{R}^+, i = 0, \ldots, M$	Element quadrature weights
$\tilde{w}_j \in \mathbb{R}^+, j = 0, \ldots, N$	Time quadrature weights
$x \in \mathbb{R}$	Space variable
$y \in \mathbb{R}$	Space variable
$\delta \in \mathbb{R}^+$	Smoothing parameter
$\varepsilon \in \mathbb{R}^+$	Small diffusion coefficient
$\eta \in \mathbb{R}$	Transformation variable for x, y
$\eta_E \in \mathbb{R}^+$	Local error estimator on E
$\eta_{E,0} \in \mathbb{R}^+$	Formal local error estimator on E
$\eta_E^{hk} \in \mathbb{R}$	Discrete local error estimator on E

$\eta_E^{*hk} \in \mathbb{R}$	Discrete dual local error estimator on E
$\eta^{hk} \in \mathbb{R}$	Discrete global error estimator
$\eta_{\text{uni}}^{hk} \in \mathbb{R}$	Discrete global error estimator on uniform grid
$\eta_{\text{ref}}^{hk} \in \mathbb{R}$	Discrete global error estimator on loc. refined grid
$\hat{\eta}_{j,E} \in \mathbb{R}^+, j = 0, \ldots, N$	Local error estimator on E at time t_j
$\eta_{j,E} \in \mathbb{R}^+, j = 0, \ldots, N$	Local error estimator on E at time t_j
$\eta_{\mathcal{E}} \in \mathbb{R}^+$	Global error estimator for $\mathcal{E}$
$\Theta \in [0, 1]$	Dörfler parameter
$\xi \in \mathbb{R}$	Transformation variable for x, y
$\Delta\rho \in \mathbb{R}$	Difference between primal and dual residual
$\tau \in \mathbb{R}$	Transformation variable for t

Sets and spaces:

$B(V, \mathbb{R})$	Set of bounded linear functionals from V to $\mathbb{R}$
$\mathcal{E} = \{E_1, \cdots, E_m\}$	Triangulation of $\bar{\Omega}$
$\mathcal{E}_h$	Triangulation with longest edge h
$\mathcal{E}_{h_{\text{ref}}}$	Refined triangulation
$\partial\mathcal{E}$	Set of edges of elements in $\mathcal{E}$
$E \in \Omega$	Elements of $\mathcal{E}$
$E_i, i = 1, \cdots, m$	Elements of $\mathcal{E}$
E'	Neighbor element of E
$\tilde{E}$	Reference element
∂E	Boundary of E
$I_{\text{ref}} = [-1, 1]$	Interval of refinement
$N_{\mathcal{E}_h}(E)$	Neighborhood of E
V	Space of test functions/ dual solutions
V^h	Finite dimensional subspace of V, (discretization in space)
V^{hk}	Finite dimensional subspace of V, (discretization in time and space)
W	Space of dual test functions/primal solutions
W^h	Finite dimensional subspace of W, (discretization in space)
W^{hk}	Finite dimensional subspace of W, (discretization in time and space)
$\Omega \subset \mathbb{R}^2$	Open rectangular domain in $\mathbb{R}^2$
$\partial\Omega$	Boundary of rectangular domain Ω

Functions:

$\tilde{e}_i \in P_p\left(\tilde{E}\right)$	Basis polynomials of order p on $\tilde{E}$
$e_i \in P_p\left(E\right)$	Basis polynomials of order p on E
$e^h \in V$	Spatial discretization error, elliptic problem
$e = u - u^{hk} \in W$	Time and space discretization error
$e^* = z - z^{hk} \in V$	Dual time and space discretization error
$\mathrm{erf} \in C^\infty(\mathbb{R}) \cap L^1(\mathbb{R})$	Error function
$f \in L^2\left(\mathbb{R}\right)$	Source term
$G : \mathbb{R}^n \times [0,T] \times \mathbb{R}^n \times [0,T]$ $\quad\quad \to \mathbb{R}^n \times [0,T]$	Green's function
$G_{\xi,\tilde{t}} : \mathbb{R} \to \mathbb{R}$	Green's function for fixed $\tilde{t}$
$H : \mathbb{R} \to \{0, 0.5, 1\}$	Heaviside function
$R : \partial E \to \mathbb{R}$	Element boundary residual, hyperbolic example
$\tilde{R} : \partial E \to \mathbb{R}$	Element boundary residual, elliptic example
$r : E \to \mathbb{R}$	Inner element residual, hyperbolic example
$\tilde{r} : E \to \mathbb{R}$	Inner element residual, elliptic example
$u \in W$	(Primal) solution
$u^h \in W^h$	(Primal) solution, space discretized
$u^{hk} \in W^{hk}$	(Primal) solution, time and space discretized
$u_{E_{\mathrm{up}}} \partial E \to \mathbb{R}$	Upwind solution on edge ∂E
$u_0 \in L^\infty\left(\mathbb{R}^n \times (0,\infty)\right)$	Solution of linear advection equation
$u_\varepsilon \in C^\infty\left(\mathbb{R}^n \times (0,\infty)\right)$	Solution of linear advection-diffusion equation
$u_{\mathrm{ini}} \in L^\infty\left(\mathbb{R}\right) \cap L^P(\mathbb{R})$	Initial data
$u_{\mathrm{ini}}^\delta \in C_c^\infty(\mathbb{R})$	Smooth approximation of u_{ini}
$u_{\mathrm{ini},\tilde{t}} \in L^\infty(\mathbb{R}) \cap L^P(\mathbb{R})$	Initial condition shifted by $v_1\tilde{t}$
$u_{\mathrm{ini},\tilde{t}}^\delta \in C_c^\infty(\mathbb{R})$	Smooth approximation of $u_{\mathrm{ini},\tilde{t}}$
$\tilde{u} \in V$	Solution of elliptic problem
$\tilde{u}^h \in V^h$	Solution of elliptic problem in V^h
$z \in V$	Dual solution
$z^h \in V^h$	Dual solution, space discretized
$z^{hk} \in V^{hk}$	Dual solution, time and space discretized
$z_0 \in L^\infty\left(\mathbb{R}^n \times (0,\infty)\right)$	Solution of dual linear advection equation
$z_\varepsilon \in C^\infty\left(\mathbb{R}^n \times (0,\infty)\right)$	Solution of dual linear advection-diffusion equation
$z_T \in L^\infty(\Omega)$	Dual initial data
$\tau : \tilde{E} \to \mathbb{R}^n$	Bilinear, affine mapping
$\phi \in W$	Test function (T.f) for the dual problem
$\phi^h \in W^h$	T.f. for the space discretized dual problem
$\phi^{hk} \in W^{hk}$	T.f. for the time and space discretized dual problem
$\psi \in V$	T.f. for the primal problem
$\psi^h \in V^h$	T.f. for the space discretized primal problem
$\psi^{hk} \in V^{hk}$	T.f. for the time and space discretized primal problem

$\tilde{\psi} \in V, W$ T.f. for elliptic problem

Vectors and matrices:

$B \in \mathbb{R}^n \times \mathbb{R}^n$	Rotation matrix
$B_E \in \mathbb{R}^p \times \mathbb{R}^p$	Discretization matrix on E
$\mathbf{c} \in \mathbb{R}^2$	Coefficient of transport equation
$D_E \in \mathbb{R}^p \times \mathbb{R}^p$	Discretization matrix on E
$e_i, i = 1, \cdots, d$	Basis element of V^h
$\mathbf{f} \in \mathbb{R}^d$	Source term vector
$J_\tau \in \mathbb{R}^n \times \mathbb{R}^n$	Jacobi matrix of τ
$M_{\tilde{E}} \in \mathbb{R}^d \times \mathbb{R}^d$	Local mass matrix on $\tilde{E}$
$M_E \in \mathbb{R}^d \times \mathbb{R}^d$	Local mass matrix on E
$M_E \in \mathbb{R}^p \times \mathbb{R}^p$	Local mass matrix on E (1D)
$\mathbf{n} \in \mathbb{R}^n$	Outwards pointing normal
$\mathbf{u} \in \mathbb{R}^d$	Basis function coefficients for u^h
$\mathbf{v} \in \mathbb{R}^n$	Advection velocity
$\mathbf{v} \in \mathbb{R}^2, \mathbf{v} = (v_1, v_2)^T$	Advection velocity
$\mathbf{x} \in \mathbb{R}^n$	Coordinate in space
$\mathbf{x} \in \mathbb{R}^2, \mathbf{x} = (x, y)^T$	Coordinate in space
$\mathbf{f} \in \mathbb{R}^n$	Coriolis parameter
$\boldsymbol{\alpha} \in \mathbb{R}^n$	Multi index for derivatives
$\boldsymbol{\xi} \in \tilde{E}, \boldsymbol{\xi} = (\xi, \eta)^T$	Coordinate in reference element $\tilde{E}$
$\boldsymbol{\xi}_0 \in \mathbb{R}^n$	Transformation parameter

Operators and functionals:

$a(\cdot,\cdot) : W \times V \to \mathbb{R}$	Semilinear form
$\tilde{a}(\cdot,\cdot) : V \times V \to \mathbb{R}$	Elliptic bilinear form
$a^*(\cdot,\cdot) : V \times V \to \mathbb{R}$	Functional for adjoint weak formulation
$a_0(\cdot,\cdot) : L^\infty\left(\mathbb{R}^n, L^2(0,1)\right) \times C_c^1(\mathbb{R} \times [0,T)) \to \mathbb{R}$	Linear form for advection
$a_\varepsilon(\cdot,\cdot) : C^\infty\left(\mathbb{R}^n, \times(0,\infty)\right) \times C_c^1(\mathbb{R} \times [0,T)) \to \mathbb{R}$	Linear form for advection-diffusion
$B(\cdot) : V \to \mathbb{R}$	Linear functional
$\mathbf{F}(\cdot) : C^1(\mathbb{R}^n) \to C^0(\mathbb{R}^n)$	Flux
$\mathbf{F}^*(\cdot) : C^1(\mathbb{R}^n) \to C^0(\mathbb{R}^n)$	Numerical flux
$\tilde{f}(\cdot) : V \to \mathbb{R}$	Bounded linear functional
$I_h : V \to V^h$	Approximation operator in space
$I_{hk} : V \to V^{hk}$	Approximation operator in time and space
$J(\cdot) : W \to \mathbb{R}$	Linear goal functional
$L(\cdot,\cdot) : W \times V \to \mathbb{R}$	Lagrangian functional
$S(\cdot) : W \to \mathbb{R}$	Source term
$\rho(\cdot,\cdot) : W \times V \to \mathbb{R}$	Primal residual
$\rho^*(\cdot,\cdot) : V \times W \to \mathbb{R}$	Dual residual
$\rho_E^{hk}(\cdot,\cdot) : W^{hk} \times V \to \mathbb{R}$	Discrete primal residual on E
$\rho_E^{*hk}(\cdot,\cdot) : V^{hk} \times W \to \mathbb{R}$	Discrete dual residual on E
$\partial_t : C^1((0,T)) \to C^0((0,T))$	Partial derivative in time
$\partial_x : C^1(\mathbb{R}) \to C^0(\mathbb{R})$	Partial derivative in x-direction
$\partial_y : C^1(\mathbb{R}) \to C^0(\mathbb{R})$	Partial derivative in y-direction
$\nabla : C^1(\mathbb{R}^n) \to C^0(\mathbb{R}^n)$	Gradient with respect to space
$\Delta : C^2(\mathbb{R}^n) \to C^0(\mathbb{R}^n)$	Laplace operator with respect to space
$O : \mathbb{R}^+ \to \mathbb{R}^+$	Landau symbol
$(\cdot,\cdot)_\Omega : L^2(\Omega) \times L^2(\Omega) \to \mathbb{R}$	$L^2(\Omega)$ inner product
$\langle \cdot,\cdot \rangle : B(V,\mathbb{R}) \times V \to \mathbb{R}$	Dual pairing

Chapter 1

Introduction

1.1 Background

Numerical simulation is a widely used tool to predict flow behavior. In weather prediction and tsunami warnings as well as in flows around cars, ships, or aircrafts. Most of these flows are advection dominated or even pure hyperbolic problems. Hyperbolic problems can cause shocks in finite time, even with smooth initial conditions. To capture these shocks, steep gradients, or local fine scale behavior of the solution the grid has to be resolved sufficiently. A globally very fine grid causes, however, a high computational effort. Static local refinement or adaptive local refinement in time is in many cases more efficient, e.g., [BB09].

Adaptive grid refinement requires local error indicators for indication of refinement areas. These indicators are often local residuals of finite element methods. Besides [AO97], [BR78a], [Ver96], many others specified residual-based error estimators for a variety of partial differential equations. In contrast to the error estimates for global error norms, the idea of goal-oriented error estimation is to control a post-processed quantity of interest, see, e.g., [AO97, BR01, EEHJ95]. This quantity could be a global or local energy, an average value on a specific area of interest, or other derived quantities.
In the goal-oriented context, the dual-weighted-residual (DWR) method, cf., [BR01], provides an error estimator for the error in a linear goal functional evaluation, consisting of weighted residuals of the primal and dual equation. While elliptic and parabolic problems provide, in general, sufficiently regular solutions for the application of DWR methods, the derivation of DWR estimates for hyperbolic problems is not straight forward. The solution to the formal dual problem might not be sufficiently regular to be used as a test function for the primal equation, see, e.g., [SH03]. A standard approach to circumvent this problem, cf., [SH03], is the consideration of an elliptic or parabolic regularization/stabilization for the corresponding set of equations. While this approach coincides with the standard discretization with continuous finite elements, additional stabilization is not so natural for discontinuous Galerkin methods (DG).

In this thesis, a DWR error representation for DG discretizations of hyperbolic problems is presented. This estimator requires a stabilization only for the, auxiliary, dual problem while leaving the primal problem unchanged.

Indeed the problem of finding a suitable representation of the error in the quantity of interest via adjoint calculus has to be expected since differentiability of such functionals w.r.t. the problem data is a subtle issue, see for instance [Ulb02], [Ulb03], and [GU10], where the problem was tackled by "shift differentiability", suitably modified adjoint based derivative computations, and application of artificial viscosity to the primal and adjoint equations, respectively.

In this thesis, the appearance of discontinuities is only suppressed in the dual solution by modification of the dual equation providing an adjoint based error representation. Due to the modified dual problem, the resulting error representation will contain an additional residual term. It is then shown numerically that this term is needed to obtain an effective error estimate, while it is not necessarily needed to obtain mesh refinement indicators.

The DWR error representation can typically not be evaluated exactly because the weights contain the unknown, primal and dual, analytic solution. Consequently, the weights need to be approximated utilizing the discrete, primal and dual, solutions. These discrete weight approximations can then be used within the DWR error representation (formal DWR); regardless of whether the exact weight is regular enough for this task or not. The difficulties in using the exact weight will consequently give rise to a more subtle matter in the DWR method; namely if the exact weight is not suitable in the representation, then it is not clear why the approximate weight should give an accurate error estimate. Indeed, this thesis shows numerically that the efficiency of the error estimate provided by a formal DWR estimator without modified dual equation will be worse then the one given by the newly proposed method, in the case where the exact weights are not suitable to be inserted into the error identity.

While there are two ways to obtain a discrete adjoint problem – either by discretization of the continuous adjoint equation or by adjoining the discrete primal equation – the non-existence of the continuous error representation will give trouble in both cases. With an adjoint consistent discretization, as pure Galerkin discretizations, both approaches generally result in the same error estimation. Due to the simplicity of applying an automatic adjoining algorithm, the discrete adjoint is often used, e.g., [RKM11], [PPF+06], and [VD00]. But also several continuous adjoint models were developed: In [BBS+14] a continuous adjoint model of the shallow water equations is derived to apply the DWR method with r-adaptivity for a finite element discretization. In [SS98] the element-wise continuous adjoint model of the Euler equations is applied and discretized by the finite volume method. In both cases the primal and dual solution were sufficiently smooth such that the solutions can be used as weights for the residuals. As mentioned above, this is not the general case as the weighted residuals of hyperbolic problems are not bounded in general, if neither the primal solution nor the dual solution are weakly differentiable in space. However, if both solutions have coinciding discontinuities, the residual of the primal equation can not be tested with the dual solution.

For a clearer understanding of the problem, the next section, which was preprinted in "Hamburger Beiträge zur Angewandten Mathematik" in September 2016, gives a motivating abstract example of the difficulty.

1.2 Motivation

For the use of the DWR method, it is suitable to rewrite the conservation law in weak form. In this context, let $a(\cdot, \cdot)\colon W \times V \to \mathbb{R}$ be a semi-linear form, i.e., it is linear in its second component, and let $F(\cdot)$ be a linear functional on V.
Suppose that $u \in W$ is a solution of

$$a(u, \psi) = F(\psi) \qquad \forall \psi \in V, \tag{1.2.1}$$

where W is a suitable function space and V is the proper test function space.
The weak form might also be utilized for discretization, such as the finite element or finite volume method. If the discrete solution u^{hk} on a spatial mesh with element size h and time step size k is to be post-processed by evaluating a goal-functional J, a natural question is the sensitivity of the functional value with respect to, small, perturbations. To this end it is useful to consider the adjoint solution $z \in V$ of

$$a'(u; \phi, z) = J'(u; \phi), \qquad \forall \phi \in W \tag{1.2.2}$$

Due to the definition of the primal and adjoint solution $u \in W$ and $z \in V$ should hold. For a reasonable problem the primal solution is indeed in W, but the adjoint problem (1.2.2) does not necessarily have a solution in the space V! To see that this is in fact a problem, we discuss this along a simple example.
For an advection equation a natural space is $W = L^\infty(\Omega; L^\infty(0, T))$ and if the initial values contain a jump no more regularity can be expected. Thus, the test functions have to be differentiable, i.e. a possible choice is $V = H^1(\Omega; H^1(0, T))$, such that the weak form has a meaning. On the other hand, the solution of the dual problem, which is again an advection equation, will only be in $L^\infty(\Omega; L^\infty(T, 0))$ and consequently not necessarily in V. Consequently, the adjoint solution z need not be regular enough to be used as a test function in (1.2.1). See also [SH03, Example B] for a more detailed exposition.
There are two obvious possibilities to match the solution spaces and test spaces in this setting: For a linear problem, modification of the goal functional, and consequently the data of the dual problem, can increase the regularity of the dual solution z and allow z to be used as a test function in (1.2.1). Second, and more generally applicable to nonlinear problems, artificial viscosity can be used to prevent shocks and obtain sufficiently smooth adjoint solutions, see for instance [SMN11]. The method presented subsequently in the thesis at hand can do without modification in the primal equation and only relies on artificial viscosity in the dual equation.
The problem of non-fitting solution spaces and test spaces for the primal and dual problem is also mentioned in [BR01, Remark 2.3].

1.3 Objective

With the above motivation in mind, this thesis has the objective to clarify the following questions:

i. What happens, if the dual problem is posed in such a way that the weights do not satisfy the necessary regularity conditions for the estimator?

ii. How does a modification of the dual problem by artificial viscosity change the error estimator?

iii. How is the numerical performance of the modified estimator?

To answer the first question, the formal DWR error estimator is evaluated for a simple advection example, in 1D (section 5.1.7) and 2D (section 5.2.5). Since this linear example with constant advection velocity cannot create a shock, a discontinuous initial condition is given and the goal functional is chosen such that the discontinuities in the dual equation coincide with the discontinuities of the primal problem.
The second question is addressed in section 5.1.5, where a modified DWR error estimator is derived. The derivation follows the idea of Becker and Rannacher, [BR01], but replaces the solution of the dual advection equation by the more regular solution of the dual advection-diffusion equation.
The modified estimator is then again tested in 1D and 2D (section 5.1.7 and 5.2.5, respectively).

1.4 Overview

This thesis is structured in the following way: Chapter 2 is a short introduction to the advection and the advection-diffusion equation and contains solution formulas and L^p-convergence of the advection-diffusion solution to the advection solution for vanishing viscosity. Both equations are discretized in Chapter 3 in detail. The discretization includes the set up of the grid structure, introduction to the finite element method and a discontinuous Galerkin discretization as well as straightforward residual error estimation. Chapter 3 closes with marking strategies and the refinement technique used in the applied codes.
The derivation of the formal dual weighted residual method used in this thesis is done in Chapter 4.
The main chapter, Chapter 5, builds on the groundwork of the chapters before. Firstly, it introduces a 1D test case in which the dual weighted residual cannot be computed right away due to discontinuities in the primal and dual solution. This difficulty is circumvented by modification of the dual problem with artificial viscosity. This causes the error estimator to have an additional term, a correction term. The extended error estimator is numerically tested for its efficiency.

The second part of Chapter 5 is concerned with two 2D test cases. The first test case, which is quasi 1D, ensures the correct implementation of the discretization of the diffusive term, as the solution is compared to the analytic solution. The second test case is treated without the knowledge of the analytic solution and therefore uses approximation of weights. Both of these test cases contain discontinuities, similar to the 1D test case. For the test case with the approximated weights the efficiency is investigated numerically.

At the end of this thesis, the numerical results are summarized and discussed in the conclusion. A short outlook describes reasonable further studies of the modified estimator and suggests a possible application.

Chapter 2

Solution theory

In this chapter solutions for the linear transport equation with and without diffusion are discussed. In both cases the initial conditions are discontinuous as these are used later on in the numerical examples.

In the first section, function spaces and norms are defined, which will be of use in the following. In the second section, the linear advection equation is introduced and a weak solution is given. The third section deals with the advection-diffusion equation and its weak solution. In the last section of this chapter the asymptotic behavior of the solution of the advection-diffusion equation towards the solution of the advection equation for vanishing viscosity is presented.

2.1 Function spaces and norms

The following definitions and notations that I used in this thesis are standard and can be found, for example, in [GT98].

Let $C^0(\Omega)$ be the set of continuous functions on the domain $\Omega \subset \mathbb{R}^n$ with real values. And let $C^K(\Omega)$, $K \in \mathbb{N}$, be the set of functions of which the derivatives up to order K are continuous in Ω. The function space of $C^K(\Omega)$ functions with compact support is denoted as $C_c^K(\Omega)$.

For $1 \leq P < \infty$, the Banach space $L^P(\Omega)$ is defined as

$$L^P(\Omega) := \left\{ u : \Omega \to \mathbb{R} \,\middle|\, u \text{ measurable and } \|u\|_{L^P(\Omega)} < \infty \right\}$$

with the norm

$$\|u\|_{L^P(\Omega)} := \left(\int_\Omega |u|^P \, \mathrm{d}\mathbf{x} \right)^{\frac{1}{P}}.$$

In case of $P = \infty$, the space $L^\infty(\Omega)$ is defined as the space of essentially bounded functions on Ω, equipped with the norm

$$\|u\|_{L^\infty(\Omega)} := \sup_\Omega |u|.$$

Besides the space of P-integrable functions and the space of K times continuous differentiable functions, spaces of functions that have derivatives in a weaker sense need to be introduced. Therefore, let $\boldsymbol{\alpha}$ be a multi index and

$$\nabla^{\boldsymbol{\alpha}} = \frac{\partial^{|\boldsymbol{\alpha}|} u}{\partial x_1^{\alpha_1} \dots \partial x_n^{\alpha_n}}$$

the derivative to the power of $\boldsymbol{\alpha}$. Let u be a locally integrable function on Ω. A locally integrable function v is called a weak derivative of u of order $\boldsymbol{\alpha}$ if

$$\int_{\Omega} \psi v \, \mathrm{d}\mathbf{x} = (-1)^{\boldsymbol{\alpha}} \int_{\Omega} u \nabla^{\boldsymbol{\alpha}} \psi \, \mathrm{d}\mathbf{x}$$

is satisfied for all $\psi \in C_c^{\boldsymbol{\alpha}}(\Omega)$.

Thus, $W^K(\Omega)$ shall be defined as the space of locally integrable functions that have weak derivatives up to K-th order, i.e., $\forall |\alpha_i| \leq K, i = 1, \dots, n$. If the functions are not only weakly differentiable, but the weak derivatives are P-integrable, the Banach space $W^{K,P}(\Omega)$ is defined as

$$W^{K,P}(\Omega) := \left\{ u \in W^K(\Omega) \, \middle| \, \forall \boldsymbol{\alpha}, |\alpha_i| \leq K : \nabla^{\boldsymbol{\alpha}} u \in L^P(\Omega) \right\}.$$

with

$$\|u\|_{W^{K,P}(\Omega)} := \left(\int_{\Omega} \sum_{|\boldsymbol{\alpha}| \leq K} |\nabla^{\boldsymbol{\alpha}} u|^P \, \mathrm{d}\mathbf{x} \right)^{\frac{1}{P}}$$

as a possible norm on $W^{K,P}(\Omega)$.

Since $W^{K,2}(\Omega)$ is a Hilbert space it is also denoted as

$$H^K(\Omega) := W^{K,2}(\Omega)$$

with the inner product

$$(u, v)_{H^K(\Omega)} := \int_{\Omega} \sum_{|\boldsymbol{\alpha}| \leq K} \nabla^{\boldsymbol{\alpha}} u \nabla^{\boldsymbol{\alpha}} v \, \mathrm{d}\mathbf{x}.$$

2.2 The linear advection equation

The linear advection equation can be used as a model for the transport of a substance which is represented as a concentration $u_0(\mathbf{x}, t)$ at $\mathbf{x} \in \mathbb{R}^n$ at time $t \in (0, \infty)$. The classical formulation of the linear advection equation with constant transport velocity $\mathbf{v} \in \mathbb{R}^n$ is

$$\partial_t u_0(\mathbf{x}, t) + \mathbf{v} \cdot \nabla u_0(\mathbf{x}, t) = 0, \qquad (\mathbf{x}, t) \in \mathbb{R}^n \times (0, \infty). \tag{2.2.1}$$

Equipped with an initial condition,

$$u_0(\mathbf{x}, 0) = u_{\mathrm{ini}}(\mathbf{x}), \qquad \mathbf{x} \in \mathbb{R}^n,$$

this problem has a unique solution

$$u_0(\mathbf{x}, t) = u_{\text{ini}}(\mathbf{x} - \mathbf{v}t), \qquad (\mathbf{x}, t) \in \mathbb{R}^n \times (0, \infty). \tag{2.2.2}$$

This is even true not only for $u_{\text{ini}} \in C^1(\mathbb{R}^n)$, but also for discontinuous initial condition, $u_{\text{ini}} \in L^\infty(\mathbb{R}^n)$. Compare, e.g., the remark in [Eva10, p. 19]. If the initial condition is discontinuous, then the solution (2.2.2) is discontinuous, too. Thus, it can obviously not satisfy the classical formulation (2.2.1) and is thus only meaningful in a weak sense.

Let $\psi \in C_c^1(\mathbb{R}^n \times [0, \infty))$. Multiplication of (2.2.1) with the test function ψ and integration by parts results in

$$\int\limits_0^\infty \int\limits_{\mathbb{R}^n} u_0 \partial_t \psi + u_0 \mathbf{v} \cdot \nabla \psi \, \mathrm{d}\mathbf{x} \, \mathrm{d}t + \int\limits_{\mathbb{R}^n} (u_{\text{ini}}(\mathbf{x}) - u_0(x, 0)) \, \psi(\mathbf{x}, 0) \, \mathrm{d}\mathbf{x} = 0, \tag{2.2.3}$$

omitting the space boundary integrals, which are zero since the test function is compactly supported. If $u_0 \in L^\infty(\mathbb{R}^n \times (0, \infty))$ satisfies (2.2.3), it is called a weak solution of problem (2.2.1).

2.3 The advection-diffusion equation

The linear advection-diffusion equation (ADE) with source term $f : \mathbb{R}^n \to \mathbb{R}$ reads

$$\partial_t u_\varepsilon(\mathbf{x}, t) + \mathbf{v} \cdot \nabla u_\varepsilon(\mathbf{x}, t) - \varepsilon \Delta u_\varepsilon(\mathbf{x}, t) = f(\mathbf{x}), \qquad (\mathbf{x}, t) \in \mathbb{R}^n \times (0, \infty), \tag{2.3.1}$$

with initial condition

$$u_\varepsilon(\mathbf{x}, 0) = u_{\text{ini}}(\mathbf{x}), \qquad \mathbf{x} \in \mathbb{R}^n. \tag{2.3.2}$$

As the in the advection equation, the substance is transported with velocity $\mathbf{v} \in \mathbb{R}^n$ but additionally a diffusion of the substance takes place. The isotropic strength of the diffusion is controlled by the diffusion coefficient $\varepsilon \in \mathbb{R}_+$. With constant advection and diffusion coefficients, the above equation can be rewritten into a conservative form as

$$\partial_t u_\varepsilon(\mathbf{x}, t) + \mathrm{div}\left(\mathbf{v} u_\varepsilon(\mathbf{x}, t) - \varepsilon \nabla u_\varepsilon(\mathbf{x}, t)\right) = f(\mathbf{x}), \qquad (\mathbf{x}, t) \in \mathbb{R}^n \times (0, \infty).$$

The argument of the divergence is called the flux term. This formulation is often used in the context of discontinuous Galerkin discretizations and is also applied in sections 5.1.6 and 5.2.4.

By changing the frame of reference, the advection-diffusion equation can be transformed into a pure diffusion equation. Thus, the ADE inherits the property of infinite speed of information transport and smoothening starts instantaneously on the whole domain after initial time. Solving the diffusion equation and retransforming it to the original space is one way to solve the problem.

An other option is the application of a Green's function . [XTB07] give an overview on Green's functions for the advection diffusion equation with various boundary conditions.

For the two dimensional case the solution to (2.3.1) with initial condition (2.3.2) is given by

$$u_\varepsilon(x,y,t) = \int\limits_0^t \int\limits_{-\infty}^\infty \int\limits_{-\infty}^\infty Gf \, \mathrm{d}\xi \, \mathrm{d}\eta \, \mathrm{d}\tau + \int\limits_{-\infty}^\infty \int\limits_{-\infty}^\infty [Gu_{\mathrm{ini}}]_{\tau=0} \, \mathrm{d}\xi \, \mathrm{d}\eta$$

$$+ \int\limits_0^t \int\limits_{-\infty}^\infty [\varepsilon\,(G\partial_\xi u_\varepsilon - \partial_\xi G u_\varepsilon) - v_1 G u_\varepsilon]_{\xi=-\infty}^\infty \, \mathrm{d}\eta \, \mathrm{d}\tau \qquad (2.3.3)$$

$$+ \int\limits_0^t \int\limits_{-\infty}^\infty [\varepsilon\,(G\partial_\eta u_\varepsilon - \partial_\eta G u_\varepsilon) - v_2 G u_\varepsilon]_{\eta=-\infty}^\infty \, \mathrm{d}\xi \, \mathrm{d}\tau$$

In this formula, $G = G(\xi,\eta,\tau;x,y,t)$ is the Green's function, a product of Green's functions for the 1D case,

$$G(\xi,\eta,\tau;x,y,t) = \frac{H(t-\tau)}{4\pi\varepsilon(t-\tau)} e^{-\frac{(\xi-x+v_1(t-\tau))^2+(\eta-y+v_2(t-\tau))^2}{4\varepsilon(t-\tau)}}, \qquad (2.3.4)$$

with the Heaviside function,

$$H(t-\tau) = \begin{cases} 1, & t > \tau \\ 0.5, & t = \tau \\ 0, & t < \tau. \end{cases}$$

The limit of the solution u_ε for $t \to 0$ exists in the distributional sense, meaning the Green's function converges to the δ-distribution and $u_\varepsilon(x,y,0) = u_{\mathrm{ini}(x,y)}$. Furthermore, due to the smoothness of the Green's function, the solution is smooth for any $t > 0$.
Because of the vanishing Dirichlet boundary condition (**??**) the evaluation of the last two summands of (2.3.3) is zero. If, additionally, the source term is zero, the solution formula (2.3.3) simplifies to

$$u_\varepsilon(x,y,t) = \int\limits_{-\infty}^\infty \int\limits_{-\infty}^\infty G u_{\mathrm{ini}}|_{\tau=0} \, \mathrm{d}\xi \, \mathrm{d}\eta. \qquad (2.3.5)$$

This is also true for non smooth initial conditions on a open but bounded domain Ω, since parabolic problems with initial data in $L^2\,(\Omega)$ and source terms in $L^2\,(0,T;H^{-1}\,(\Omega))$ have solutions in $L^2\,(0,T;H^1\,(\Omega))$, [Eva10, pp.351].
For the 1D case, the Green's function is

$$G(\xi,\tau;x,t) = \frac{H(t-\tau)}{\sqrt{4\pi\varepsilon(t-\tau)}} e^{-\frac{(\xi-x+v_1(t-\tau))^2}{4\varepsilon(t-\tau)}},$$

and the solution formula is

$$u_\varepsilon(x,t) = \int\limits_{-\infty}^\infty G u_{\mathrm{ini}}|_{\tau=0} \, \mathrm{d}\xi. \qquad (2.3.6)$$

Since the Green's function is a Schwartz function for $t \neq \tau$ and therefore all derivatives are uniformly bounded, the homogeneous problem with a bounded and continuous initial condition, $u_{\text{ini}} \in C\left(\mathbb{R}^n\right) \cap L^\infty\left(\mathbb{R}^n\right)$, has a smooth solution, $u_\varepsilon \in C^\infty\left(\mathbb{R}^n \times (0, \infty)\right)$. For a problem with source term, the regularity of the solution is depending on the regularity of the source term.

2.4 Asymptotics for vanishing viscosity

In the previous sections solution formulas for the advection and the advection-diffusion equation were given. Since this thesis focuses on the replacement of a solution of the advection equation by the solution of the advection-diffusion equation this section is about the convergence of these two solutions for vanishing diffusion. Convergence is not obvious, due to the fact that the analytic behavior of the solutions is influenced primarily be the derivatives of the highest order. [Eva10] gives an example of a singularly perturbed transport equation and the convergence of solutions. In [BLN79] convergence of solutions is proven for $u_{\text{ini}} \in C^2\left(\mathbb{R}\right)$.

In this thesis, convergence in $L^P\left(\mathbb{R}\right)$ is shown for $u_{\text{ini}} \in L^\infty\left(\mathbb{R}\right) \cap L^p\left(\mathbb{R}\right)$ and the special 1D case of constant advection velocity. This means, the following Lemma is especially true for piecewise continuous initial conditions with a compact support.

Recalling the solution formulas, the solution of the advection equation is

$$u_0(x,t) = u_{\text{ini}}(x - vt) \tag{2.4.1}$$

and the solution to the advection-diffusion equation is

$$u_\varepsilon(x,t) = \int_{\mathbb{R}} \frac{1}{\sqrt{4\pi\varepsilon t}} e^{-\frac{(\xi - x + vt)^2}{4\varepsilon t}} u_{\text{ini}}(\xi) \, \mathrm{d}\xi. \tag{2.4.2}$$

Lemma 1. *Let the initial condition $u_{ini} \in L^\infty\left(\mathbb{R}\right) \cap L^P\left(\mathbb{R}\right)$ and the advection and advection-diffusion equation have the solution formulas (2.4.1) and (2.4.2), then*

$$\lim_{\varepsilon \to 0} \left\| u_0(\cdot, \tilde{t}) - u_\varepsilon(\cdot, \tilde{t}) \right\|_{L^P(\mathbb{R})} = 0.$$

holds for $P \in [1, \infty)$ and arbitrary but fixed $\tilde{t} \in (0, \infty)$.

To prove this, the solution formula of the diffusion equation is rewritten into a convolution form for fixed $\tilde{t} \in (0, \infty)$

$$u_\varepsilon(x, \tilde{t}) = G_{\varepsilon, \tilde{t}}(\xi - x) * u_{\text{ini}}(\xi)$$

with the heat kernel $G_{\varepsilon, \tilde{t}}(\xi - x) := \frac{1}{\sqrt{4\pi\varepsilon\tilde{t}}} e^{-\frac{(\xi - x + v\tilde{t})^2}{4\varepsilon\tilde{t}}}$. The solution of the advection equation at fixed time $\tilde{t} \in (0, \infty)$ is also rewritten to

$$u_0(x, \tilde{t}) = u_{\text{ini}}(x - v\tilde{t}) =: u_{\text{ini}, \tilde{t}}(x).$$

Let $u_{\text{ini},\tilde{t}}^{\delta} \in C_c^{\infty}(\mathbb{R})$ be a smooth approximation with compact support of $u_{\text{ini},\tilde{t}} \in L^{\infty}(\mathbb{R}) \cap L^P(\mathbb{R})$ and $u_{\text{ini}}^{\delta} \in C_c^{\infty}(\mathbb{R})$ be a smooth approximation with compact support of $u_{\text{ini}} \in L^{\infty}(\mathbb{R}) \cap L^P(\mathbb{R})$, respectively. Thus, it is

$$\left\| u_0(\cdot, \tilde{t}) - u_{\varepsilon}(\cdot, \tilde{t}) \right\|_{L^P(\mathbb{R})}$$

$$= \left\| u_{\text{ini},\tilde{t}} - G_{\varepsilon,\tilde{t}} * u_{\text{ini}} \right\|_{L^P(\mathbb{R})}$$

$$= \left\| u_{\text{ini},\tilde{t}} - u_{\text{ini},\tilde{t}}^{\delta} + u_{\text{ini},\tilde{t}}^{\delta} - G_{\varepsilon,\tilde{t}} * u_{\text{ini}}^{\delta} + G_{\varepsilon,\tilde{t}} * u_{\text{ini}}^{\delta} - G_{\varepsilon,\tilde{t}} * u_{\text{ini}} \right\|_{L^P(\mathbb{R})}$$

$$\leq \left\| u_{\text{ini},\tilde{t}} - u_{\text{ini},\tilde{t}}^{\delta} \right\|_{L^P(\mathbb{R})} + \left\| u_{\text{ini},\tilde{t}}^{\delta} - G_{\varepsilon,\tilde{t}} * u_{\text{ini}}^{\delta} \right\|_{L^P(\mathbb{R})} + \left\| G_{\varepsilon,\tilde{t}} * u_{\text{ini}}^{\delta} - G_{\varepsilon,\tilde{t}} * u_{\text{ini}} \right\|_{L^P(\mathbb{R})}$$

$$\tag{2.4.3}$$

The last norm can be approximated by Young's inequality for convolutions

$$\left\| G_{\varepsilon,\tilde{t}} * u_{\text{ini}}^{\delta} - G_{\varepsilon,\tilde{t}} * u_{\text{ini}} \right\|_{L^P(\mathbb{R})} \leq \left\| G_{\varepsilon,\tilde{t}} \right\|_{L^1(\mathbb{R})} \left\| u_{\text{ini}}^{\delta} - u_{\text{ini}} \right\|_{L^P(\mathbb{R})}.$$

The integral of the Green's function is one independent of ε, see (A.1.3).
$\left\| u_{\text{ini},\tilde{t}} - u_{\text{ini},\tilde{t}}^{\delta} \right\|_{L^P(\mathbb{R})}$ and $\left\| u_{\text{ini}} - u_{\text{ini}}^{\delta} \right\|_{L^P(\mathbb{R})}$ can become arbitrary small, depending on the choice of δ, since $C_c^{\infty}(\mathbb{R})$ is dense in $L^p(\mathbb{R})$. So I chose δ such that both terms are smaller then an arbitrary small, positive κ. With this choice (2.4.3) becomes

$$\left\| u_0(\cdot, \tilde{t}) - u_{\varepsilon}(\cdot, \tilde{t}) \right\|_{L^P(\mathbb{R})} \leq 2\kappa + \left\| u_{\text{ini},\tilde{t}}^{\delta} - G_{\varepsilon,\tilde{t}} * u_{\text{ini}}^{\delta} \right\|_{L^P(\mathbb{R})}$$

For initial condition $u_{\text{ini}}^{\delta} \in C^2(\mathbb{R})$ the solution of the advection-diffusion equation converges to the solution of the advection equation in L^p sense, see [BLN79]. I.e.,

$$\lim_{\varepsilon \to 0} \left\| u_{\text{ini},\tilde{t}}^{\delta} - G_{\varepsilon,\tilde{t}} * u_{\text{ini}}^{\delta} \right\|_{L^P(\mathbb{R})} = 0,$$

and it follows

$$\lim_{\varepsilon \to 0} \left\| u_0(\cdot, \tilde{t}) - u_{\varepsilon}(\cdot, \tilde{t}) \right\|_{L^P(\mathbb{R})} \leq 2\kappa + \lim_{\varepsilon \to 0} \left\| u_{\text{ini},\tilde{t}}^{\delta} - G_{\varepsilon,\tilde{t}} * u_{\text{ini}}^{\delta} \right\|_{L^P(\mathbb{R})} = 2\kappa.$$

Since $\kappa > 0$ can become arbitrary small, the limit has to be zero. $\qquad\square$

This shows that for the special case of the 1D advection equation with constant velocity and initial condition $u_{\text{ini}} \in L^{\infty}(\mathbb{R}) \cap L^P(\mathbb{R})$ the solution of the perturbed problem converges to the solution of the unperturbed problem in L^P sense. This convergence is of interest if the solution of the advection equation is replaced by the solution of the advection-diffusion equation in the computation of an integral, as for instance the later used residuals.

This chapter introduced the advection equation and the advection-diffusion equation with constant velocity. For both problems solution formulas were given which depended

on the initial condition. In the last section of this chapter, it was shown that the solution of the advection-diffusion equation converged pointwise to the solution of the advection equation if the diffusion decreases to zero and the initial condition satisfies several restraining conditions.

In the next chapter the advection equation and the advection-diffusion equation are reformulated to equations in conservative form and discretized by a discontinuous Galerkin scheme.

Chapter 3

Discretization

Numerical solution of differential equations by a finite element method bears different sources of computational errors, [EEHJ95]: For the Galerkin discretization the solution is represented by piecewise polynomials, which introduces a discretization error, if the solution is not a polynomial of the respective order. The necessary quadrature for the finite element method can raise an additional error if the quadrature rule is not exact. Furthermore, the resulting discrete system has to be solved and if this is only done approximately, another approximation error is introduced.

In a discontinuous Galerkin method, the approximation of the boundary terms is an other source of computational errors [Riv08].

For elliptic problems, solutions are generally smooth and grid refinement is most useful if the computational domain has a reentrant corner or the equation discontinuous coefficients. For hyperbolic problems though, a static grid refinement with respect to the initial conditions is in most cases not enough to resolve the solution sufficiently. Since the solution is changing with time and can even exhibit shocks in finite time, it is essential to capture these shocks and adapt the grid in each time step. Of course, if one were to know the region of the shocks, one could refine the grid beforehand and keep it static while the shock is traveling on the refined area.

To detect shocks or other areas of high influence to the computational error, local error indicators – or even better – local error estimators are used. Depending on these estimators, elements are marked for refinement or coarsening and are then refined/coarsened.

The numerical computations in this thesis were done with two different codes: I extended the 1D DG code *hypy1D*, which has been used so far to solve the shallow water equations and was written in Python by Dr.Stefan Vater, such that it can solve problems including diffusion. And I implemented the DWR error estimator for the advection equation. 1D results in this thesis are all computed with *hypy1D*.

The 2D results are obtained by simulations with *StormFlash2D*, a Fortran code programmed by several different members of the working group of Prof. Dr. Jörn Behrens. *StormFlash2D* solves 2D shallow water equations with DG discretization in time and explicit time stepping schemes as the explicit Euler scheme or different explicit

Runge-Kutta methods. *StormFlash2D* uses *amatos*, [BRH$^+$05], for grid generation and management. I added routines to *StormFlash2D* in order to solve the advection and the advection-diffusion equation. The DG method for diffusion is thus also included in *StormFlash2D*. For the 2D test cases in this thesis, I extended the code to compute local DWR error estimators for the advection equation.

The following sections partly refer to the used codes. The first section deals with the general introduction to finite elements for elliptic equations. Tough the advection equation discussed in this thesis is hyperbolic and the advection-diffusion equation is parabolic, the theory for elliptic problems gives the basic ideas of discretization.

The second section, describing and defining admissible grids, is related to the triangular mesh used in *amatos*. Having the basic grid structure, DG elements are introduced, giving first and second order polynomials for basis functions on a reference interval and a reference triangle. These reference elements are related to *hypy1D* and *amatos*. The next section introduces a discontinuous Galerkin method for the advection and the advection-diffusion equation.

In the section about error estimation a residual based error estimator for an elliptic example is introduced to see the basic idea of residual based error estimation and to make it clear, that this kind of estimator does not work on hyperbolic equations as the advection equation. The second part of the error estimator section gives an example for an estimator for a hyperbolic equation.

The last two short sections are about the Dörfler marking strategy and grid refinement by bisection. With these two and the error estimation, the discretization schemes, and the grid structure, all tools are given to obtain a numerical solution on an adaptive grid.

3.1 Discretization schemes

Let $V = V(\Omega), W = W(\Omega)$ be Banach spaces equipped with norms $\|\cdot\|_V$ and $\|\cdot\|_W$. And let $a(\cdot, \cdot) : V \times W \to \mathbb{R}$ be an elliptic bilinear mapping, for which $u \in V(\Omega)$ is a solution of the variational formulation

$$a(u, \psi) = (f, \psi)_\Omega, \qquad \forall \psi \in W. \tag{3.1.1}$$

The right hand side of the equation is the standard L^2 inner product $(f, \psi)_\Omega = \int_\Omega f\psi \, \mathrm{d}x$, for $f, \psi \in L^2(\Omega)$.

If the test function space is equivalent to the solution space, problem (3.1.1) can be rewritten into

$$a(u, \psi) = (f, \psi)_\Omega, \qquad \forall \psi \in V. \tag{3.1.2}$$

If now the space V is not only a Banach space, but also a Hilbert space, the Lemma of Lax-Milgram gives existence and uniqueness of a solution to (3.1.2) under certain assumptions.

Lemma 2. Lax-Milgram

Let V be a Hilbert space with norm $\|\cdot\|_V$ and inner product, and let $a : V \times V \to \mathbb{R}$ be a bilinear mapping, which is

- *continuous, $\exists C > 0 \quad \forall u, \psi \in V : \quad |a(u,\psi)| \le C\|u\|_V\|\psi\|_V$*

- *and coercive, $\exists c > 0 \quad \forall u \in V : \quad c\|u\|_V^2 \le a(u,u).$*

And let $\tilde{f} : V \to \mathbb{R}$ be a bounded linear functional on V. Then,

$$\exists! u \in V \quad \forall \psi \in V : \quad a(u,\psi) = \langle \tilde{f}, \psi \rangle.$$

In this Lemma, the right hand side is represented as dual pairing $\langle \cdot, \cdot \rangle$, with $\tilde{f}, \psi \in L^2(\Omega)$ and $V \hookrightarrow L^2(\Omega) \hookrightarrow V^*$, respectively. The *Riesz Representation Theorem* allows to identify the dual pairing with the inner product in L^2,

$$\langle \tilde{f}, \psi \rangle = (f, \psi)_\Omega, \quad \forall \psi \in V,$$

for some element $f \in V$. For proof of the lemma or further reading on the representation theorem see for instance [Eva10].

Keeping in mind the existence and uniqueness of the solution, (3.1.1) shall be solved numerically. The infinite dimensional space V is approximated by a finite dimensional subspace $V^h \subset V$, compare [Rit09], and a solution $u^h \in V^h$ to

$$a(u^h, \psi^h) = \left(f, \psi^h\right)_\Omega, \qquad \forall \psi^h \in V^h(\Omega) \tag{3.1.3}$$

is to be computed. u^h is called the *Ritz projection* of u.

Since V^h is finite dimensional, it can be represented as the span of a finite basis

$$V^h = \mathrm{span}\{e_1, \dots, e_d\}$$

and thus any $u^h \in V^h$ can be uniquely represented as

$$u^h = \sum_{i=1}^d u_i e_i. \tag{3.1.4}$$

with coefficients $\mathbf{u}^T = (u_1, \dots, u_d) \in \mathbb{R}^d$. The basis also represents a suitable set of test functions, representing the whole space V^h, and problem (3.1.3) becomes

$$a\left(\sum_{i=1}^d u_i e_i, e_j\right) = (f, e_j)_\Omega, \qquad j = 1, \dots, d. \tag{3.1.5}$$

Since a is assumed bilinear, the n equations from (3.1.5) can be rewritten into a matrix vector multiplication

$$A\mathbf{u} = \mathbf{f} \tag{3.1.6}$$

with system matrix $A = a\left(e_j, e_i\right)_{i,j}$.

If the problem in (3.1.3) is symmetric and definite, the approximation by a finite subspace is often called *Ritz-Galerkin* method. In case the problem might contain singularities, the Lemma of Lax-Milgram does not hold. Therefore, it might be a good choice to have a different test space than the solution space, as stated in the beginning of this section. The finite spaces are then V^h and W_h and the method is called *Petrov-Galerkin* method. Galerkin methods for linear problems have the convenient property that the approximation error, $u - u^h$, is orthogonal in the sense of the linear form a to the test and ansatz function space,

$$a\left(u - u^h, \psi^h\right) = 0, \quad \forall \psi^h \in V^h.$$

The approximation error is thus in the complement of V^h in V. The norm of the error can be bounded by the error of the best possible approximation in the respective subspace times a constant, independent of h. This is stated in Céas Lemma.

Lemma 3. Céa

Let $a : V \times V \to \mathbb{R}$ be a bilinear mapping, continuous and coercive as in Lemma (2) and let V be Hilbert space with finite dimensional subspace $V^h\left(\Omega\right) \subset V$ and norm $\|\cdot\|_V$. Furthermore, let u be the solution to (3.1.2) and u^h solution to (3.1.3). Then

$$\|u - u^h\|_V \leq \frac{C}{c} \inf_{\psi^h \in V^h} \|u - \psi^h\|_V$$

For proof and further reading, see for example [Bra07].

Céas Lemma shows that the *Ritz-Galerkin* approximation is the best possible solution in V^h, up to a constant. Furthermore it demonstrates that it is essential to take care of the choice of the finite dimensional subspace, because the subspace influences the approximation quality of u^h to u. The space of polynomials of order n shall serve as an example: If the solution u is smooth, a polynomial approximation is fine, but if u has steep gradients, higher order polynomials will not be a good approximation due to oscillations. Thus, it is a better idea to define piecewise polynomials of low order and decrease the size of the pieces. This type of refinement is called *h-refinement*.

Céas Lemma requires conform elements, i.e., $V^h \subset V$, the later applied discontinuous Galerkin method uses, however, non-conforming elements. Strangs Lemmas, see for instance in [Bra07], give similar statements for non-conforming methods. The second Lemma of Strang assumes the discrete bilinear form a_h to be continuous and elliptic, and deduces

$$\|u - u^h\|_h \leq C \left(\inf_{\psi^h \in V^h} \|u - \psi^h\|_h + \sup_{\tilde{\psi}^h \in V^h} \frac{\left| a_h\left(u, \tilde{\psi}^h\right) - \left(f, \tilde{\psi}^h\right)_\Omega \right|}{\|\tilde{\psi}^h\|_h} \right)$$

with a mesh dependent norm $\|\cdot\|_h$. The additional supremum term represents the consistency error.

Tough this theory is on elliptic problems it shall serve as basic idea for parabolic and hyperbolic equations, for which sometimes existence and uniqueness of solutions is not yet proven, but numerical computations are done nevertheless.

3.1.1 Grid structure

The idea of piecewise polynomials gives rise to the necessity of decomposing the domain Ω into 'pieces'. This decomposition is called *triangulation*, if the domain is subdivided into simplices. A triangulation in 1D is thus the partition into intervals, in 2D into triangles, and in 3D into tetrahedrons. Though the partition into other polytopes is also possible, the work in this thesis is restricted to intervals and triangles. Furthermore, it is assumed that Ω is a polygon, since domains with curved boundaries require special treatment of the boundaries, see for instance [Bra07].

Definition 3.1.7. *Let the polygonal domain $\bar{\Omega}$ be a closed set in $\mathbb{R}^n$, $n = 1, 2$. A triangulation $\mathcal{E} = \{E_1, \ldots, E_m\}$ of $\bar{\Omega}$ is called*

- *structure regular if the intersection of any two E_i, E_j, $i \neq j$, contains*

    - *either a single point or is empty, (1D),*
    - *either a vertex or an edge or the intersection is empty, (2D).*

- *admissible if*

$$\bar{\Omega} = \bigcup_{E \in \mathcal{E}} E.$$

    and $\mathcal{E}$ structure regular.

The property of *structure regularity* ensures the absence of hanging nodes. Hanging nodes need some more treatment and further insight gives e.g. [CO84].

In the case of a 2D domain, there is some freedom to choose the type of element: while in 1D an element is an interval, in 2D an element can be triangular, quadrilateral, or other types of polygonals, covering non-overlappingly the domain. Though in quadrilateral grids the spatial derivatives are easier to compute, since the direction of derivatives is along the coordinate axes, (unstructured) triangular grids are usually more fit to approximate non-trivial boundaries. As the numerics in this thesis are done on triangular grids, only the properties of triangular grids will be discussed in the following. For triangles, h can stand for the maximum values of the following properties of all triangles in the grid: the circumcircle diameter, the incircle diameter, or the longest side of a triangle in the grid. If a grid with grid size h is refined, the new grid size h_{ref} satisfies $h_{\mathrm{ref}} \leq h$ and the amount of elements in the refined triangulation is higher than before, $\mathrm{card}(\mathcal{E}_{h_{\mathrm{ref}}}) \succeq \mathrm{card}(\mathcal{E}_h)$.

The smallest angle of all triangles in the triangulation, γ, is also of interest. If there exist constants $c, C \in (0, \pi)$ such that

$$0 < c \leq \gamma \leq C < \pi$$

then the triangulation is called *regular* and the triangles are *not degenerated.*

The triangulation $\mathcal{E}_h$ is called *locally quasi-uniform* if it is admissible and for all possible partitions of the triangulation exists a common non-degeneration constant c. A typical partition is a neighborhood. A neighborhood of a triangle E in triangulation $\mathcal{E}_h$ can be defined as

$$N_{\mathcal{E}_h}(E) = \{E' \in \mathcal{E}_h | E' \cap E \neq \emptyset\}.$$

In a *locally quasi-uniform* triangulation the maximal number of neighbors is bounded for all $E \in \mathcal{E}_h$ and this is true for all grid sizes $h > 0$. Furthermore, the size ratio of any two triangles sharing a neighborhood are be bounded, meaning, neighboring triangles have relatively equal size.

While the *admissibility* of the triangulation is geometrically essential, the properties *regularity* and *local quasi-uniformity* ensure conformity of nodal interpolation for the finite element approximation as well as for the discontinuous Galerkin schemes.

3.1.2   Realization in *amatos and hypy1D*

Having decomposed Ω into a set $\mathcal{E}$ of elements E, on each element a polynomial of low order is used to represent u^h. To avoid computation of the coefficients for the basis functions for each element, the effort is done only for a reference element, $\tilde{E}$, to which the degrees of freedom are mapped by metric terms. For example, the local mass matrix $M_{\tilde{E}}$ of the reference element $\tilde{E}$ is computed as

$$M_{\tilde{E}} = \left(\int\limits_{\tilde{E}} \tilde{e}_i(\boldsymbol{\xi}) \tilde{e}_j(\boldsymbol{\xi}) \, \mathrm{d}\boldsymbol{\xi} \right)_{i,j},$$

where $\boldsymbol{\xi} \in \tilde{E}$ is the local coordinate in the reference element and $\tilde{e}_i, i = 1, \ldots, n$ are the local basis functions. Gaining the integral value on the reference element, only the transformation is needed to translate the information from the reference element to each element in the grid. Let

$$\tau: \quad \tilde{E} \mapsto E, \qquad \tau(\boldsymbol{\xi}) = \boldsymbol{\xi}_0 + B\boldsymbol{\xi}$$

be a bijective and affine mapping with a non singular matrix B.
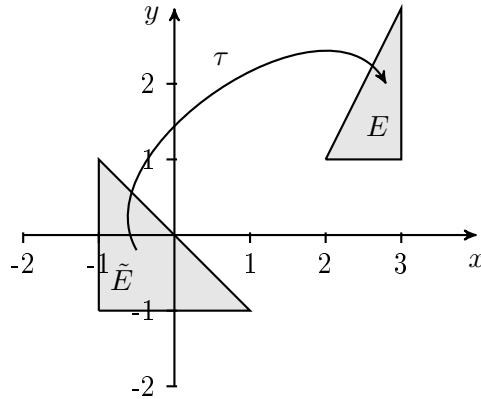
Figure 3.1: Reference triangle $\tilde{E}$ and mapping τ

For the computation of the local integral values in each element, the transformation rule is applied. For the mass matrix this is

$$M_E = \int\limits_E e_i(\mathbf{x})e_j(\mathbf{x})\,\mathrm{d}\mathbf{x} = \int\limits_{\tilde{E}} |\det(J_\tau)|e_i(\tau(\boldsymbol{\xi}))e_j(\tau(\boldsymbol{\xi}))\,\mathrm{d}\xi$$
$$= |\det(B)| \int\limits_{\tilde{E}} \tilde{e}_i(\boldsymbol{\xi})\tilde{e}_j(\boldsymbol{\xi})\,\mathrm{d}\xi.$$

In this way, the integrals of the basis function products can be precomputed and stored. Thus, the mass matrix for each adapted mesh can be computed by a multiplication with the determinant of the rotation and scaling matrix B. The precomputed integral values are now only dependent on the reference element. The reference triangle in *amatos* is placed as in Figure 3.1 and the reference interval in *hypy1D* is $[-1,1]$. For these special reference elements basis functions are given below.

The basis functions $\tilde{e}_i, i = 1, \ldots, n$ on the reference interval, triangle respectively, are chosen such that they are a partition of one on the element. In the 1D linear case, the basis functions are straight lines with function values zero and one at node points at the element ends. For the quadratic case, each element has three nodes and the basis function values are zero at two of them and one at the other node, see Fig. 3.2.
For the reference interval $[-1,1]$ the linear basis functions are

$$\tilde{e}_1(\xi) = \frac{1}{2}\xi + \frac{1}{2},$$
$$\tilde{e}_2(\xi) = -\frac{1}{2}\xi + \frac{1}{2},$$
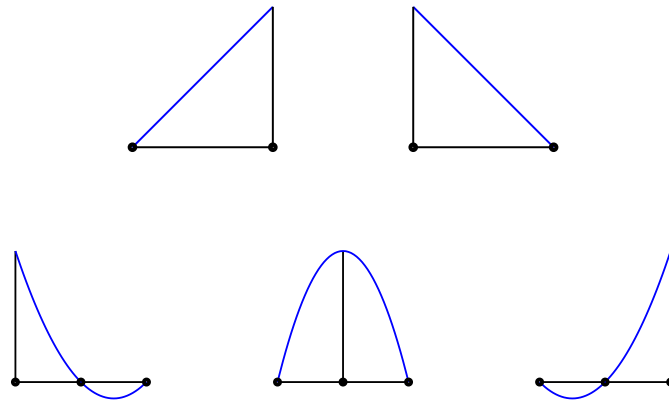
Figure 3.2: Basis functions on the reference interval: linear functions (top), quadratic functions (bottom)
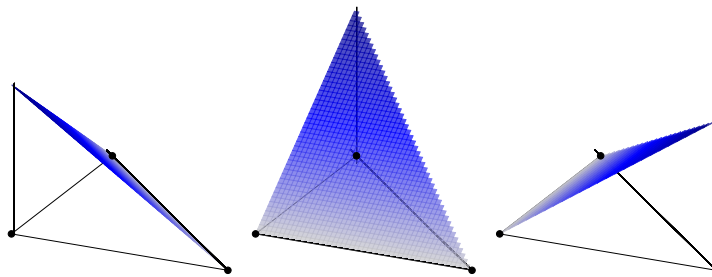
Figure 3.3: Linear basis functions on the reference triangle

and quadratic basis functions on $[-1, 1]$ are

$$\tilde{e}_1(\xi) = \frac{1}{2}\xi^2 - \frac{1}{2}\xi,$$
$$\tilde{e}_2(\xi) = -\xi^2 + 1,$$
$$\tilde{e}_3(\xi) = \frac{1}{2}\xi^2 + \frac{1}{2}\xi.$$

In 2D, linear basis functions have more degrees of freedom than the linear functions in 1D. Therefore three nodes per element are necessary to determine a linear function uniquely, see Fig. 3.3. For the reference triangle shown in Fig. 3.1 the linear basis functions are
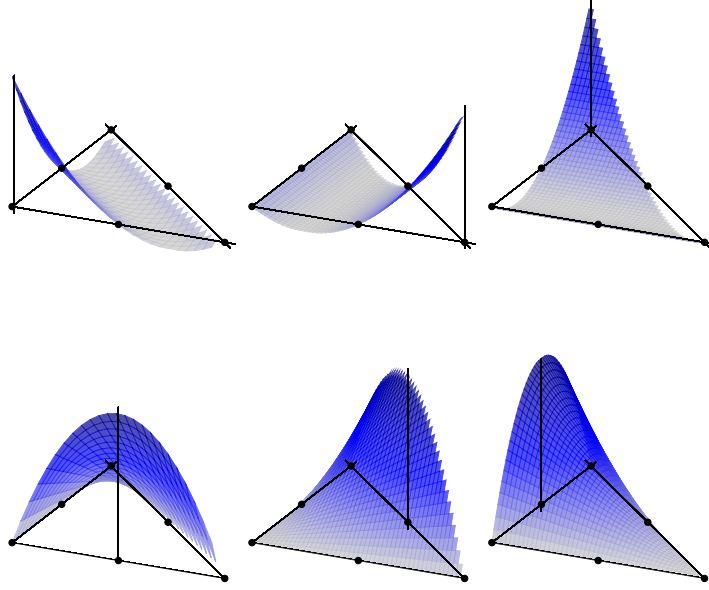
Figure 3.4: Quadratic basis functions on the reference triangle

$$\tilde{e}_1(\xi, \eta) = -\frac{1}{2}\xi - \frac{1}{2}\eta,$$

$$\tilde{e}_2(\xi, \eta) = \frac{1}{2}\eta + \frac{1}{2},$$

$$\tilde{e}_3(\xi, \eta) = \frac{1}{2}\xi + \frac{1}{2}.$$

For the same reference triangle quadratric basis functions are

$$\tilde{e}_1(\xi, \eta) = \frac{1}{2}\xi^2 + \xi\eta + \frac{1}{2}\eta^2 + \frac{1}{2}\xi + \frac{1}{2}\eta,$$

$$\tilde{e}_2(\xi, \eta) = \frac{1}{2}\xi^2 + \frac{1}{2}\xi,$$

$$\tilde{e}_3(\xi, \eta) = \frac{1}{2}\eta^2 + \frac{1}{2}\eta,$$

$$\tilde{e}_4(\xi, \eta) = -\xi^2 - \xi\eta - \xi - \eta,$$

$$\tilde{e}_5(\xi, \eta) = \xi\eta + \xi + \eta + 1,$$

$$\tilde{e}_6(\xi, \eta) = -\xi\eta - \eta^2 - \xi - \eta,$$

which were determined by function values on six nodes: Five of them have zero value and one has the function value one. Fig. 3.4 shows the quadratic basis functions $\tilde{e}_i, i = 1, 2, 3$ in the first row and $\tilde{e}_i, i = 4, 5, 6$ in the second row.

The system matrix A in the linear equation system, equation (3.1.6), might contain boundary integrals due to partial integration for the weak formulation or just to include

boundary conditions. For finite elements the solution is assumed to be continuous over element edges, i.e., the left and right boundary value on an inner edge cancels- it is never considered at all, respectively.

Ignoring the idea of continuity over the edges, as done in discontinuous Galerkin methods, results in more degrees of freedom and a better parallelizability. For a global understanding of the basis functions defined on the reference triangle the functions are extended by zero outside of their respective element.

3.1.3 Discontinuous Galerkin method

First to introduce a discontinuous Galerkin (DG) method were Reed and Hill, [RH73], discretizing the neutron transport equation

$$\bar{c}u + \mathrm{div}(\mathbf{c}u) = f, \tag{3.1.8}$$

$\bar{c} \in \mathbb{R}$ and $\mathbf{c} \in \mathbb{R}^2$. While keeping the advantages of the finite element methods (FEM), e.g. the handling of complicate geometries and formal high order approximations, DG methods for linear equations are also better suited for parallelizing and adaption of the grid and for capturing discontinuities and steep gradients without spurious oscillations, [Coc99]. In combination with Runge-Kutta methods, [Kut01] [But87], for time discretization, Runge-Kutta discontinuous Galerkin (RKDG) methods are often used to discretize nonlinear hyperbolic equations, such as the shallow water equations (SWE), the Euler equations, and the compressible Navier-Stokes equations.

As for finite elements, a weak form has to be derived on each element, introducing element boundary integrals. Since the solution is not continuous over element edges, as in the FEM case, each edge has values with respect to its left element and values with respect to its right element. A unification of these values is done by a so called numerical flux.

Let $\mathbf{F} : \mathbb{R} \to \mathbb{R}^n$ be the linear flux operator of which the weak form of the divergence shall be computed on each element E. And $\mathbf{F}^* : \mathbb{R} \to \mathbb{R}^n$ serves as approximation of $\mathbf{F}$ on the boundaries.

For an evolution equation of the form

$$\partial_t u + \mathrm{div}\left(\mathbf{F}(u)\right) = S(u) \quad \text{on } \Omega \times (0,T)$$

with source term $S : W \to \mathbb{R}$ the DG discretization is achieved by multiplication with any test function of a suitable test function space, $\psi \in V$, and two times integration by parts. For all $E \in \mathcal{E}$ holds the strong form of the differential equation,

$$\int_E \partial_t u\psi + \mathrm{div}\left(\mathbf{F}(u)\right)\psi - S(u)\psi \, \mathrm{d}\mathbf{x} = \int_{\partial E} \left(\mathbf{F}^*(u) - \mathbf{F}(u)\right) \cdot \mathbf{n}\psi \, \mathrm{d}s. \tag{3.1.9}$$

The normal $\mathbf{n}$ is depending on the considered edge and points always outwards of element E.

For a linear advection equation the flux term is a simple multiplication with the advection velocity, $v \in \mathbb{R}$ or $\mathbf{v} \in \mathbb{R}^2$, respectively. For a constant velocity field the up wind scheme delivers an exact element boundary value for the approximation $\mathbf{F}^*(u)$ on ∂E, with $u_{E_{\mathrm{up}}}$ the function value of the upwind element, i.e. E or neighbor E', on the common edge ∂E.

$$\int\limits_E \partial_t u\psi + \mathrm{div}(\mathbf{v}u)\psi \, \mathrm{d}\mathbf{x} = \int\limits_{\partial E} \left(u_{E_{\mathrm{up}}} - u\right) \mathbf{v} \cdot \mathbf{n}\psi \, \mathrm{d}s.$$

For discretization, $u \in W$ is approximated by $u^h \in W^h$ and $\psi \in V$ by $\psi^h \in V^h$, see the representation in equation (3.1.4). The discretization of the time derivative can be done for instance by Runge-Kutta schemes. Further details of the full discretization are given in section 5.2.4.

Linear advection-diffusion with advection velocity $\mathbf{v} \in \mathbb{R}^2$ and constant diffusion coefficient $\varepsilon \in \mathbb{R}^+$ is modeled by

$$\mathbf{F}(u) = \mathbf{v}u - \varepsilon\nabla u.$$

Using the general equation (3.1.9) for the advection-diffusion flux yields

$$\int\limits_E \partial_t u\psi + \mathrm{div}(\mathbf{v}u - \varepsilon\nabla u)\psi \, \mathrm{d}\mathbf{x} = \int\limits_{\partial E} (\mathbf{F}^*(u) - \mathbf{v}u + \varepsilon\nabla u) \cdot \mathbf{n}\psi \, \mathrm{d}s. \qquad (3.1.10)$$

The approximation of the element boundary values for advection-diffusion is not as straight forward as for advection. The advection part on the boundary can still be approximated by the upwind scheme, but the diffusion part needs some extra stabilization terms. [Riv08] suggests the numerical flux to be

$$\mathbf{F}^*(u) = -\{\varepsilon\nabla u\} + b[u] + \mathbf{v} \cdot \mathbf{n}u_{E_{\mathrm{up}}}. \qquad (3.1.11)$$

where $\{\nabla u\} = \frac{1}{2}\left(\nabla u_E + \nabla u_{E'}\right)$ is the average gradient of u on ∂E with respect to E and E' and $[u] = (u_E - u_{E'})$ is the jump between the function values of E and E' on ∂E. The last term in (3.1.11) is again the upwind term of u, depending on the direction of $\mathbf{v}$.

The coefficient $b \geq p^2/h$ regulates the penalization of jumps between the elements and provides stability of the algorithm, [FŠ04]. Here p is the polynomial degree and h the maximal edge length.

With a further stabilization term with coefficient $\tilde{c}$, which is in general chosen to be minus one or one to penalize kinks between the elements, and a forcing to satisfy the domain boundary conditions, the edge evaluation of equation (3.1.10) for all edges is

$$\sum_{E \in \mathcal{E}} \int\limits_{\partial E} (\mathbf{F}^*(u) - \mathbf{v}u + \varepsilon\nabla u) \cdot \mathbf{n}\psi \, \mathrm{d}s$$

$$= \sum_{e \in \partial\mathcal{E}} \int\limits_e \left(-\{\varepsilon\nabla u \cdot \mathbf{n}\}_e + b[u]_e + \mathbf{v} \cdot \mathbf{n}u_{E_{\mathrm{up}}}\right) [\psi]_e - \tilde{c}\{\varepsilon\nabla\psi \cdot \mathbf{n}\}_e[u]_e$$

$$- [(\mathbf{v}u - \varepsilon\nabla u) \cdot \mathbf{n}\psi]_e \, \mathrm{d}s + [(b\psi + \varepsilon\nabla\psi \cdot \mathbf{n})\, u_{\partial\Omega}]_{\partial\Omega}. \qquad (3.1.12)$$

$\partial\mathcal{E}$ is the collection of all edges of the element set $\mathcal{E}$.

The given Dirichlet boundary conditions on the domain boundary are denoted as $u(\mathbf{x},t) = u_{\partial\Omega}(t)$ for all $(\mathbf{x},t) \in \partial\Omega \times (0,T)$. For vanishing viscosity and thus the pure advection problem, boundary conditions would over-determine the problem. For the numerical computations in this thesis, domain boundary values were set to zero. This is reasonable because the computational domain was chosen large enough for the advection solution not to reach the boundaries in finite time T and the solution of the diffusion equation is quickly decreasing to zero at the boundaries, such that it is assumed, that the actual values of the boundary conditions are below the range of computational accuracy. Substituting the numerical flux from (3.1.12) into the advection-diffusion equation (3.1.10) yields an equation which is ready to be discretized by replacement of u and ψ with their spatial approximations u^h and ψ^h.

$$
\sum_{E\in\mathcal{E}} \int_E \partial_t u^h \psi + \mathrm{div}(\mathbf{v}u^h - \varepsilon\nabla u^h)\psi^h \; \mathrm{d}\mathbf{x}
$$
$$
= \sum_{e\in\partial\mathcal{E}} \int_e \left(-\{\varepsilon\nabla u^h \cdot \mathbf{n}\}_e + b[u^h]_e + \mathbf{v}\cdot\mathbf{n}u_{E_{\mathrm{up}}}^h \right) [\psi^h]_e - \tilde{c}\{\varepsilon\nabla\psi^h\cdot\mathbf{n}\}_e[u^h]_e
$$
$$
- [\left(\mathbf{v}u^h - \varepsilon\nabla u^h\right)\cdot\mathbf{n}]_e[\psi^h]_e \; \mathrm{d}s + \left[\left(b\psi^h + \varepsilon\nabla\psi^h\cdot\mathbf{n}\right)u_{\partial\Omega}^h\right]_{\partial\Omega}. \qquad (3.1.13)
$$

The test and basis functions were previously only defined elementwise, but as they are used globally in this notation each function is extended to the whole domain by zero.

Unlike in [Riv08] the equation here is given in its strong from, such that the actual Laplacian of u is evaluated inside the elements and not the gradient of u times the gradient of the test function. This is also the reason, why the boundary terms in (3.1.10) do not only contain the numerical flux $\mathbf{F}^*$ but also evaluations of the flux (3.1.11) using the limiting values from within the element. More details of the full discretization can be found in section 5.2.4.

With a given grid and an approximation $u^h \in W^h$ of the solution, which can be represented as linear combination of polynomials with elementwise support, the task is to improve the grid such that the approximation is 'close' to the actual solution. The distance of the approximation to the solution is measured in error norms. These norms can be evaluated on each single element, including element boundary errors, and thereby give a local error. However, since the analytic solution is not known in general, the error can only be estimated.

3.2 Error estimation

In general, error estimators are classified into two groups: *a priori* error estimators, estimating the error without knowledge of the actual numeric solution, and *a posteriori* error estimators, for which the computation is based on the numeric solution to assess the accuracy. Since the goal oriented error estimator used and extended in this thesis

is of *a posteriori* type, this section gives a small introduction to the general idea of *a posteriori* error estimation.

Pioneering work in the area of *a posteriori* error estimation for finite elements was done by Babuška and Rheinboldt, [BR78a]. Thenceforward, local error estimators, η_E, for each element E were developed which approximated the error in the energy norm. This was the basis of adaptive meshing, and interest in controlling and minimizing error caused by discretization arose. Babuška and Rheinbold did more work on this topic, e.g. [BR78b] and [BR81].

In 1984 and 1985 Demkowitcz *et al.*, [DOS84], [DOS85], and Bank and Weiser, [BW85], presented the element residual method, which is applicable for h and p refinement. Further extensive studies were done, e.g. by Oden *et al.* [ODRW89].

An important paper on explicit error residual methods by Baranger and El-Amri [BEA91] covers error estimation for a broad class of boundary value problems, including nonlinear problems.

Most of the error estimation theory was done for elliptic problems until Eriksson and Johnson, [EJ87], [EJ91], [EJ95] progressed in the error estimation for parabolic and hyperbolic problems.

The work done was mostly focus on global bounds in energy norms. In the end of the 20th century the focus shifted to the theory extension of local error estimates and especially local error estimates in a quantity of interest. The idea that local error can be influenced by errors far outside the direct vicinity was considered and the interest in goal oriented error estimation increased. One realization of a goal oriented error estimation is the dual weighted residual method, which is further discussed in section 4.

An error estimator should be *reliable* and *efficient*. This means, that the error estimator is always larger than the true error and in this way *reliable*. But the estimator should also not over estimate the error too much such that the effort to decrease the estimated error by grid refinement is in fact the effort needed to decrease the true error down to a specified tolerance and not much more, being *efficient*.

3.2.1   Explicit residual based error estimator for an elliptic example

This section gives a rough understanding in the functionality of a residual based error estimator for an elliptic equation, compare [AO97]. This shall give an idea, how local error estimates can be obtained by residuals, but shall also raise the awareness that this kind of estimator is unfit to deal with influences from more remote elements to the element error; influences caused for instance by singularities, which might arise in hyperbolic problems.

Let $\tilde{a}(\cdot, \cdot)$ be an elliptic, coercive bilinear form on $H^1(\Omega) \times H^1(\Omega)$, for example

$$\tilde{a}\left(\tilde{u}, \tilde{\psi}\right) := -\int_\Omega \tilde{u}\mathbf{v} \cdot \nabla\tilde{\psi} - \varepsilon\nabla\tilde{u} \cdot \nabla\tilde{\psi} \,\mathrm{d}\mathbf{x} + \int_{\partial\Omega} \mathbf{v} \cdot \mathbf{n}\tilde{u}\tilde{\psi} - \varepsilon\left(\mathbf{n} \cdot \nabla\tilde{u}\right)\tilde{\psi} \,\mathrm{d}s, \qquad (3.2.1)$$

which is the operator for the above advection-diffusion equation (2.3.1), without the time dependence and the time derivative. The now only space dependent functions $\tilde{u}, \tilde{\psi} \in H^1(\Omega)$ shall satisfy

$$\tilde{a}\left(\tilde{u}, \tilde{\psi}\right) = B\left(\tilde{\psi}\right) \quad \forall\tilde{\psi} \in H^1(\Omega) \qquad (3.2.2)$$

with the right hand side given as

$$B\left(\tilde{\psi}\right) := \int_\Omega f\tilde{\psi} \,\mathrm{d}\mathbf{x} \qquad (3.2.3)$$

Evaluating the bilinear operator $\tilde{a}$ at the spatial discretization error $e^h := \tilde{u} - \tilde{u}^h$ gives

$$\tilde{a}\left(e^h, \tilde{\psi}\right) = \tilde{a}\left(\tilde{u}, \tilde{\psi}\right) - \tilde{a}\left(\tilde{u}^h, \tilde{\psi}\right)$$
$$= \tilde{B}\left(\tilde{\psi}\right) - \tilde{a}\left(\tilde{u}^h, \tilde{\psi}\right).$$

From definitions (3.2.1) and (3.2.3) follows that,

$$\tilde{a}\left(e^h, \tilde{\psi}\right) = \int_\Omega f\tilde{\psi} + \tilde{u}^h\mathbf{v} \cdot \nabla\tilde{\psi} - \varepsilon\nabla\tilde{u}^h \cdot \nabla\tilde{\psi} \,\mathrm{d}\mathbf{x}$$
$$- \int_{\partial\Omega} \mathbf{v} \cdot \mathbf{n}\tilde{u}^h\tilde{\psi} - \varepsilon(\mathbf{n} \cdot \nabla\tilde{u}^h)\tilde{\psi} \,\mathrm{d}s.$$

Splitting the integrals into elementwise contributions yields

$$\tilde{a}\left(e^h, \tilde{\psi}\right) = \sum_{E\in\mathcal{E}} \int_E f\tilde{\psi} + \tilde{u}^h\mathbf{v} \cdot \nabla\tilde{\psi} - \varepsilon\nabla\tilde{u}^h \cdot \nabla\tilde{\psi} \,\mathrm{d}\mathbf{x}$$
$$- \int_{\partial E\cap\partial\Omega} \mathbf{v} \cdot \mathbf{n}\tilde{u}^h\tilde{\psi} - \varepsilon(\mathbf{n} \cdot \nabla\tilde{u}^h)\tilde{\psi} \,\mathrm{d}s.$$

Integration by parts and rearranging leads to a formulation in terms of element residual $\tilde{r} = f - \mathbf{v} \cdot \nabla\tilde{u}^h + \varepsilon\Delta\tilde{u}^h$ and boundary residual $\tilde{R}|_{\partial\Omega} = \mathbf{v} \cdot \mathbf{n}\left(\tilde{u}^h - \tilde{u}\right) - \varepsilon\mathbf{n} \cdot \nabla\left(\tilde{u}^h - \tilde{u}\right)$,

$$\tilde{a}\left(e^h, \tilde{\psi}\right) = \sum_{E\in\mathcal{E}} \int_E \tilde{r}\tilde{\psi} \,\mathrm{d}\mathbf{x} + \int_{\partial E\cap\partial\Omega} \tilde{R}\tilde{\psi} \,\mathrm{d}s + \int_{\partial E\setminus\partial\Omega} \mathbf{v} \cdot \mathbf{n}\left(\tilde{u}^h\tilde{\psi}\right) - \varepsilon\mathbf{n} \cdot \nabla\left(\tilde{u}^h\tilde{\psi}\right) \,\mathrm{d}s.$$

$$(3.2.4)$$

For continuous Galerkin methods test functions are continuous on element boundaries. Therefore, for neighboring elements E and E', sharing edge e, holds $\tilde{\psi}_E|_e = \tilde{\psi}_{E'}|_e$. With smoothness of data and regularity of the approximation $\tilde{u}^h$ in the interior of every element the interior edges in (3.2.4) can be reorganized such that each edge evaluation has to be computed only once,

$$\sum_{E \in \mathcal{E}} \int_{\partial E \backslash \partial \Omega} \mathbf{v} \cdot \mathbf{n} \left(\tilde{u}^h \tilde{\psi} \right) - \varepsilon \mathbf{n} \cdot \nabla \left(\tilde{u}^h \tilde{\psi} \right) \, \mathrm{d}s = \sum_{e \in \partial \mathcal{E}} \int_e \left[\mathbf{v} \cdot \mathbf{n} \left(\tilde{u}^h \right) - \varepsilon \mathbf{n} \cdot \nabla \left(\tilde{u}^h \right) \right] \tilde{\psi} \, \mathrm{d}s.$$

(3.2.5)

Here, $[\cdot]$ is the jump between the evaluation of the left and right element on one edge. In case of discontinuous Galerkin methods, the expression in (3.2.5) becomes more complicated by an additional jump term for the test functions.

Augmenting $\tilde{R}$ to the interior edges as $\tilde{R}|_{\partial \mathcal{E} \backslash \partial \Omega} := \left[\mathbf{v} \cdot \mathbf{n} \left(\tilde{u}^h \right) - \varepsilon \mathbf{n} \cdot \nabla \left(\tilde{u}^h \right) \right]$ yields

$$\tilde{a} \left(e^h, \tilde{\psi} \right) = \sum_{E \in \mathcal{E}} \int_E \tilde{r} \tilde{\psi} \, \mathrm{d}\mathbf{x} + \sum_{e \in \partial \mathcal{E}} \int_e \tilde{R} \tilde{\psi} \, \mathrm{d}s.$$

(3.2.6)

Galerkin orthogonality, $\tilde{a} \left(e^h, \tilde{\psi}^h \right) = 0$, permits the extension

$$\tilde{a} \left(e^h, \tilde{\psi} \right) = \tilde{a} \left(e^h, \tilde{\psi} - I^h \tilde{\psi} \right),$$

(3.2.7)

with $I^h \tilde{\psi} \in V^h$ an approximation to $\tilde{\psi} \in H^1(\Omega)$, in the sense of V^h being the space of continuous piecewise polynomials on Ω.

Application of the Cauchy-Schwarz inequality to (3.2.6) in combination with (3.2.7) gives

$$\tilde{a} \left(e^h, \tilde{\psi} \right) \leq \sum_{E \in \mathcal{E}} \|\tilde{r}\|_{L^2(E)} \|\tilde{\psi} - I^h \tilde{\psi}\|_{L^2(E)} + \sum_{e \in \partial \mathcal{E}} \|\tilde{R}\|_{L^2(e)} \|\tilde{\psi} - I^h \tilde{\psi}\|_{L^2(e)}.$$

For a local quasi uniform mesh $\mathcal{E}$, the approximation errors of the test functions can be approximated in the H^1 norm on the subdomain $N_{\mathcal{E}_h}(E)$, consisting of all elements which share an edge with element E, see [AO97, Theorem 1.1.],

$$\|\tilde{\psi} - I^h \tilde{\psi}\|_{L^2(E)} \leq c_1 h_E \|\tilde{\psi}\|_{H^1(N_{\mathcal{E}_h}(E))},$$

(3.2.8)

$$\|\tilde{\psi} - I^h \tilde{\psi}\|_{L^2(\partial E)} \leq c_2 h_E^{\frac{1}{2}} \|\tilde{\psi}\|_{H^1(N_{\mathcal{E}_h}(E))}.$$

(3.2.9)

Reusing the Cauchy-Schwarz inequality and shape regularity yield

$$\tilde{a} \left(e^h, \tilde{\psi} \right) \leq c_2 \|\tilde{\psi}\|_{H^1(\Omega)} \left(\sum_{E \in \mathcal{E}} h_E^2 \|\tilde{r}\|_{L^2(E)}^2 + \sum_{e \in \partial \mathcal{E}} h_E \|\tilde{R}\|_{L^2(e)}^2 \right)^{\frac{1}{2}}$$

As assumed above, $\tilde{a}$ is coercive, meaning $\forall \tilde{u} \in H^1(\Omega) : \tilde{a}(\tilde{u}, \tilde{u}) \geq c_3 \|\tilde{u}\|_{H^1(\Omega)}^2$, and thus

$$c_3 \|e^h\|_{H^1(\Omega)}^2 \leq \tilde{a} \left(e^h, e^h \right) \leq c_2 \|e^h\|_{H^1(\Omega)} \left(\sum_{E \in \mathcal{E}} h_E^2 \|\tilde{r}\|_{L^2(E)}^2 + \sum_{e \in \partial \mathcal{E}} h_E \|\tilde{R}\|_{L^2(e)}^2 \right)^{\frac{1}{2}}$$

Rearrangement of the above inequality yields

$$\|e^h\|^2_{H^1(\Omega)} \leq c_4 \sum_{E \in \mathcal{E}} \left(h_E^2 \|\tilde{r}\|^2_{L^2(E)} + h_E \|\tilde{R}\|^2_{L^2(\partial E)} \right).$$

In this way an elementwise error estimator can be defined as

$$\eta_E^2 := h_E^2 \|\tilde{r}\|^2_{L^2(E)} + h_E \|\tilde{R}\|^2_{L^2(\partial E)}$$

and the global error can be estimated as

$$\|e^h\|^2_{H^1(\Omega)} \leq c_4 \sum_{E \in \mathcal{E}} \eta_E^2.$$

With this definition of a local error estimator, the elements contributing most to the estimated error can be identified and refined. As mentioned in the beginning of this subsection, this is an example of a residual based error estimator which is not suited for hyperbolic problems. In (3.2.5) and for the coercivity, regularity of $\tilde{u}^h$ is needed in the sense that $\tilde{u} \in H^1(\Omega)$. If the solution is only $\tilde{u} \in L^\infty(\Omega)$, or even worse, $\tilde{u}$ contains a singularity, the above theory would not suffice.

The error estimation for hyperbolic equations covers the idea of an area of influence to the elements of interest and is depending on a dual solution. The next subsection gives an example for an error estimator for a hyperbolic equation.

3.2.2 Error estimators for hyperbolic equations

In [SH03] Süli and Huston present *a posteriori* error estimators for first order hyperbolic problems. Similar to their presented simple residual based error estimator, in this section an residual based error estimator is derived for the linear advection equation. Based on the weak form of the advection equation (2.2.3), a bilinear form a can be defined as

$$a(u, \psi) := \int\limits_0^T \int\limits_\Omega u \partial_t \psi + u \mathbf{v} \cdot \nabla \psi \, \mathrm{d}\mathbf{x} \, \mathrm{dt} + \int\limits_\Omega \left(u(\mathbf{x}, 0) - u_{\text{ini}}(\mathbf{x}) \right) \psi(\mathbf{x}, 0) \, \mathrm{d}\mathbf{x},$$

and the weak problem is to find $u \in L^\infty\left(\Omega; L^2(0, T)\right)$ such that

$$a(u, \psi) = \int\limits_0^T \int\limits_\Omega f \psi \, \mathrm{d}\mathbf{x} \, \mathrm{dt} \qquad \forall \psi \in C_{\mathrm{c}}^1\left(\Omega \times (0, T)\right).$$

Here all functions are not only depending on space but also on time.
Since a is bilinear in this example, the adjoint equation is

$$a(\phi, z) = J(\phi) \qquad \forall \phi \in L^\infty\left(\Omega; L^2(0, T)\right),$$

where J is a bounded linear functional of interest, for instance a weighted mean value over the domain Ω, and is chosen such that $z \in C_{\mathrm{c}}^1\left(\Omega \times (0, T)\right)$.

After computing the space and time discrete solution u^{hk} the goal functional can be evaluated. But $J\left(u^{hk}\right)$ is only an approximation to $J(u)$. To refine the mesh with respect to the error in the functional of interest, one likes to know the error in the functional of interest and the local contributions to it.

Using the adjoint equation and the linearity of a in its first component, it is straight forward

$$
\begin{aligned}
J(u) - J\left(u^{hk}\right) &= J\left(u - u^{hk}\right) \\
&= a\left(u - u^{hk}, z\right) \\
&= a\left(u - u^{hk}, z - z^{hk}\right) \\
&= a\left(u, z - z^{hk}\right) - a\left(u^{hk}, z - z^{hk}\right) \\
&= \left(f, z - z^{hk}\right)_\Omega - a\left(u^{hk}, z - z^{hk}\right)
\end{aligned}
$$

Now, with the definition of a

$$
\begin{aligned}
J(u) - J\left(u^{hk}\right) &= \left(f, z - z^{hk}\right)_\Omega - a\left(u^{hk}, z - z^{hk}\right) \\
&= \int_0^T \int_\Omega f\left(z - z^{hk}\right) - u^{hk}\partial_t\left(z - z^{hk}\right) - u^{hk}\mathbf{v}\cdot\nabla\left(z - z^{hk}\right)\ \mathrm{d}\mathbf{x}\,\mathrm{dt} \\
&\quad - \int_\Omega \left(u^{hk}(\mathbf{x}, 0) - u_{\mathrm{ini}}(\mathbf{x})\right)\left(z - z^{hk}\right)(\mathbf{x}, 0)\ \mathrm{d}\mathbf{x}.
\end{aligned}
$$

Analogue to the estimator for elliptic equations, the integrals are split and integrated by parts. Since $z - h^{hk}$ has to be assumed to be in $C_c^1\left(\Omega \times (0, T)\right)$, compare the function space of test functions for the advection equation, no boundary integrals on $\partial\Omega$ appear. The error in the functional of interest is thus

$$
\begin{aligned}
J(u) - J\left(u^{hk}\right) &= \sum_{j=0}^N \sum_{E\in\mathcal{E}} \left(\int_{t_j}^{t_{j+1}} \int_E r\left(z - z^{hk}\right)\ \mathrm{d}\mathbf{x}\,\mathrm{dt} - \int_E u^{hk}\left(z - z^{hk}\right)\Big|_{t_j}^{t_{j+1}}\ \mathrm{d}\mathbf{x} \right) \\
&\quad - \sum_{j=0}^N \sum_{E\in\mathcal{E}} \int_{t_j}^{t_{j+1}} \int_{\partial E} R\left(z - z^{hk}\right)\ \mathrm{ds}\,\mathrm{dt} - \sum_{E\in\mathcal{E}} \int_E \left(u^{hk} - u_{\mathrm{ini}}\right)\left(z - z^{hk}\right)\Big|_{t=0}\ \mathrm{d}\mathbf{x},
\end{aligned}
$$

$$(3.2.10)$$

with the element residual $r = f - \partial_t u^{hk} + \nabla\cdot\mathbf{v}$ and edge residual $R = (\mathbf{v}\cdot\mathbf{n})u^{hk}$.

Sorted as above, each time-space element can be connected to a local error estimator for $j = 0, \ldots, N$:

$$
\hat{\eta}_{j,E} := \int_{t_j}^{t_{j+1}} \int_E r\left(z - z^{hk}\right)\ \mathrm{d}\mathbf{x}\,\mathrm{dt} - \int_{t_j}^{t_{j+1}} \int_{\partial E} R\left(z - z^{hk}\right)\ \mathrm{ds}\,\mathrm{dt} - \int_E u^{hk}\left(z - z^{hk}\right)\ \mathrm{d}\mathbf{x}\Big|_{t_j}^{t_{j+1}}.
$$

The last integral evaluated at times t_{j+1} and t_j is a telescoping time sum for continuous time discretization and cancels apart from its first and last entry. For zeroth order discretization, as for instance the explicit Euler method, the solution is piecewise constant in time and has jumps in t_j, t_{j+1} respectively, and therefore does not cancel out.
With local error contributions as

$$
\begin{aligned}
\eta_{0,E} &:= \hat{\eta}_{0,E} - \int_E \left(u^{hk} - u_{\mathrm{ini}} \right) \left(z - z^{hk} \right) \Big|_{t=0} \, \mathrm{d}\mathbf{x} \\
\eta_{j,E} &:= \hat{\eta}_{j,E}, \qquad j = 1, \ldots, N
\end{aligned}
$$

the global error in the functional of interest is

$$
J(u) - J\left(u^{hk} \right) = \sum_{j=0}^{N} \sum_{E \in \mathcal{E}} \eta_{j,E}. \tag{3.2.11}
$$

The exact discretization errors of the dual solution, $z - z^{hk}$, can normally not be computed, since the analytic solution is unknown. To circumvent this problem, the discretization errors can be approximated similar to (3.2.8) or by computations with higher order solutions, as later done in section 5.2.4.

This thesis focuses on spatial adaptivity and does not handle time step control, the local errors in (3.2.12) are summed over time,

$$
\eta_E := \sum_{j=0}^{N} \eta_{j,E}.
$$

Together with the approximation of the dual discretization error the global error estimator is now

$$
J(u) - J\left(u^{hk} \right) \approx \eta_{\mathcal{E}} := \sum_{E \in \mathcal{E}} \eta_E. \tag{3.2.12}
$$

In this context, the bilinear form a does not have to be coercive but the dual solution must at least be $z \in C_c^1 \left(\Omega \times (0, T) \right)$. Here this regularity condition is only on the dual solution. However, this error estimator is based on the assumption that a is a bilinear form. The general estimation of errors in a quantity of interest for also nonlinear problems is discussed in section 4.

3.3 Marking strategies

Based on an elementwise error estimator elements for refinement have to be chosen. In [BR03] several strategies are given, as for example the error balancing strategy. For the balancing, the mesh has to be adapted until each element contributes the same share

to the error and the sum of local estimators is in the order of the desired tolerance, TOL. This means for the local error estimator η_{E_i} on element E_i

$$\eta_{E_i} \approx \frac{\text{TOL}}{\#E}, \tag{3.3.1}$$

for a total number of $\#E$ elements. Though this method would return an potentially optimal mesh, it is rather impracticable since each refinement or coarsening of a single triangle changes $^{\text{TOL}}/_{\#E}$ and (3.3.1) is not satisfied for the other elements anymore. The other elements have to be refined/coarsened and change $^{\text{TOL}}/_{\#E}$ in turn.

Dörfler marking, [Dö96], marks elements such that the estimated error of this set is larger than a specific percentage of the estimated error for the whole triangulation.

Let $\mathcal{E}_{\text{ref}}$ be the set of marked elements in the triangulation $\mathcal{E}$ such that

$$\eta_{\mathcal{E}_{\text{ref}}} \geq (1 - \Theta)\, \eta_{\mathcal{E}}.$$

For $\Theta = 0$ this means, that global refinement is performed, for $\Theta = 1$ no element at all has to be marked.

3.4 Refinement

After marking the elements accordingly to a marking strategy, the marked elements have to be refined. Refinement of an interval can be most easily achieved by subdividing the interval into smaller intervals. For triangles in 2D there are several different methods, how to refine the triangle, see, e.g., [Bän91].

There is the very common *red refinement*, which divides the triangle into four triangles of similar shape.
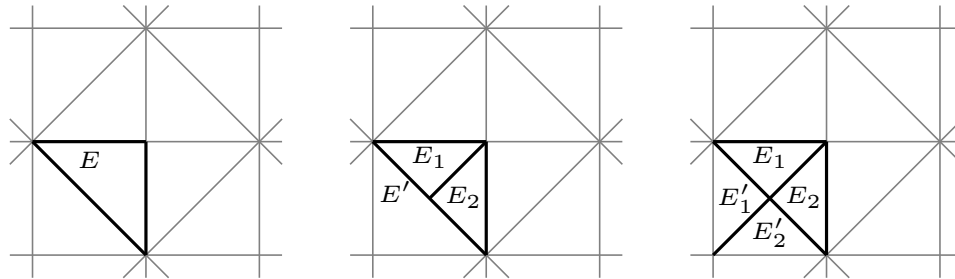
Figure 3.5: Bisection of element E into E_1 and E_2.

A simpler refinement, the *green refinement*, splits the triangles of a mesh by bisection. in this case the edge, which is to be bisected, has to be chosen. A choice to prevent the mesh from degeneration is the bisection of the longest edge. For right triangles, this is the hypotenuse. Fig. 3.5 shows the element E marked for refinement in a structured mesh of right triangles, which is supported by the mesh generator *amatos*. After the

bisection of E there would be a hanging node, unless the neighboring element E' is also bisected. But simultaneous refinement of the neighboring element results in a regular grid.

Summarizing this chapter, all necessary tools for adaptive numerical solution of hyperbolic problems are given. However, the estimator for hyperbolic equations introduced in this section is only valid for linear problems. Therefore the next chapter introduces the complete dual weighted residual method to obtain a general error estimator based on a primal and a dual residual.

Chapter 4

The dual weighted residual method

In the previous chapter error estimators were introduced which are not suitable for hyperbolic problems in general. This chapter is therefore introducing the dual weighted residual method which includes two residuals, the primal residual and the dual residual. Becker and Rannacher, [BR01], did a comprehensive study on the subject and the following introduction is along the lines of this study.

The first section is about the derivation of the DWR error estimator and the second section discusses some properties and limitations.

4.1 Derivation

As in the previous sections, a partial differential equation in its weak form is considered. Let $a(\cdot, \cdot) : W \times V \to \mathbb{R}$ be a semilinear form and $B(\cdot) : V \to \mathbb{R}$ a linear functional on V. For instance $B(\psi) = (f, \psi)_\Omega$ where $(\cdot, \cdot)_\Omega : V \times V \to \mathbb{R}$ is the L^2 inner product on Ω. Let $u \in W$ be the unique solution to

$$a(u, \psi) = B(\psi) \qquad \forall \psi \in V. \tag{4.1.1}$$

The solution shall be post-processed in the evaluation of a linear goal functional $J : W \to \mathbb{R}$. Since the analytic solution is however not given, an approximation is needed. For a Galerkin approximation u^{hk} of u in a finite dimensional subspace $W^{hk} \subset W$ the variational formulation (4.1.1) is still satisfied,

$$a(u^{hk}, \psi^{hk}) = B(\psi^{hk}) \qquad \forall \psi^{hk} \in V^{hk}, \tag{4.1.2}$$

and again it is assumed, that the solution is unique. Now, the solution u^{hk} serves to approximate the quantity $J(u)$ by $J\left(u^{hk}\right)$. The question at hand is, how big is the error in the evaluation of the goal functional, $\left| J(u) - J\left(u^{hk}\right) \right|$? To answer this question, the Lagrangian is defined as

$$L(u, \psi) := J(u) + B(\psi) - a(u, \psi) \quad \forall \psi \in V. \tag{4.1.3}$$

And the difference in the goal functional can be expressed as a difference in the Lagrangian for any $\psi \in V$ and any $\psi^{hk} \in V^{hk}$

$$
\begin{aligned}
J(u) - J\left(u^{hk}\right) &= L(u, \psi) - B(\psi) + a(u, \psi) - L\left(u^{hk}, \psi^{hk}\right) - B(\psi^{hk}) + a\left(u^{hk}, \psi^{hk}\right) \\
&= L(u, \psi) - L\left(u^{hk}, \psi^{hk}\right), \tag{4.1.4}
\end{aligned}
$$

since (4.1.1) and (4.1.2) are satisfied.

At a stationary point $(u, z) \in W \times V$, the first derivatives of the Lagrangian are zero in any direction $\phi \in W$ and $\psi \in V$,

$$
\begin{aligned}
L'(u; \phi, z) &= J'(u; \phi) - a'(u; \phi, z) \overset{!}{=} 0, \tag{4.1.5} \\
L'(u, z; \psi) &= B'(z; \psi) - a'(u, z; \psi) \overset{!}{=} 0. \tag{4.1.6}
\end{aligned}
$$

The notation of the derivatives means that the (semi-)linear forms are differentiated with respect to the function in front of the semicolon and evaluated with the function behind the semicolon. J and B are linear and a is linear in its second component. Therefore the first order optimality conditions (4.1.5) and (4.1.6) become

$$
\begin{aligned}
J(\phi) - a'(u; \phi, z) &\overset{!}{=} 0 \quad \forall \phi \in W, \tag{4.1.7} \\
B(\psi) - a(u, \psi) &\overset{!}{=} 0 \quad \forall \psi \in V. \tag{4.1.8}
\end{aligned}
$$

Obviously, equation (4.1.8) is again the original, primal problem (4.1.1). Condition (4.1.7) is called the adjoint or dual problem. If the primal and dual problem are solved on finite dimensional subspaces, primal and dual residual are

$$
\begin{aligned}
\rho\left(u^{hk}, \psi\right) &:= B(\psi) - a(u^{hk}, \psi) & \forall \psi \in V, \\
\rho^*\left(z^{hk}, \phi\right) &:= J(\phi) - a'\left(u^{hk}; \phi, z^{hk}\right) & \forall \phi \in W.
\end{aligned}
$$

For this setting proposition 2.1 in [BR01] gives a representation of the difference of the Lagrangian of the analytic solutions and the discrete ones under the assumption, L is convex.

$$
\begin{aligned}
L(u, z) - L\left(u^{hk}, z^{hk}\right) = {} &\frac{1}{2} \min_{\phi^{hk} \in W^{hk}} L'\left(u^{hk}; u - \phi^{hk}, z^{hk}\right) \\
&+ \frac{1}{2} \min_{\psi^{hk} \in V^{hk}} L'\left(u^{hk}, z^{hk}; z - \psi^{hk}\right) + R.
\end{aligned}
$$

The error in the goal functional evaluation is equal to the error in the Lagrangian, see (4.1.4), and with the computation of the Lagrangian and the definition of the residuals it is

$$
J(u) - J\left(u^{hk}\right) = \frac{1}{2} \min_{\phi^{hk} \in W^{hk}} \rho^*\left(z^{hk}, u - \phi^{hk}\right) + \frac{1}{2} \min_{\psi^{hk} \in V^{hk}} \rho\left(u^{hk}, z - \psi^{hk}\right) + R.
$$

Proposition 2.2. in [BR01] gives the remainder term in terms of the primal and dual error, $e := u - u^{hk}$ and $e^* := z - z^{hk}$,

$$
\begin{aligned}
R := \frac{1}{2} \int_0^1 & \left(J''' \left(u^{hk} + se; e, e, e \right) - a''' \left(u^{hk} + se; e, e, e, z^{hk} + se^* \right) \right. \\
& \left. -3a'' \left(u^{hk} + se; e, e, e^* \right) \right) s(s-1) \, \mathrm{ds}.
\end{aligned}
\tag{4.1.9}
$$

For bilinear a and linear J the remainder term vanishes, since the derivatives are zero.

4.2 Properties and limitations

This section shortly lists some properties of the error estimator in the quantity of interest. As mentioned in the last section, the remainder (4.1.9) vanishes if a is bilinear and J quadratic. This means especially, that the error estimator

$$
J(u) - J\left(u^{hk} \right) \approx \frac{1}{2} \min_{\phi^{hk} \in W^{hk}} \rho^* \left(z^{hk}, u - \phi^{hk} \right) + \frac{1}{2} \min_{\psi^{hk} \in V^{hk}} \rho \left(u^{hk}, z - \psi^{hk} \right)
\tag{4.2.1}
$$

is not only an estimator but an error identity. This will be of special interest in section 5.1.7. The relation between the primal and dual residual is characterized in [BR01, proposition 2.3.]. Adapted to the notation in this thesis it reads

Lemma 4 (Becker & Rannacher).

$$
\min_{\phi^{hk} \in W^{hk}} \rho^* \left(z^{hk}, u - \phi^{hk} \right) = \min_{\psi^{hk} \in V^{hk}} \rho \left(u^{hk}, z - \psi^{hk} \right) + \Delta\rho.
$$

with the difference

$$
\Delta\rho = \int_0^1 a'' \left(u^{hk} + see; e, e, z^{hk} + se^* \right) - J'' \left(u^{hk} + se; e, e \right) \, ds,
$$

and the errors $e := u - u^{hk}$ and $e^* := z - z^{hk}$.

Since the difference $\Delta\rho$ is only depending on the second derivative of the semilinear form and of the goal functional the two minima are equal in case of bilinear a and linear J.
The DWR method yields *reliable* error estimators, as long as the error caused by the numerical approximation of the dual solution is negligible. [NVV09] give an example in which the approximation error of the dual solution is not negligible and propose a safe guard method for these cases.
Furthermore, the DWR error estimator, as given in 4.2.1, is by construction *efficient*, only indicating elements which contribute to the error in the quantity of interest, see also [BR01].
But the method also does have some limitations. The derivation in the above section

needs the goal functional to be linear. Linearization of the goal functional by a Taylor series and neglecting the nonlinear terms would introduce another source of inaccuracy. Another drawback of this method is the dependence on the primal and dual analytic solution, u and z. Since these are normally unknown, the solutions are approximated by interpolations of there discrete solutions, u^{hk} and z^{hk}. How these interpolations can be done is described in section 5.2.4.

The limitation I like to stress is the eligibility of primal and dual solution to work as weights in the error estimation. To do so, the residual of the advection equation (2.2.3) is recalled: $u \in L^\infty(\Omega \times (0, \infty))$ is a (weak) solution of the advection equation, if for all $\psi \in C_c^1(\Omega \times (0, \infty))$ holds

$$\rho(u, \psi) = \int\limits_0^\infty \int\limits_\Omega u \partial_t \psi + u\mathbf{v} \cdot \nabla \psi \, \mathrm{d}\mathbf{x} \, \mathrm{dt} + \int\limits_\Omega \left(u_{\mathrm{ini}}(\mathbf{x}) - u(x, 0) \right) \psi(\mathbf{x}, 0) \, \mathrm{d}\mathbf{x} = 0. \quad (4.2.2)$$

Now, if by choice of the goal functional the dual equation has a solution $z \in L^\infty(\Omega \times (0, \infty))$, the weight $z - h^{hk}$ is in the same space. Since $L^\infty(\Omega \times (0, \infty))$ is not a true subspace of $C_c^1(\Omega \times (0, \infty))$ the weight $z - h^{hk}$ is not necessarily (weakly) differentiable and cannot be used in the place of test function ψ. A similar problem arises for the dual residual. The next chapter presents an example which exhibits the afore mentioned problem and proposes a solution.

Chapter 5

DWR and shocks

The following section about the one dimensional problem was submitted to Springer in October 2016, to be published in the journal "Numerische Mathematik". Slight changes were done to the article to fit into this thesis and to improve the flow of reading.

5.1 1D linear transport equation

5.1.1 Discontinuous test case (one dimensional)

In this section, the solutions of a 1D advection problem and a 1D advection diffusion problem with discontinuous initial data are computed analytically. Additionally, for both cases an adjoint problem with discontinuous initial data is given and the analytic solutions are determined. The four solutions, two primal and two dual, are used to compute weighted residuals which are needed for the DWR method.

It is shown, that the weighted residual for the advection equation with weight given by the adjoint solution for advection-diffusion equation, do not converge for vanishing viscosity in the adjoint problem. This shows the capriciousness of evaluating the weighted residual of the advection equation with the formal dual given by (1.2.2).

5.1.2 The pure advection equation and its dual

A simple advection problem for $x \in \mathbb{R}$ and $t \in (0, T)$ is given by

$$\partial_t u_0(x, t) + \partial_x u_0(x, t) = 0, \quad \text{in } \mathbb{R} \times (0, T), \tag{5.1.1}$$

with initial condition

$$u_0(x, 0) = u_{ini}(x) = \begin{cases} 1, & -1 \leq x \leq 0, \\ 0, & \text{else.} \end{cases} \tag{5.1.2}$$

Since the advection-diffusion equation is introduced later in this thesis, the solution of the advection equation is marked as u_0, which is compatible with zero diffusion. With

the discontinuous initial condition the problem is only reasonable in weak sense: For all $\psi \in C_c^1(\mathbb{R} \times [0, T))$, differentiable test functions with compact support in $\mathbb{R}$, it holds

$$
\begin{aligned}
a_0(u_0, \psi) := &- \int\limits_0^T \int\limits_{\mathbb{R}} u_0 \partial_t \psi + u_0 \partial_x \psi \, \mathrm{dx} \, \mathrm{dt} \\
&+ \int\limits_{\mathbb{R}} \left(u_{\mathrm{ini}}(x) - u_0(x, 0) \right) \psi(x, 0) \, \mathrm{dx} \\
&= 0.
\end{aligned}
\tag{5.1.3}
$$

The weak solution for $t \leq T$ is given by

$$
u_0(x, t) = u_{\mathrm{ini}}(x - t) = \begin{cases} 1, & -1 + t \leq x \leq t, \\ 0, & \text{else} \end{cases}
\tag{5.1.4}
$$

which is simply a translation of the initial condition along the characteristic curves. Since this problem does not include viscosity, i.e.,- $\varepsilon = 0$, the solution is denoted with subscript "0".

Choosing the goal functional as

$$
J(u_0) = \int\limits_{\mathbb{R}} u_0(x, T) z_T(x) \, \mathrm{dx},
\tag{5.1.5}
$$

with the weight z_T indicating an area of interest

$$
z_T(x) := \begin{cases} 1, & 0 \leq x \leq 1, \\ 0, & \text{else} \end{cases}
$$

gives a dual problem of the above advection equation, an advection equation backwards in time with discontinuous initial data. This dual problem of finding z_0 can be formulated in the weak sense as: For all $\psi \in C_c^1(\mathbb{R} \times (0, T]) :$

$$
\int\limits_0^T \int\limits_{\mathbb{R}} z_0 \partial_t \psi + z_0 \partial_x \psi \, \mathrm{dx} \, \mathrm{dt} - \int\limits_{\mathbb{R}} \left(z_T(x) - z_0(x, T) \right) \psi(x, T) \, \mathrm{dx} = 0,
$$

with initial condition $z_0(x, T) = z_T(x)$.
Fixing $T = 1$, the solution for $t \in (0, 1)$ is

$$
z_0(x, t) = \begin{cases} 1, & -1 + t \leq x \leq t, \\ 0, & \text{else}, \end{cases}
$$

which coincides with the primal solution.
As we have seen above, the advection equation and its adjoint provide solutions in $L^\infty(\mathbb{R}; L^2(0, 1))$. To obtain solutions in $H^1(\mathbb{R}; H^1(0, 1))$ the advection problem can be

modified with a small diffusion, as done in the vanishing viscosity method, e.g., [Eva10, pp 403]. Notice, that in [Eva10] the initial condition is in $H^1(\mathbb{R})$ and the solution therefore of higher regularity than in the case considered below. In the following, the advection-diffusion equation is initialized with the same step function as before, which is only $L^\infty(\mathbb{R})$. The solution is calculated analytically and examined regarding its regularity.

5.1.3 The advection-diffusion equation and its dual

The one dimensional advection-diffusion equation with diffusion coefficient $\varepsilon > 0$ reads

$$\partial_t u_\varepsilon(x,t) + \partial_x u_\varepsilon(x,t) - \varepsilon \partial_{xx} u_\varepsilon(x,t) = 0 \qquad (5.1.6)$$

in the domain $\mathbb{R} \times (0,1)$. Again, the following initial condition (5.1.2) is assumed. The weak solution u_ε of the advection-diffusion equation satisfies

$$
\begin{aligned}
a_\varepsilon(u_\varepsilon, \psi) = {} & -\int_0^1 \int_{\mathbb{R}} u_\varepsilon \partial_t \psi + u_\varepsilon \partial_x \psi - \varepsilon \partial_x u_\varepsilon \partial_x \psi \ \mathrm{dx} \ \mathrm{dt} \\
& + \int_{\mathbb{R}} \left(u_{\mathrm{ini}}(x) - u_0(x,0) \right) \psi(x,0) \ \mathrm{dx} \\
= {} & 0,
\end{aligned}
\qquad (5.1.7)
$$

for all sufficiently regular ψ. The known Green's function for this problem (see [XTB07, pp. 9–12]) is

$$G(x, \xi, t) = \frac{1}{\sqrt{4\pi t \varepsilon}} e^{-\frac{(x-\xi-t)^2}{4t\varepsilon}}$$

for $\xi \in \mathbb{R}$. Thus, the solution u_ε is given by

$$u_\varepsilon(x,t) = \frac{1}{\sqrt{\pi}} \int_{\frac{x-t}{2\sqrt{t\varepsilon}}}^{\frac{x+1-t}{2\sqrt{t\varepsilon}}} e^{-y^2} \ \mathrm{dy},$$

where the integral and its factor $\frac{1}{\sqrt{\pi}}$ can be expressed in terms of the error function (see [NG69, Definition 3.1.1]), providing the alternative representation

$$u_\varepsilon(x,t) = \frac{1}{2} \left(\mathrm{erf}\left(\frac{x+1-t}{2\sqrt{t\varepsilon}} \right) - \mathrm{erf}\left(\frac{x-t}{2\sqrt{t\varepsilon}} \right) \right). \qquad (5.1.8)$$

This solution corresponds to the one provided in the test case 'Advection and diffusion of a plane wave in a channel' in [CL00].

Fig. 5.1 shows the initial step function and the solution at $t = 1$ which propagates to the right. Furthermore, one can see the smoothing caused by diffusion with diffusion parameter $\varepsilon = 0.01$. Having the primal solution, the adjoint solution is to be computed next.
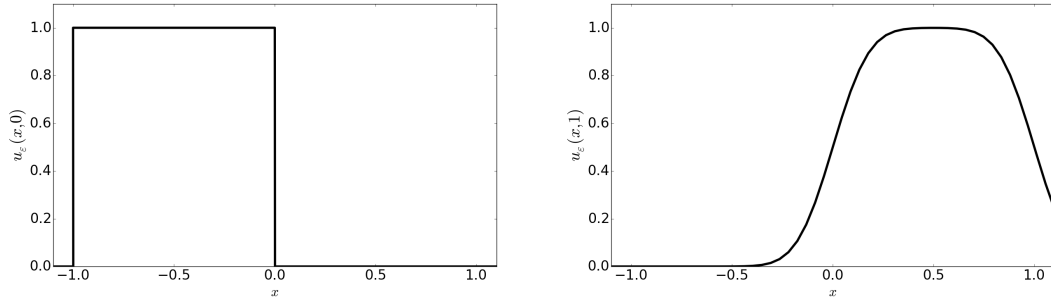
Figure 5.1: Initial condition $u_\varepsilon(x,0)$ (left) and solution $u_\varepsilon(x,1)$ (right).

The adjoint equation to the one dimensional advection-diffusion equation, with respect to the same goal functional (5.1.5) as in the advection case, is

$$-\partial_t z_\varepsilon(x,t) - \partial_x z_\varepsilon(x,t) - \varepsilon \partial_{xx} z_\varepsilon(x,t) = 0 \quad \text{in } \mathbb{R} \times (1,0) \tag{5.1.9}$$

with the initial conditions $z_\varepsilon(x,1) = z_{\mathrm{T}}(x)$. In analogy to the primal case the solution of the dual problem is given by

$$z_\varepsilon(x,t) = \frac{1}{2}\left(\mathrm{erf}\left(\frac{-x + 1 - (1-t)}{2\sqrt{(1-t)\varepsilon}} \right) - \mathrm{erf}\left(\frac{-x - (1-t)}{2\sqrt{(1-t)\varepsilon}} \right) \right), \tag{5.1.10}$$

using the transformation $(x,t) \to (-x, 1-t)$. Here the dual solution z_ε is regular enough and therefore the weak derivative necessary for the residual can be applied to z_ε.

5.1.4 Pure advection residual

Application of the DWR method to the purely advective case needs the evaluation of $a_0(\cdot, \cdot)$ at $(u_0, z_0 - z_0^{hk})$, compare equation (5.2.11), where z_0^{hk} is the solution of the time and space discretized advection equation. In the example at hand, the solution z_0 is in $L^\infty\left(\mathbb{R}; L^2(0,1)\right)$, as is $z_0 - z_0^{hk}$. To evaluate (5.2.11), time and space derivatives of $z_0 - z_0^{hk}$ have to be considered. This could be done in the distributional sense, but only if the function to which the distribution is applied to is smooth enough. This is not the case for $u_0 \in L^\infty\left(\mathbb{R}; L^2(0,1)\right)$ which does not have a weak derivative. The nonexistence of derivatives of the primal and dual solution at the same point is due to coinciding discontinuities of the solutions.

To avoid coinciding discontinuities at $t = T$, the dual initial condition would have to be modified but this can only be done by modification of the goal functional which is not in the interest of applications. Thus, for the weighted residuals in Section 5.1.5, the solution of the dual advection-diffusion equation is taken, since this solution is differentiable on $\Omega \times (0,T)$.

More general, it is necessary that one solution - primal or dual - is sufficiently smooth, the weighted residual can be computed and thus be used for error estimation in the
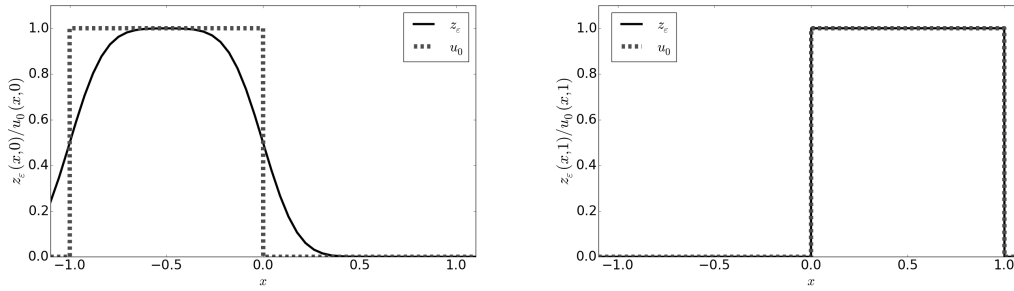
Figure 5.2: Artificial viscosity (here $\varepsilon = 0.01$) in the dual asserts that coinciding discontinuities appear only at $t = 1$ (right) and not at $t = 0$ (left).

DWR method. This suggests to force one solution to be smooth with a modification in the equation, an artificial viscosity. Since the interest lies in the primal solution it is reasonable to modify the dual equation and thus obtain a slightly different, smoother dual solution. In doing this, the question of the thereby introduced error arises. Therefore, in the next section, the DWR error estimator for a modified dual equation is determined.

5.1.5 Error estimator with correction term

In this section, an additional term in the goal oriented error estimator is identified, which is caused by a modification of the dual equation. The primal equation is considered with a source term as

$$a_0(u_0, \psi) = S(\psi) =: \int\limits_0^1 \int\limits_{\mathbb{R}} f\psi \, \mathrm{dx} \, \mathrm{dt} \quad \forall \psi \in V. \tag{5.1.11}$$

Following [BR01], the Lagrangian is set to

$$L(u_0, z_0) := J(u_0) + S(z_0) - a_0(u_0, z_0). \tag{5.1.12}$$

The formal dual problem is obtained as a stationary point of the Lagrangian, and gives the known problem

$$a_0'(u_0; \phi, z_0) = J'(u_0; \phi) \quad \forall \phi \in V. \tag{5.1.13}$$

As we have seen above, this dual problem might return a z_0 which is not in the intersection $V \cap W$, and thus z_0 might not be an admissible function in the test function space of the primal equation, (5.1.11). For this reason, we add artificial viscosity to the dual problem and the new dual equation with the smooth dual solution $z_\varepsilon \in V$ reads

$$a_\varepsilon'(u_0; \phi, z_\varepsilon) = J'(u_0; \phi) \quad \forall \phi \in V$$

and it holds $\lim\limits_{\varepsilon \to 0} \|z_\varepsilon - z_0\|_{L^2(\mathbb{R})}$, see section 2.4. With this, the difference between the value of the goal functional of the exact solution u_0 and the value of the goal functional of the numerically approximated solution u^{hk}, can be represented as the difference of the

Lagrangian of the exact solution and of the discrete one. The commonly applied test function is the -usually smooth- dual solution z_0 because it makes an additional residual vanish, compare [BR01]. But here the solution of the modified dual equation, z_ε, needs to be used. In the following, the influence of this change shall be determined. For this, the Lagrangian has to be differentiated. Let $L'_u(u_0; u_0 - u_0^{hk}, z_\varepsilon)$ be the derivative with respect to the first variable in direction of $u_0 - u_0^{hk}$, and $L'_z(u_0, z_\varepsilon; z_\varepsilon - z_\varepsilon^{hk})$ be the derivative with respect to the second variable in $z_\varepsilon - z_\varepsilon^{hk}$ direction. Thus,

$$
\begin{aligned}
J(u_0) - J(u_0^{hk}) &= L(u_0, z_\varepsilon) - L(u_0^{hk}, z_\varepsilon^{hk}) \\
&= \frac{1}{2} L'_u(u_0; u_0 - u_0^{hk}, z_\varepsilon) + \frac{1}{2} L'_u(u_0^{hk}; u_0 - u_0^{hk}, z_\varepsilon^{hk}) \\
&\quad + \frac{1}{2} L'_z(u_0, z_\varepsilon; z_\varepsilon - z_\varepsilon^{hk}) + \frac{1}{2} L'_z(u_0^{hk}, z_\varepsilon^{hk}; z_\varepsilon - z_\varepsilon^{hk}) \\
&\quad + \tilde{R},
\end{aligned}
\tag{5.1.14}
$$

where the remainder term $\tilde{R}$ is given in terms of the error $e := (u_0, z_\varepsilon) - (u_0^{hk}, z_\varepsilon^{hk})$, analogous to [BR01], as

$$
\tilde{R} = \frac{1}{2} \int_0^1 L''((u_0^{hk}, z_\varepsilon^{hk}) + se; e, e) \, \mathrm{d}s = 0.
$$

Here the remainder is zero, since the Lagrangian is linear in this example. The definition of the Lagrangian, (5.1.12), is plugged into expansion of the Lagrangian (5.1.14) and the difference in the goal functional reads

$$
\begin{aligned}
J(u_0) - J(u_0^{hk}) = \frac{1}{2} \Big[&\rho^*(z_\varepsilon^{hk}, u_0 - u_0^{hk}) + \rho(u_0^{hk}, z_\varepsilon - z_\varepsilon^{hk}) \\
&+ \rho^*(z_\varepsilon, u_0 - u_0^{hk}) + \rho(u_0, z_\varepsilon - z_\varepsilon^{hk}) \Big]
\end{aligned}
$$

with the primal and dual residuals

$$
\rho(u_0, z_\varepsilon - z_\varepsilon^{hk}) := S(z_\varepsilon - z_\varepsilon^{hk}) - a_0(u_0, z_\varepsilon - z_\varepsilon^{hk}),
\tag{5.1.15}
$$

$$
\rho^*(z_\varepsilon, u_0 - u_0^{hk}) := J'(u_0; u_0 - u_0^{hk}) - a'_0(u_0; u_0 - u_0^{hk}, z_\varepsilon).
\tag{5.1.16}
$$

Since, u_0 solves equation (5.1.11) the primal residual (5.1.15) vanishes in u_0. Normally the weighted dual residual of the analytic dual solution vanishes. But for z_ε it does not. Thus, the error in the goal functional is given as

$$
\begin{aligned}
J(u_0) - J(u_0^{hk}) = \frac{1}{2} \Big[&\rho^*(z_\varepsilon^{hk}, u_0 - u_0^{hk}) + \rho(u_0^{hk}, z_\varepsilon - z_\varepsilon^{hk}) \\
&+ \rho^*(z_\varepsilon, u_0 - u_0^{hk}) \Big].
\end{aligned}
\tag{5.1.17}
$$

In comparison to the error given in [BR01] the first two residuals now contain z_ε instead of z_0, as was expected, but an additional dual residual, $\rho^*(z_\varepsilon, u_0 - u_0^{hk})$ has to be taken into account.

Concluding, in this section it was shown that a modification in the dual equation introduces an additional dual residual. Given the goal functional of the above mentioned advection problem the error in the goal functional can be computed easily. This representation of the error in the goal functional which is due to the introduction of diffusion in the dual equation is going to be evaluated numerically in the next section.

5.1.6 Discretization schemes

Advection can develop or maintain discontinuities in the solutions, as seen in the advection example in Section 5.1.1. One approach for an accurate and efficient method to solve advection dominated problems numerically are the discontinuous Galerkin (DG) methods. These methods combined with slope limiters are able to capture the physically relevant discontinuities without producing spurious oscillations, [CKS00].
Some of the first to apply the DG method were W. Reed and T. Hill, [RH73], in 1973. DG methods are generalizations of finite volume methods but possess also properties of finite element methods, as for instance the simple handling of complex geometries and of boundary conditions. The advantage of DG lies in the discontinuities at the element boundaries and the thereby resulting simple routines for parallelization and adaptivity. These advantages, however, have to be bought by the price of a higher number of degrees of freedom than for the continuous finite element schemes.
In this section, the primal advection equation and the dual diffusion equation from the examples above shall be spatially discretized in DG manner to compute the dual weighted residual as necessary for the error estimation in the goal functional, see equation (5.1.17). Usually the weight in the residuals is approximated by a global higher order approximation, a patchwise higher order interpolation, or a cellwise interpolation estimate, [BR01], since the analytic solution is not given.
In the case at hand, the analytic solutions are known and thus an approximation is not necessary, which will be useful to demonstrate the advantage of our modified dual without considering the additional source of difficulties given by the weight approximation.
For the discretization the interval $\Omega = (a, b)$ is decomposed into a set $\mathcal{E}$ of n non-overlapping elements E of length h such that

$$\overline{\Omega} = \bigcup_{\overline{E} \in \mathcal{E}} \overline{E}.$$

For each element $E \in \mathcal{E}$ the flux in the element is defined as

$$F(u_\varepsilon)(x, t) := u_\varepsilon(x, t) - \varepsilon \partial_x u_\varepsilon(x, t), \quad (x, t) \in E \times (0, 1)$$

and thus for each E the weak form of the advection-diffusion equation, with no source

term, can be represented as

$$0 = a_\varepsilon(u_\varepsilon, \psi) = \sum_{E \in \mathcal{E}} \left\{ \int_0^1 \int_E \partial_t u_\varepsilon \psi + \partial_x F(u_\varepsilon) \psi \ \mathrm{dx} \ \mathrm{dt} + \int_E u_{ini}(x) \psi(x, 0) \ \mathrm{dx} \right\}$$

$$= \sum_{E \in \mathcal{E}} \left\{ \int_0^1 \int_E \partial_t u_\varepsilon \psi - F(u_\varepsilon) \partial_x \psi \ \mathrm{dx} \ \mathrm{dt} + \int_E u_{ini}(x) \psi(x, 0) \ \mathrm{dx} \right.$$

$$\left. + \int_0^1 F(u_\varepsilon) \psi|_{\partial E} \ \mathrm{dt} \right\}.$$

Evaluation on the boundaries of the elements E is not straightforward, since a discontinuous Galerkin method allows jumps on the boundaries and thus the function value is not unique. In the application of DG methods, it is common, compare [CKS00], to approximate the flux over the edge by a numerical flux F^*. For the computation of these boundary terms, the symmetric interior penalty Galerkin (SIPG) method, [Whe78], is applied to the problem in this thesis. With regard to the previously mentioned DG method in (3.1.12), the parameters are chosen to be $b = \frac{p^2}{h}$ and $c = 1$. This gives the boundary fluxes

$$\sum_{E \in \mathcal{E}} \int_0^1 F^*(u_\varepsilon) \psi|_{\partial E} \ \mathrm{dt} := \sum_{\partial E \in \partial \mathcal{E}} \left\{ \int_0^1 \frac{p^2}{h} [u_\varepsilon][\psi] - \{\varepsilon \partial_x \psi\} [u_\varepsilon] - \{\varepsilon \partial_x u_\varepsilon\} [\psi] \ \mathrm{dt} \right.$$

$$\left. + \int_0^1 u_{\varepsilon, E_{\mathrm{up}}} \psi_{E_{\mathrm{up}}} \ \mathrm{dt} \right\}$$

$$+ \int_0^1 \left(-\frac{p^2}{h} \psi(a, t) + \varepsilon \partial_x \psi_\varepsilon(a, t) \right) u_{\varepsilon, \mathrm{bound}}(a, t) \ \mathrm{dt}$$

$$+ \int_0^1 \left(\frac{p^2}{h} \psi(b, t) - \varepsilon \partial_x \psi_\varepsilon(b, t) \right) u_{\varepsilon, \mathrm{bound}}(b, t) \ \mathrm{dt}$$

$[\cdot]$ is the jump at the element edges, $\{\cdot\}$ is the average of two element values at one edge, and $u_{\varepsilon, E_{\mathrm{up}}}$ is the evaluation of the left element on an element edge to obtain an upwind flux for the advection. Furthermore, Dirichlet boundary conditions at a and b are assumed and to mimic these values the boundary values $u_{\varepsilon, \mathrm{bound}}(\cdot, t)$ are taken as values of the analytic solution. To obtain the strong form as used in (3.1.12), the additional jump term $[(u_\varepsilon - \varepsilon \partial_x u_\varepsilon) \psi]$ has to be subtracted in the boundary summation.

Choosing the test functions ψ^h in the finite dimensional space $V^h = \{\psi \in L^2(\Omega) : \forall E \quad \psi|_E \in P_p(E)\}$ where $P_p(E)$ is the space of polynomials of degree p on element E and the ansatz functions $\psi_i|_E$ such that they construct a basis of V^h. The test function

- the ansatz function respectively - can be represented as

$$\psi^h(x) = \sum_{i=0}^{p} \psi_i(x),$$

$$u_\varepsilon^h(x,t) = \sum_{i=0}^{p} u_{\varepsilon,i}(t)\psi_i(x).$$

With these representations the semi-discrete form on each element E is obtained:

$$0 = \partial_t u_{\varepsilon,i} \int\limits_E \psi_i \psi_j \, \mathrm{dx} - F(u_\varepsilon) \int\limits_E \partial_x \psi_i \psi_j \, \mathrm{dx} + F^*(u_{\varepsilon,i})\psi_i\psi_j|_{\partial E}.$$

With the definition of element-wise matrices

$$M_{E,i,j} := \int\limits_E \psi_i \psi_j \, \mathrm{dx}, \quad D_{E,i,j} := \int\limits_E \partial_x \psi_i \psi_j \, \mathrm{dx}, \quad B_{E,i,j} := \psi_i \psi_j|_{\partial E}, \qquad (5.1.18)$$

it is

$$M_{E,i,j}\partial_t u_{\varepsilon,i} = -D_{E,i,j} F(u_{\varepsilon,i}) - B_{E,i,j} F^*(u_{\varepsilon,i}).$$

Inverting the mass matrix $M_E = (M_{E,i,j})_{i,j}$ gives a semi discrete form

$$\partial_t u_\varepsilon = -M_E^{-1} D_E F(u_\varepsilon) - M_E^{-1} B_E F^*(u_\varepsilon), \qquad (5.1.19)$$

which can be treated with time discretization schemes.

The primal advection equation is treated in a similar way, but the numerical flux is only the up-winding term $F^*(u_0) = u_0^l$.

In the example at hand, the explicit Euler method is used for time discretization and Lagrange Polynomials of degree two are used for spatial discretization by the above introduced DG method without any limiter. Though the explicit time discretization requires a step size restriction by the CFL condition, it is chosen to have an explicit representation of the discrete time derivative which is of value in the computation of the residuals. The time step size for the solution, plotted in Fig. 5.3 and Fig. 5.4, is $k = 0.001$ and the spatial discretization uses elements of the size $h = 0.125$. With the DG method the box-shaped initial condition for the primal and the dual case can be initialized without any initialization error. For the purely advective primal case, the box is advected to the right hand side with the unit velocity. The numerical advection causes some over and under shootings in front of steep gradients since no limiter is applied. The dual problem with diffusion advects the box to the left hand side and smooths the steep gradients. In this case, the numerical solution is close to the analytical one.

The dual initial condition is set at $t = T$ and the simulation runs down to $t = 0$ with a diffusion coefficient $\varepsilon = 0.1$. For sufficiently smooth solutions the SIPG method provides convergence of L^2-errors of the order $p + 1$, where p is the order of the polynomial, compare [Riv08]. For discontinuous initial conditions, the order of convergence is lower.
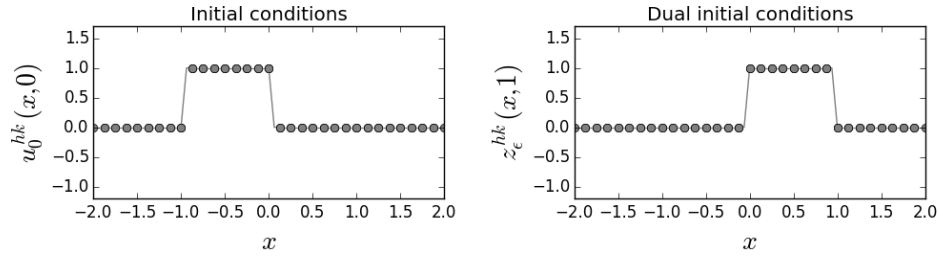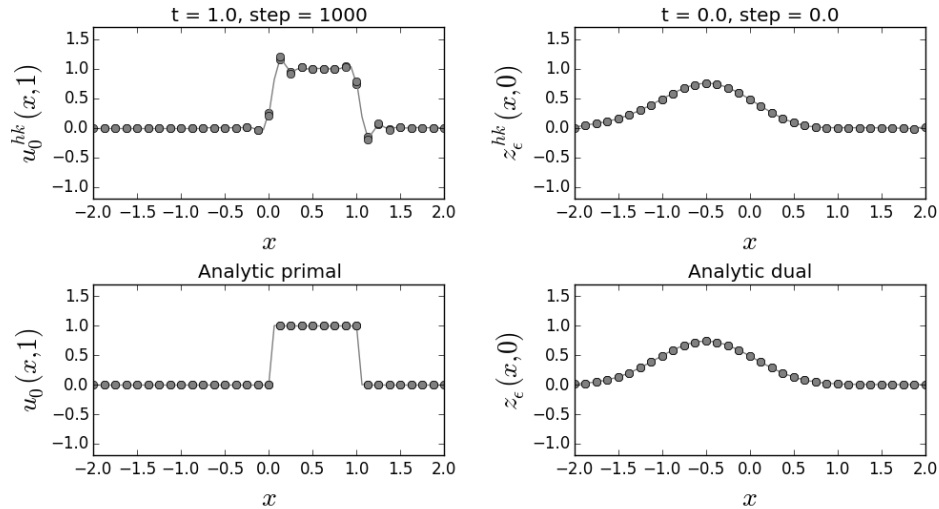
Figure 5.3: Initial condition of the primal and the dual problem

Figure 5.4: Solution of the primal (left) and the dual problem (right) at $t = 1$ and $t = 0$, respectively, with $k = 0.001$, $h = 0.125$, and dual diffusion coefficient $\varepsilon = 0.1$ (first line). The second line shows the corresponding values of the known solution.

In the numerical example at hand, the global L^2-error at final time $T = 1$ of the primal solution of the advection equation (black dots) decreases proportional to $\sqrt{h}$, marked with a dashed line, as seen in Fig. 5.5.

The right hand side of Fig. 5.5 shows the decreasing global L^2-error of the dual problem of the advection-diffusion equation. In this case, the error tends to a convergence rate of 1 (dashed line).

With the discrete solution of the dual advection-diffusion equation and the discrete solution of the primal advection equation the weighted residuals, necessary for the error estimation in the goal functional, can be computed.

For the error estimation, the residuals are integrated by parts, such that the derivatives are applied to u_0^{hk}, for the primal problem, and z_ε^{hk}, for the dual problem, respectively. The integrals are computed by quadrature formulas on each of the elements/time intervals that are combined for the global space time integral. If $M + 1$ quadrature points per
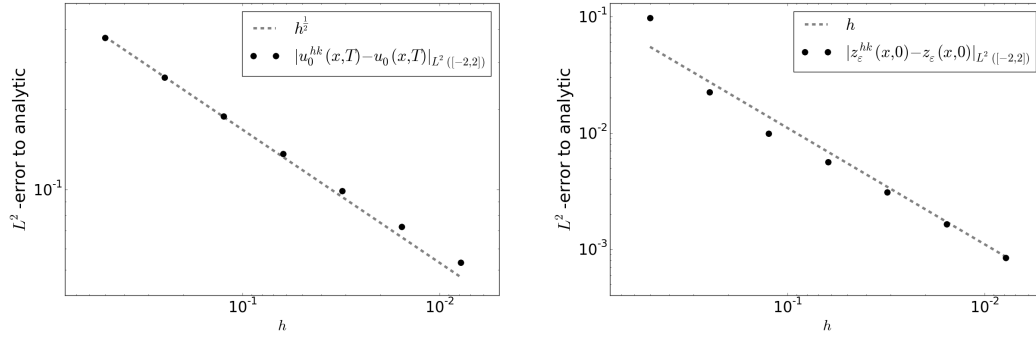
Figure 5.5: Global L^2-error of the (primal) advection problem at final time $t = 1$ (left) and dual advection-diffusion problem at final time $t = 0$ (right) with $\varepsilon = 0.1$. The timestep in both cases is $k = 0.001$.

element are used in space and a total of $N + 1$ quadrature points in time the discrete, global in time, element-wise residual is evaluated as:

$$
\begin{aligned}
\rho_E^{hk}(u_0^{hk}, z_\varepsilon - z_\varepsilon^{hk}) := & \sum_{i=0}^{M} \sum_{j=0}^{N} w_i \tilde{w}_j u_0^{hk}(x_i, t_j) \\
& \qquad \left((z_\varepsilon - z_\varepsilon^{hk})(x_i, t_{j+1}) - (z_\varepsilon - z_\varepsilon^{hk})(x_i, t_j) \right) \\
& - k \sum_{i=0}^{M} \sum_{j=0}^{N} w_i \tilde{w}_j \partial_x u_0^{hk}(x_i, t_j) \left(z_\varepsilon - z_\varepsilon^{hk} \right)(x_i, t_j) \\
& + k \sum_{j=0}^{N} \tilde{w}_j u_0^{hk}(x_{E,\text{right}}, t_j) \left(z_\varepsilon - z_\varepsilon^{hk} \right)(x_{E,\text{right}}, t_j) \\
& - k \sum_{j=0}^{N} \tilde{w}_j u_0^{hk}(x_{E,\text{left}}, t_j) \left(z_\varepsilon - z_\varepsilon^{hk} \right)(x_{E,\text{left}}, t_j) \\
& - \sum_{i=0}^{M} w_i u_0^{hk}(x_i, 1) \left(z_\varepsilon - z_\varepsilon^{hk} \right)(x_i, 1),
\end{aligned}
\tag{5.1.20}
$$

where w_i are the element-wise quadrature weights in space and $\tilde{w}_i$ are the weights in time. The discrete residual, equation (5.1.20), serves as element-wise error estimator

$$
\eta_E^{hk} := \frac{1}{2} \rho_E^{hk}(u_0^{hk}, z_\varepsilon - z_\varepsilon^{hk}).
$$

The dual residual is treated analogously:

$$
\begin{aligned}
\rho_E^{*hk}(z_\varepsilon, u_0 - u_0^{hk}) = {}& -\sum_{i=0}^{M} w_i(u_0 - u_0^{hk})(x_i, 1) z_\varepsilon(x_i, 1) \\
& + k \sum_{i=0}^{M} \sum_{j=0}^{N} w_i \tilde{w}_j u_0(x_i, t_j) \partial_x z_\varepsilon(x_i, t_j) \\
& + k \sum_{i=0}^{M} \sum_{j=0}^{N} w_i \tilde{w}_j \partial_x u_0^{hk}(x_i, t_j) z_\varepsilon(x_i, t_j) \\
& + \sum_{i=0}^{M} \sum_{j=0}^{N} w_i \tilde{w}_j (u_0 - u_0^{hk})(x_i, t_j) \\
& \qquad (z_\varepsilon(x_i, t_{j+1}) - z_\varepsilon(x_i, t_j)) \\
& + k \sum_{j=0}^{N} \tilde{w}_j u_0^{hk}(x_{E,\text{right}}, t_j) z_\varepsilon(x_{E,\text{right}}, t_j) \\
& - k \sum_{j=0}^{N} \tilde{w}_j u_0^{hk}(x_{E,\text{left}}, t_j) z_\varepsilon(x_{E,\text{left}}, t_j)
\end{aligned}
\tag{5.1.21}
$$

and the same for $\rho_E^{*hk}(z_\varepsilon^{hk}, u_0 - u_0^{hk})$. The sum of the dual residuals is set to be the element-wise dual error estimator

$$
\eta_E^{*hk} := \frac{1}{2} \rho_E^{*hk}(z_\varepsilon, u_0 - u_0^{hk}) + \frac{1}{2} \rho_E^{*hk}(z_\varepsilon^{hk}, u_0 - u_0^{hk}).
$$

Since we are interested in the quality of the global error estimate, we refrain from a separation of the indicators into a separate space and time contribution.

Following equation (5.1.17), the element-wise evaluated discrete primal and dual weighted residuals define a local error estimator

$$
\eta_E := \eta_E^{hk} + \eta_E^{*hk}
\tag{5.1.22}
$$

and the sum over all elements is an approximation of the global error

$$
\eta^{hk} := \sum_{E \in \mathcal{E}} \eta_E \approx J(u_0) - J\left(u_0^{hk}\right).
\tag{5.1.23}
$$

We remark, that although all terms in the residuals are known, due to the integration error only an approximation of the residuals is computed. Since we will consider the limit $\varepsilon \to 0$ this quadrature error needs to be kept in mind.

5.1.7   Numerical experiments

In this section, the dependence of the absolute value of the additional residual on the spatial grid size is studied numerically. Then, the behavior of the local error estimators

with and without the additional dual residual is further investigated, and, in the end, the global error estimator including the additional residual is found to gain a better effectivity index as the global estimator without the artificial viscosity.

In the following, the spatial discretization on $\Omega = (-2, 2)$ in DG manner uses basis and test function polynomials of order 2 and the discrete solutions are evaluated such that a numerical quadrature, using a composite trapezoidal rule on each element, can be performed. An example shows the influence of the choice of the quadrature rule. The value of the goal functional for the discrete solution, $J(u_0^{hk})$, is also determined exactly by the trapezoidal rule. The goal value of the analytic solution, $J(u_0)$, is one.

In this setting, the global value of the additional residual was computed for different spatial resolutions and a fixed time step size of $k = 0.0001$.
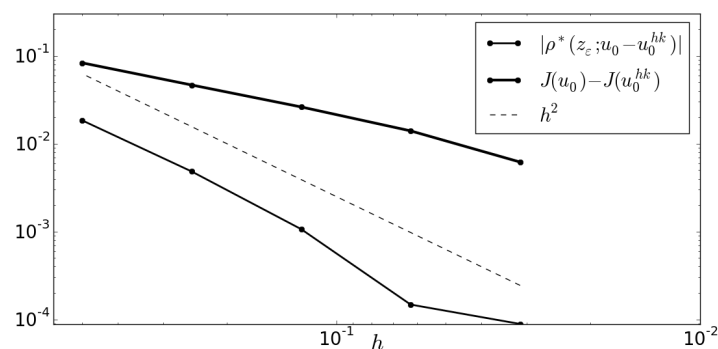

Figure 5.6: Absolute value of the additional residual, $k = 0.0001$, $\varepsilon = 0.1$.

Fig. 5.6 shows the absolute global value of the additional residual for $\varepsilon = 0.1$. This extra term converges with second order to zero and is thus faster than the actual error in the goal functional, implying the finer the mesh, the less important the additional residual. However, the difference to the classical formulation is not only the additional residual, but also the replacement of the discontinuous dual function by the solution of the dual advection-diffusion equation.

All three residuals together, element-wise evaluated, give the local error estimators, see (5.1.22). For a uniform grid the local error estimator $\eta_{E,uni}$ indicates the area of influence for the goal functional, (5.1.5).

The area of interest, on which the goal functional is evaluated, is the interval $[0, 1]$. Thus, for the discontinuous test case presented in this thesis, each element over which the box shaped function moves, has theoretically an equally high local error estimator, while the regions outside are of minor influence to the value of the goal functional. This is reflected in the numerical results, as, e.g., in Fig. 5.7, despite the diffusion in the dual the estimator does not smear.

Dörfler marking, [Dö96], would suggest to refine the elements in the middle of Fig. 5.7, namely in the interval $I_{\text{ref}} = [-1, 1]$, such that the sum of the absolute values of the estimators in the set which is going to be refined, $\mathcal{E}_{\text{ref}}$, is larger then a specific percentage
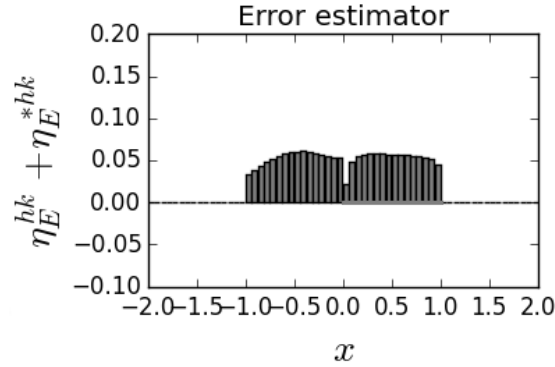
Figure 5.7: Absolute value of local error estimators on a uniform grid with $h = 0.0625$ and artificial viscosity $\varepsilon = 0.05$

of the sum of the absolute values of the estimators in the whole set $\mathcal{E}$,

$$\sum_{E \in \mathcal{E}_{\text{ref}}} \left| \eta_E^{hk} + \eta_E^{*hk} \right| \geq (1 - \Theta) \sum_{E \in \mathcal{E}} \left| \eta_E^{hk} + \eta_E^{*hk} \right|,$$

for some $\Theta \in (0, 1)$. In the test case at hand, refinement in I_{ref} is achieved with $1 - \Theta \approx 1 - 10^{-6}$, showing that most of the estimated error is in I_{ref}.

The summation over each element of the signed local spatial error estimators on the uniform grid brings the global estimator η_{uni}^{hk}, while the sum of the estimators over the locally refined, grid brings η_{ref}^{hk}.

Table 5.1: Dependence of the global error estimators and the error in the goal functional on the grid size. Uniform grid size h is marked in bold. $\varepsilon = 0.1$

h	η_{uni}^{hk}	η_{ref}^{hk}	$\lvert J(u_0) - J(u_{0,\text{uni}}^{hk}) \rvert$	$\lvert J(u_0) - J(u_{0,\text{ref}}^{hk}) \rvert$
0.5/0.25	0.0674	0.0552	0.0832	0.0466
0.25/0.125	0.0437	0.0324	0.0466	0.0262
0.125/0.0625	0.0258	0.0174	0.0262	0.0140
0.0625/0.03125	0.0140	0.0080	0.0140	0.0062

Table 5.1 shows that the global error estimator on a uniform grid is greater than the estimator on a mesh which is locally refined once by bisection according to the error indicators. The bold h indicates the uniform grid size, the normal style h is the size of the refined elements. Also the error in the goal functional evaluated on a locally refined grid is smaller than on the uniform grid. On each element, the quadrature rule is the same, such that the approximation of the integral is better in the refined elements. But the numerically evaluated error estimator does not satisfy the error identity, as suggested in equation (5.1.17). This could be caused by several reasons, for instance by a quadrature error or by a non-adjoint consistent implementation [Har07]. However, as

the difference between estimator and error decrease with decreasing element size h, we do not investigate this issue further.
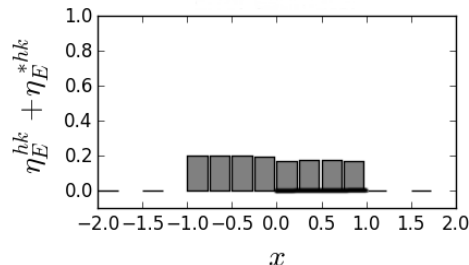

Figure 5.8: Absolute value of local error estimators on a locally refined grid with $h = 0.5, 0.25,$ and $\varepsilon = 0$

If the dual equation is not modified and the computations are done nevertheless by evaluating only

$$\eta_{E0} := \rho_E^{hk}\left(u_0^{hk}, z_0 - z_0^{hk}\right) + \rho_E^{*hk}\left(z_0^{hk}, u_0 - u_0^{hk}\right), \qquad (5.1.24)$$

compare equation (5.1.22), the local error estimators are even more evenly distributed on the area which is expected to be refined, as shown in Fig. 5.8. For the computation it was naively assumed, that $\partial_x z_0 = \partial_t z_0 = 0$ in $[-2, 2]$, since this is true almost everywhere – and in particular in the chosen quadrature points.
Concluding, the modification of the dual equation does not harm the local error indication, and even the approach without modification – ignoring the unboundedness in the analytic case – results in reasonable local error indication. So far, there seems to be no advantage in the modification, but this is different for the global error estimation:
The quality of the global error estimators is measured by the effectivity index, see, e.g., [Ver94], [BDR92], and [BR78a], which is the ratio of the estimator to the true error. Here it is

$$\text{eff} = \frac{J(u_0) - J(u_0^{hk})}{\eta^{hk}}. \qquad (5.1.25)$$

Fig. 5.9 shows the behavior of the effectivity index with respect to the spatial grid size. The index for the global error estimator without viscosity, e.g., equation (5.1.24), is increasing at first. If it ever converges to one, it is much later as in case of the modified error estimator.
The right hand side of Fig. 5.9 shows that the error estimator including the additional residual gains a better effectivity on coarse grids than the estimator without the additional term, e.g., equation (5.1.23) with and without the last residual. Fig. 5.10 depicts this relation also for different values of ε. For any tested $\varepsilon \in [0.0001, 0.1]$ the effectivity of the estimator including the addition was closer to one, but obviously depending on the diffusion coefficient. Thus, the relation of the error and the error estimator to the diffusion parameter ε is of interest. Table 5.2 shows the different global spatial error
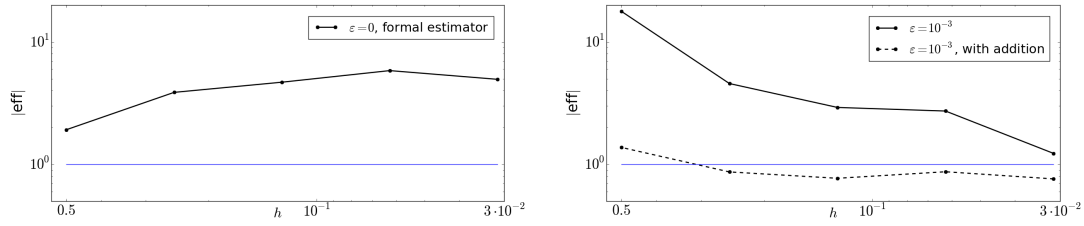
Figure 5.9: Effectivity of the global estimator without artificial viscosity in the dual equation (left) and with and without the additional residual, $\rho^*(z_\varepsilon, u_0 - u_0^{hk})$ with viscosity $\varepsilon = 0.001$ in the dual equation (right).
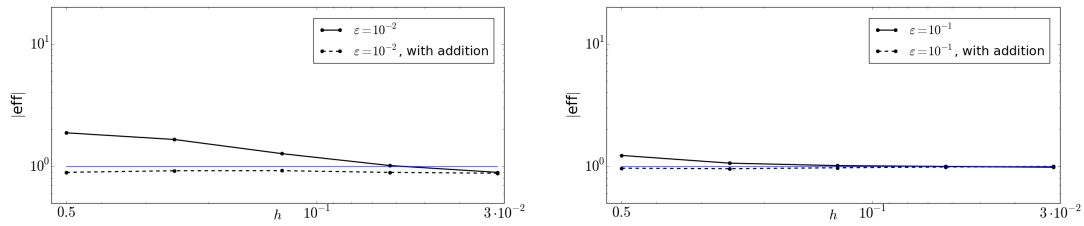

Figure 5.10: Effectivity of the global estimator with and without the additional residual, $\rho^*(z_\varepsilon, u_0 - u_0^{hk})$, for $\varepsilon = 0.01$ (left) and $\varepsilon = 0.1$ (right).

estimators for a decreasing diffusion coefficient. For stability reasons, the time step size was chosen to be $k = 0.0001$ and the spatial grid size was fixed at $h = 0.0625$. Since neither the primal problem nor the goal functional are modified, the error in the goal functional is constant for a fixed grid size.

Table 5.2: Dependence of the global spatial error estimators on the dual diffusion coefficient ε, with $J(u_0) - J(u_0^{hk}) = 0.0140$

ε	$|\eta_{\mathrm{uni}}^{hk}|$	$|\mathrm{eff}|$
0.0	0.0028	4.9515
0.0001	0.0076	1.8389
0.001	0.0051	2.7269
0.01	0.0138	1.0154
0.1	0.0140	0.9986

While the error in the goal functional is not influenced by the modification in the dual equation, the error estimator and thus the effectivity is. Notice, that for an exact evaluation of the residuals the effectivity is always one - since an error identity is evaluated. However, with a fixed integration accuracy smaller values of ε increase the quadrature error and consequently effectivity deteriorates. Once the mesh is sufficiently refined the quadrature - fixed per element - gains accuracy and thus the effectivity converges to one.

The same effect has to be expected when numerically recovering the unknown primal and dual solutions for the weights, as the accuracy of the discrete primal and dual solutions are fixed on a given mesh and can only be increased by refinement.

A ratio of the advection to the diffusion is given by the Peclet number, see, e.g., [Pat80]. Here, P_h shall be the approximation of the Peclet number for a constant advection velocity of one, depending on the mesh size as $P_h = \frac{h}{\varepsilon}$.

Table 5.3: Effectivity and approximated Peclet number for $\varepsilon = 0.0001$ (left), $\varepsilon = 0.01$ (middle), and $\varepsilon = 0.1$ (right), with $k = 10^{-4}$ constant and 40 quadrature points for a composite trapezoidal rule.

	$\varepsilon = 0.0001$		$\varepsilon = 0.01$		$\varepsilon = 0.1$	
h	P_h	eff	P_h	eff	P_h	eff
0.5	5000	-1.995	50	1.924	5	1.235
0.25	2500	-3.815	25	1.678	2.5	1.065
0.125	1250	7.290	12.5	1.277	1.25	1.016
0.0625	625	1.885	6.26	1.018	0.626	1.000

Table 5.3 shows that the effectivity of the global error estimator is getting better, the more the diffusion is of influence in the discretized scheme. Thus, it is suggested that, if the diffusion is resolved sufficiently, the modified dual weighted residual error estimator gives an effective approximation of the global error in the goal functional.

Concluding, these experiments suggest that in this setting the modified dual weighted residual error estimator for a spatial refinement is a reasonable indicator for grid refinement with respect to some goal functional and moreover the modified global error estimator is in this case of discontinuities a better approximation of the actual global error than the classical approach.

5.2 2D linear transport equation

5.2.1 Discontinuous test case (two dimensional)

In this section, the solutions of a 2D advection problem and a 2D advection diffusion problem with discontinuous initial data are computed. Additionally, for both cases an adjoint problem with discontinuous initial data is given and solved numerically. With second order DG in space and Euler steps in time, the test and ansatz functions are quadratic on each spatial element and constant during each time step. The discretization error is approximated with help of an interpolation of the discrete primal and dual solution and is used as weight in the DWR method. In the end of this section, local error indicators of the modified DWR method are examined and efficiency of the global error estimator is tested.

5.2.2 The pure advection equation and its dual

A simple advection problem for $\mathbf{x} = (x,y)^T \in \mathbb{R}^2$ and $t \in (0,T)$ with velocity $\mathbf{v} \in \mathbb{R}^2$ is given by

$$\partial_t u_0(\mathbf{x},t) + \operatorname{div}(\mathbf{v}u_0(\mathbf{x},t)) = 0, \quad \text{in } \mathbb{R}^2 \times (0,T), \tag{5.2.1}$$

with initial condition (A)

$$u_0(\mathbf{x},0) = u_{ini,A}(\mathbf{x}) = \begin{cases} 1, & -1 \le x \le 0, \\ 0, & \text{else.} \end{cases} \tag{5.2.2}$$

or initial condition (B)

$$u_0(\mathbf{x},0) = u_{ini,B}(\mathbf{x}) = \begin{cases} 1, & -1 \le x, y \le 0, \\ 0, & \text{else.} \end{cases} \tag{5.2.3}$$

Again, the solution to the pure advection equation is marked as u_0, which is compatible with zero diffusion. With the discontinuous initial condition the problem is only reasonable in weak sense: For all $\psi \in C_c^1(\mathbb{R}^2 \times [0,T))$, differentiable test functions with compact support in $\mathbb{R}^2$, it holds

$$\begin{aligned} a_0(u_0, \psi) := & -\int\limits_0^T \int\limits_{\mathbb{R}^2} u_0 \partial_t \psi + u_0 \mathbf{v} \cdot \nabla \psi \, \mathrm{d}\mathbf{x} \, \mathrm{d}t \\ & + \int\limits_{\mathbb{R}^2} (u_{\text{ini,A,B}}(\mathbf{x}) - u_0(x,0))\, \psi(\mathbf{x},0) \, \mathrm{d}\mathbf{x} \\ = & \; 0. \end{aligned} \tag{5.2.4}$$

For initial data (A) and the velocity vector $\mathbf{v} = (1,0)$ the weak solution for $t \le T$ is given by

$$u_{0,A}(\mathbf{x},t) = u_{\text{ini},A}(x-t,y) = \begin{cases} 1, & -1+t \le x \le t, \\ 0, & \text{else,} \end{cases} \tag{5.2.5}$$

which is a constant extension in y-direction of the one dimensional solution.
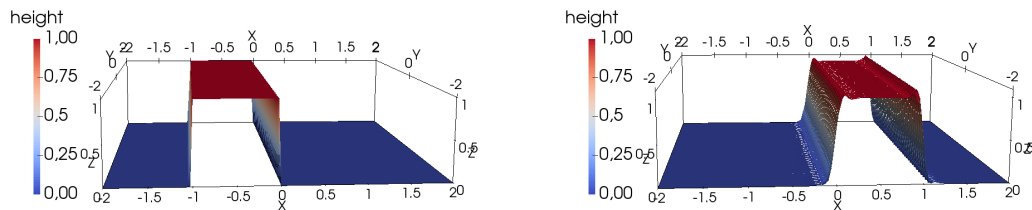

Figure 5.11: Left: Initial condition (A). Right: Numerical solution for (A) at $t = 1$

For the box shaped initial condition (B) the solution of the advection equation with constant velocity $\mathbf{v} = (1,1)^T$ is also a translation along the characteristics and it is

$$u_{0,B}(\mathbf{x},t) = u_{\text{ini},B}(x-t,y-t) = \begin{cases} 1, & -1+t \le x,y \le t, \\ 0, & \text{else.} \end{cases} \tag{5.2.6}$$
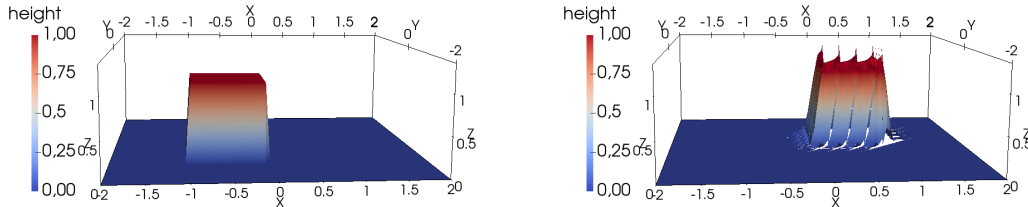

Figure 5.12: Left: Initial condition (B). Right: Numerical solution for (B) at $t = 1$

Since this problem does not include viscosity, i.e., $\varepsilon = 0$, the solution is denoted with subscript "0". The discrete solution $u_{0,B}^{hk}(\mathbf{x},t)$ shows slightly more oscillations than the discrete solution to problem (A), $u_{0,A}^{hk}(\mathbf{x},t)$, due to diagonal advection over a triangular grid, compare 5.11 and 5.12.

Choosing the goal functional analogously to the 1D test case as

$$J(u_0) = \int_{\mathbb{R}} u_0(\mathbf{x},T) z_T(\mathbf{x}) \, \mathrm{d}\mathbf{x}, \tag{5.2.7}$$

with the weight z_T indicating an area of interest for test case (A) and (B)

$$z_{T,A}(\mathbf{x}) := \begin{cases} 1, & 0 \le x \le 1, \\ 0, & \text{else} \end{cases} \tag{5.2.8}$$

$$z_{T,B}(\mathbf{x}) := \begin{cases} 1, & 0 \le x,y \le 1, \\ 0, & \text{else} \end{cases} \tag{5.2.9}$$

gives again a dual problem of the above advection equation. The problem of finding z_0 for all $\phi \in C_c^1(\mathbb{R}^2 \times (0,T])$:

$$\int_0^T \int_{\mathbb{R}} z_0 \partial_t \phi + z_0 \mathbf{v} \cdot \nabla \phi \, \mathrm{d}\mathbf{x} \, \mathrm{dt} - \int_{\mathbb{R}} (z_T(\mathbf{x}) - z_0(\mathbf{x},T)) \, \phi(\mathbf{x},T) \, \mathrm{d}\mathbf{x} = 0,$$

with initial condition $z_0(\mathbf{x},T) = z_{T,A/B}(\mathbf{x})$. Fixing again $T = 1$, the solution test case (A) and time $t \in (0,1)$ is

$$z_{0,A}(\mathbf{x},t) = \begin{cases} 1, & -1+t \le x \le t, \\ 0, & \text{else.} \end{cases}$$

while the solution for test case (B) and time $t \in (0, 1)$ is

$$z_{0,B}(\mathbf{x}, t) = \begin{cases} 1, & -1 + t \le x, y \le t, \\ 0, & \text{else.} \end{cases}$$

Both coincide with corresponding the primal solution.

5.2.3 The advection-diffusion equation and its dual

A linear advection-diffusion problem for $\mathbf{x} = (x, y)^T \in \mathbb{R}^2$ and $t \in (0, T)$ with velocity $\mathbf{v} \in \mathbb{R}^+$ and diffusion coefficient $\varepsilon \in \mathbb{R}^+$ is given by

$$\partial_t u_0(\mathbf{x}, t) + \operatorname{div}(\mathbf{v} u_0(\mathbf{x}, t) - \varepsilon \nabla u) = 0. \quad \text{in } \mathbb{R}^2 \times (0, T), \qquad (5.2.10)$$

With discontinuous initial conditions (A), (5.2.2), and (B), (5.2.3), the problem is posed in weak form: For all $\psi \in C_c^1(\mathbb{R}^2 \times [0, T))$, bounded test functions with compact support in $\mathbb{R}^2$ holds

$$\begin{aligned} a_0(u_0, \psi) &:= -\int\limits_0^T \int\limits_{\mathbb{R}^2} u_0 \partial_t \psi + u_0 \mathbf{v} \cdot \nabla \psi - \varepsilon \nabla u_0 \cdot \nabla \psi \, \mathrm{d}\mathbf{x} \, \mathrm{dt} \\ &\quad + \int\limits_{\mathbb{R}^2} \left(u_{\mathrm{ini,A,B}}(\mathbf{x}) - u_0(\mathbf{x}, 0) \right) \psi(\mathbf{x}, 0) \, \mathrm{d}\mathbf{x} \\ &= 0. \end{aligned} \qquad (5.2.11)$$

For initial data (A) the solution is analogue to the one dimensional case. For case (B) the analytic solution could also be obtained by the application of a Green's function, e.g. as given in (2.3.4). However, here it is assumed, that the analytic solution to this test case is not known. This is of interest for the DWR error estimator general cases. Choosing the goal functional again as

$$J(u_0) = \int\limits_{\mathbb{R}} u_0(\mathbf{x}, T) z_T(\mathbf{x}) \, \mathrm{d}\mathbf{x},$$

with z_T as before in case (A) and in case (B) the resulting dual equation reads

$$-\partial_t z_\varepsilon(\mathbf{x}, t) - \mathbf{v} \cdot \nabla z_\varepsilon(\mathbf{x}, t) - \varepsilon \Delta z_\varepsilon(\mathbf{x}, t) = 0 \quad \text{in } \mathbb{R}^2 \times (1, 0) \qquad (5.2.12)$$

with dual initial condition (5.2.8) or (5.2.9) at final time $t = T$.
Fig. 5.13 shows the dual initial condition of test case A on the left hand side. On the right hand side, the discrete dual solution of case (A) is depicted for diffusion coefficient $\varepsilon = 0.1$. Fig. 5.14 shows the same for test case (B).
With its analytic solution given, case (A) is used to check the L^2-convergence for decreasing h and fixed diffusion coefficient $\varepsilon > 0$, see Fig. 5.15.
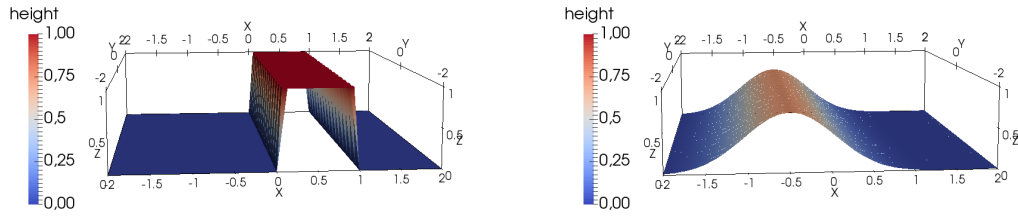
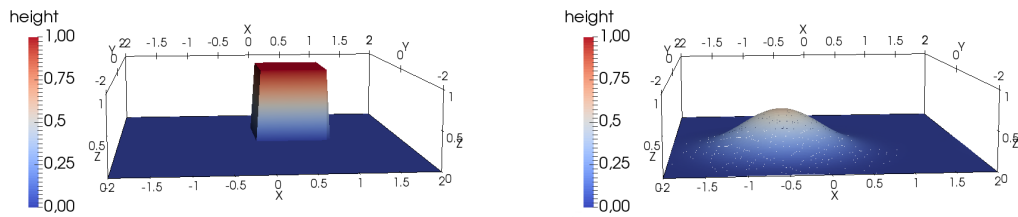Figure 5.13: Left: Dual initial condition (A). Right: Numeric solution for (A) at $t = 0$

Figure 5.14: Left: Dual initial condition (B). Right: Numeric solution for (B) at $t = 0$
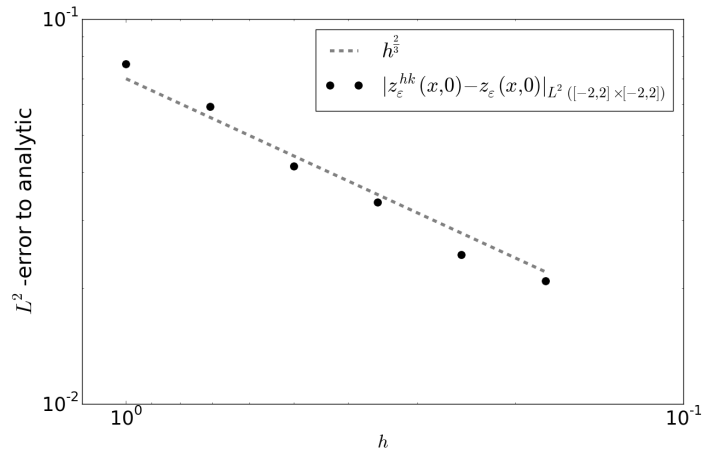

Figure 5.15: Global L^2-error of the dual advection-diffusion problem at final time $t = 0$ with $\varepsilon = 0.1$. The time step size is $k = 10^{-4}$.

5.2.4 Discretization schemes and approximation of weights

As in the 1D test case, advection residual evaluation means the evaluation of $a_0(\cdot, \cdot)$ at $\left(u_0, z_0 - z_0^{hk}\right)$. Here, z_0^{hk} is again the solution of the time and space discretized dual advection equation and u_0 and z_0 are the analytic solutions to the primal and dual advection problem. With $z_0 - z_0^{hk} \in L^\infty\left(\mathbb{R}^2; L^2(0,1)\right)$, and $u_0 \in L^\infty\left(\mathbb{R}^2; L^2(0,1)\right)$ the

formal evaluation of $a_0(\cdot, \cdot)$ is not allowed.

Analogue to the 1D case, the residuals are evaluated with the more regular dual solution of the advection-diffusion equation, z_ε and z_ε^{hk}, respectively. With discretization similar to the 1D case, but now on the domain $\bar{\Omega} = [-2, 2] \times [-2, 2]$, space discretization matrices M_E, D_E, and B_E, see (5.1.18), are set up and the system (5.1.19) is solved in each time step. With an explicit Euler time stepping u_0^{hk} and z_ε^{hk} are obtained. Recalling the error in the goal functional with additional dual residual, caused by the inconsistent dual problem, it is

$$J(u_0) - J(u_0^{hk}) = \frac{1}{2}\Big[\rho^*(z_\varepsilon^{hk}, u_0 - u_0^{hk}) + \rho(u_0^{hk}, z_\varepsilon - z_\varepsilon^{hk}) \\ + \rho^*(z_\varepsilon, u_0 - u_0^{hk})\Big]. \tag{5.2.13}$$

Since the goal functional and the advection (diffusion) equation were linear, the error was not only estimated but exactly represented. While the analytic solutions u_0 and z_ε are known in the 1D test case and in the quasi 1D case with initial conditions (5.2.2), in general the analytic solution of posed problems is not known. Thus, the error identity as in (5.2.13) can only be evaluated as an error estimation $\tilde{\eta}^{hk}$. One possibility, for instance, is to replace the discretization error with an a priori error estimation of the form

$$u_0 - u_0^{hk} \approx \mathcal{O}\left(h^{c_1}\right) + \mathcal{O}\left(k^{c_2}\right). \tag{5.2.14}$$

This would lead to a decrease of the DWR error estimator for finer resolution in time and space, but not necessarily to an efficient error estimator. An error representation like

$$J(u_0) - J(u_0^{hk}) = \tilde{\eta}^{hk} + \mathcal{O}\left(h^{c_3}\right) + \mathcal{O}\left(k^{c_4}\right). \tag{5.2.15}$$

would ensure the efficiency. To obtain such a formulation, the discretization error, which works as a weight to the residual, is split into two parts: The error introduced by discretization in space and the error caused by discretization in time.

$$u_0 - u_0^{hk} = u_0 - u_0^h + u_0^h - u_0^{hk}. \tag{5.2.16}$$

An more suitable approximation to the spatial discretization error $u_0 - u_0^h$ and $z_\varepsilon - z_\varepsilon^h$ as the a priori estimation (5.2.14) can, for instance, be achieved by a patch-wise quadratic interpolation of the linear Ritz projections u_0^h and z_ε^h: $I_{2h}^{(2)} u_0 - u_0^h$ and $I_{2h}^{(2)} z_\varepsilon - z_\varepsilon^h$, respectively, [BR03]. This method satisfies (5.2.15) with $c_3 = 3$, see section five of [BR01]. Other methods to approximate the analytic solution by a different approximation than the computed numeric solution are local and global higher order approximations or an approximation by difference quotients.

In the test cases at hand, the basis functions are already quadratic such that inner element diffusion is also taken into account. Higher order interpolation would lead to cubic functions having ten degrees of freedom instead of six and causing high computational costs. Less effort is the application of a linear solution and the approximation of the approximation error by

$$u_0 - u_0^{hk} \approx I_h^{(1)} u_0^{hk} - u_0^{hk} \qquad (5.2.17)$$

and

$$z_\varepsilon - z_\varepsilon^{hk} \approx I_h^{(1)} z_\varepsilon^{hk} - z_\varepsilon^{hk}. \qquad (5.2.18)$$

For the lower order interpolation on an element, a linear interpolation between the function values of three neighboring nodes, e.g., P_1, P_4, P_5, is used to obtain the function value in Q. Function values in P and R are similarly obtained by linear interpolation between P_3, P_5, P_6 and P_2, P_4, P_6. The values in P, Q, and R define a plane, which allows linear extrapolations back to the nodes P_1 to P_6.
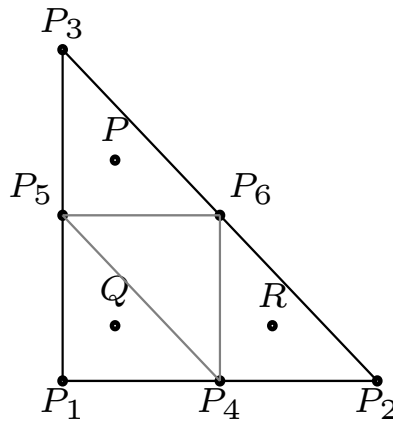

Figure 5.16: Nodes of quadratic basis functions, $P_i, i = 1, \ldots, 6$, and interpolation points P, Q, and R.

The discretization error in time can also be approximated by the difference of the fully discrete solution and its interpolation in time.

$$u_0^h - u_0^{hk} \approx I_k^{(1)} u_0^{hk} - u_0^{hk} \qquad (5.2.19)$$

and

$$z_\varepsilon^h - z_\varepsilon^{hk} \approx I_k^{(1)} z_\varepsilon^{hk} - z_\varepsilon^{hk}. \qquad (5.2.20)$$

[GRW15] use a linear interpolation for a discretization in time by the implicit Euler method. Interpolation such that the effectivity of the error estimator is converging towards one is up to now only known for the Euler method, but not for Runge-Kutta methods. All predefined time discretization methods in *StormFlash2d* are explicit and for the reason of effectivity, the explicit Euler and the corresponding linear interpolation are used in the application section of this thesis.

For the explicit Euler method, the linear interpolation for equidistant time steps $k = t_j - t_{j-1}, j = 1, \ldots, N$ is

$$I_k^{(1)} u_0^{hk}(t) = \frac{t_j - t}{k} u_{0,j}^{hk} + \frac{t - t_{j-1}}{k} u_{0,j+1}^{hk},$$
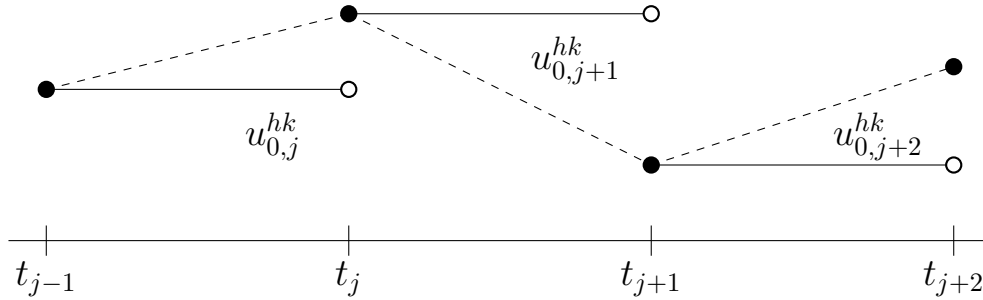
for $t \in [t_{j-1}, t_j)$.

Figure 5.17: Linear interpolation (dashed line) of the piecewise constant explicit Euler solution.

With this interpolation operator, the derivative for $t \in (t_{j-1}, t_j)$ is

$$\partial_t I_k^{(1)} u_0^{hk}(t) = \frac{u_{0,j+1}^{hk} - u_{0,j}^{hk}}{k},$$

which is of use for the discrete evaluation of the residuals.
The total discretization error (5.2.16) of the primal solution is approximated by

$$
\begin{aligned}
u_0 - u_0^{hk} &= u_0 - u_0^h + u_0^h - u_0^{hk} \\
&\approx I_h^{(1)} u_0^h - u_0^h + I_k^{(1)} u_0^{hk} - u_0^{hk} \\
&\approx I_h^{(1)} I_k^{(1)} u_0^{hk} - u_0^{hk} \\
&= I_{hk}^{(1)} u_0^{hk} - u_0^{hk},
\end{aligned}
$$

by usage of $u_0^h \approx I_k^{(1)} u_0^{hk}$ and the definition $I_{hk}^{(1)} := I_h^{(1)} I_k^{(1)}$. The discrete dual solution z_ε^{hk} is interpolated in space and time in the same way and the error estimator (5.2.13) without the analytic solution reads

$$\tilde{\eta}^{hk} = \frac{1}{2} \Big[\rho^*(z_\varepsilon^{hk}, I_{hk}^{(1)} u_0^{hk} - u_0^{hk}) + \rho(u_0^{hk}, I_{hk}^{(1)} z_\varepsilon^{hk} - z_\varepsilon^{hk}) + \rho^*(I_{hk}^{(1)} z_\varepsilon^{hk}, I_{hk}^{(1)} u_0^{hk} - u_0^{hk}) \Big]$$
(5.2.21)

As in 1D, the evaluation at quadrature points for numeric integration is done with the

linear interpolation and the local primal and dual residuals are

$$
\begin{aligned}
\rho_E^{hk}(u_0^{hk}, z_\varepsilon - z_\varepsilon^{hk}) &\approx \rho_E^{hk}(u_0^{hk}, I_{hk}^{(1)} z_\varepsilon^{hk} - z_\varepsilon^{hk}) \\
&= \sum_{i=0}^{M} \sum_{j=0}^{N} w_i \tilde{w}_j u_0^{hk}(\mathbf{x}_i, t_j) \\
&\qquad\qquad \left((I_{hk}^{(1)} z_\varepsilon^{hk} - z_\varepsilon^{hk})(\mathbf{x}_i, t_{j+1}) - (I_{hk}^{(1)} z_\varepsilon^{hk} - z_\varepsilon^{hk})(\mathbf{x}_i, t_j) \right) \\
&\quad - k \sum_{i=0}^{M} \sum_{j=0}^{N} w_i \tilde{w}_j \mathbf{v} \cdot \nabla u_0^{hk}(\mathbf{x}_i, t_j) \left(I_{hk}^{(1)} z_\varepsilon^{hk} - z_\varepsilon^{hk} \right) (\mathbf{x}_i, t_j) \\
&\quad + k \sum_{j=0}^{N} \tilde{w}_j \int_{\partial E} \mathbf{v} \cdot \mathbf{n} u_0^{hk}(s, t_j) \left(I_{hk}^{(1)} z_\varepsilon^{hk} - z_\varepsilon^{hk} \right)(s, t_j) \, \mathrm{d}s \\
&\quad - \sum_{i=0}^{M} w_i u_0^{hk}(\mathbf{x}_i, 1) \left(I_{hk}^{(1)} z_\varepsilon^{hk} - z_\varepsilon^{hk} \right)(\mathbf{x}_i, 1),
\end{aligned}
$$

$$(5.2.22)$$

and

$$
\begin{aligned}
\rho_E^{*hk}(z_\varepsilon, u_0 - u_0^{hk}) &\approx \rho_E^{*hk}(z_\varepsilon, I_{hk}^{(1)} u_0^{hk} - u_0^{hk}) \\
&= - \sum_{i=0}^{M} w_i (I_{hk}^{(1)} u_0^{hk} - u_0^{hk})(\mathbf{x}_i, 1) I_{hk}^{(1)} z_\varepsilon^{hk}(\mathbf{x}_i, 1) \\
&\quad + k \sum_{i=0}^{M} \sum_{j=0}^{N} w_i \tilde{w}_j I_{hk}^{(1)} u_0^{hk}(\mathbf{x}_i, t_j) \mathbf{v} \cdot \nabla \left(I_{hk}^{(1)} z_\varepsilon^{hk}(\mathbf{x}_i, t_j) \right) \\
&\quad + k \sum_{i=0}^{M} \sum_{j=0}^{N} w_i \tilde{w}_j \mathbf{v} \cdot \nabla u_0^{hk}(\mathbf{x}_i, t_j) I_{hk}^{(1)} z_\varepsilon^{hk}(\mathbf{x}_i, t_j) \\
&\quad + \sum_{i=0}^{M} \sum_{j=0}^{N} w_i \tilde{w}_j \left(I_{hk}^{(1)} u_0^{hk} - u_0^{hk} \right)(\mathbf{x}_i, t_j) \\
&\qquad\qquad \left(I_{hk}^{(1)} z_\varepsilon^{hk}(\mathbf{x}_i, t_{j+1}) - I_{hk}^{(1)} z_\varepsilon^{hk}(\mathbf{x}_i, t_j) \right) \\
&\quad + k \sum_{j=0}^{N} \tilde{w}_j \int_{\partial E} \mathbf{v} \cdot \mathbf{n} u_0^{hk}(s, t_j) I_{hk}^{(1)} z_\varepsilon^{hk}(s, t_j) \, \mathrm{d}s,
\end{aligned}
$$

$$(5.2.23)$$

Because of the modification in the dual equation, the dual residual has to be evaluated twice: Once with the discrete dual solution, $\rho_E^{*hk}(z_\varepsilon^{hk}, u_0 - u_0^{hk})$, and once with the analytic dual solution, $\rho_E^{*hk}(z_\varepsilon, u_0 - u_0^{hk})$. But the analytic dual solution is in this case also replaced with the interpolant of the discrete solution.

In the introduction of the DWR error estimator in section 4.2, it was stated that the primal and dual residual are equal in a linear case. Though this 2D test case is a linear

problem, the computation of the residuals showed that the residuals are not equal. They are only in the same order of magnitude. This might be cause by the facts that, firstly, the used dual solution z_ε is not the solution of the dual advection problem, and secondly, that the discretization error of a smooth solution is in general much better than the discretization error of a discontinuous solution.

5.2.5 Numerical experiments

In this section, the dependence of the absolute value of the additional residual on the spatial grid size in 2D is studied numerically by the means of test case (B). Again, the behavior of the local error estimators with and without the additional dual residual is further investigated, and, as in 1D, the global error estimator including the additional residual is found to gain a better effectivity index as the formal global estimator.

In the following, the spatial DG discretization on $\bar{\Omega} = [-2, 2] \times [-2, 2]$ uses basis and test function polynomials of order 2 and the discrete solutions are evaluated such that a numerical quadrature, using a composite box rule on each element, can be performed. The value of the goal functional for the discrete solution, $J(u_0^{hk})$, is also determined exactly by a second order spatial quadrature rule. The goal value of the analytic solution, $J(u_0)$, is one.
In this setting, the global value of the additional residual was computed for different spatial resolutions, a fixed time step size of $k = 10^{-5}$ and a fixed diffusion coefficient $\varepsilon = 0.1$.
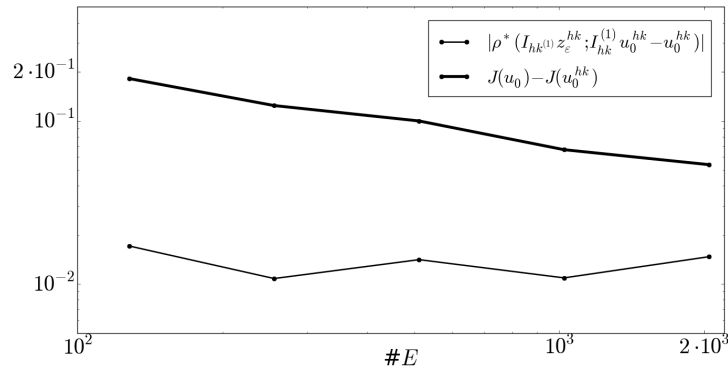

Figure 5.18: Absolute value of the additional residual, $k = 10^{-5}$, $\varepsilon = 0.1$.

Fig. 5.18 shows the absolute global value of the additional residual, $\rho^* \left(I_{hk}^{(1)} z_\varepsilon^{hk}; I_{hk}^{(1)} u_0^{hk} - u_0^{hk} \right)$. In contrast to the 1D test case, the additional term seems not to converge to zero. However, with the used parameters ($\varepsilon = 0.1$, $k = 10^{-5}$, and $\#E = 128, 256, 512, 1024, 2048$) the additional residual is approximately ten times smaller than the error in the quantity of interest. Further refinement might help the

estimator to be more efficient. Additionally, it is not clear, if and how the approximation of weights influenced the estimator. Further investigation in this area is needed, for instance at the example of 2D test case (A), with a given analytic solution.

Negligence of the diffusion and the additional dual residual results in a formal element-wise error estimator, as defined in the 1D test case in (5.1.24). The formal local estimator indicates similar elements as the proposed modified error estimator, see Fig. 5.19, especially taking into consideration that also neighboring elements will be refined to avoid hanging nodes. This suggests that both estimators, modified and formal, serve equally well as error indicators for grid refinement.
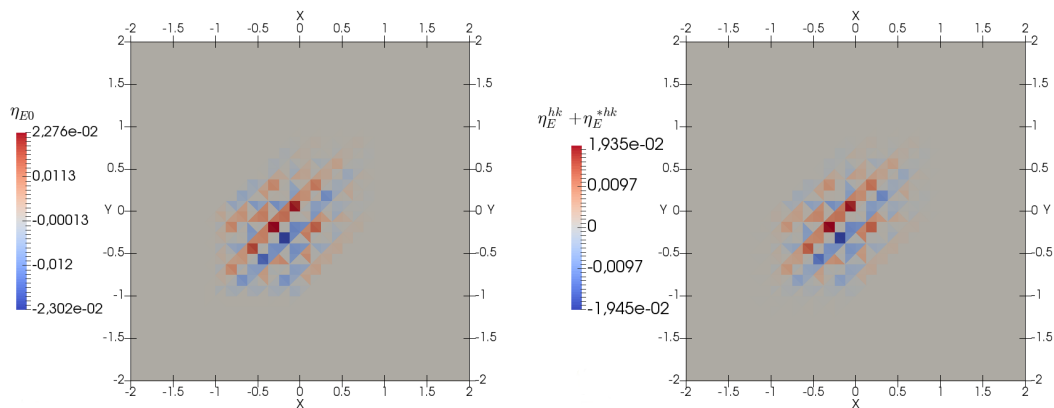

Figure 5.19: Local error indicators obtained by formal evaluation (left) and with dual modification with viscosity $\varepsilon = 0.1$, (right).

The effectivity index, see (5.1.25), for the example at hand is shown in Table 5.4. For a fixed time step size of $k = 10^{-5}$ the effectivity index of the modified error estimator improves, though not monotone. I assume, that higher spatial grid resolution would bring the effectivity index closer to one, as the diffusion might not be sufficiently resolved with 2048 elements and a longest edge $h \approx 0.177$, compare the 1D test regarding the Peclet number in section 5.1.7.

Table 5.4: Dependence of the modified global error estimator and the error in the goal functional on the grid size (2D)

#E	η_{uni}^{hk}	$\left\vert J\left(u_0\right) - J\left(u_0^{hk}\right) \right\vert$	|eff|
128	0.0615	0.1818	2.9584
256	0.0247	0.1242	5.0346
512	0.0467	0.0999	2.1386
1024	0.0283	0.0666	2.3554
2048	0.0477	0.0539	1.130

These results have to be considered in relation to the performance of the formal error estimator. Fig. 5.20 shows on the left hand side the dependency of the effectivity index of the formal error estimator on the total number of elements of the uniform grid. The right side depicts the effectivity index of the modified error estimator. Noticing that the vertical axes have a different scaling, the efficiency of the formal error estimator is worse than the efficiency of the modified one. This is even true if the residuals are evaluated with the solution of the dual advection-diffusion equation, but without the additional residual $\rho^* \left(I_{hk}^{(1)} z_\varepsilon^{hk}; I_{hk}^{(1)} u_0^{hk} - u_0^{hk} \right)$. With the additional term though, the efficiency is even better, see Table 5.5.
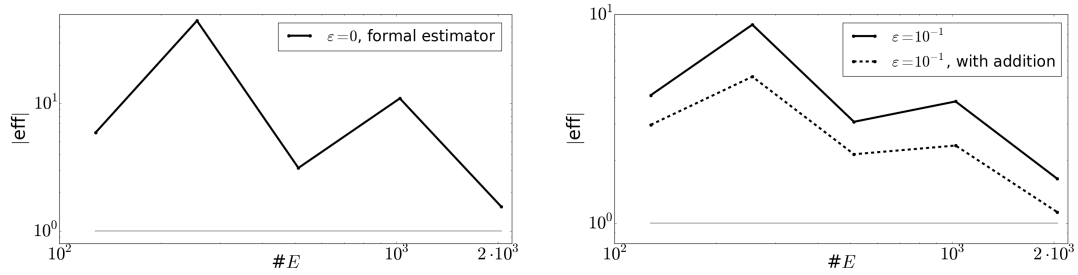

Figure 5.20: Effectivity of the global estimator without artificial viscosity in the dual equation (left) and with and without the additional residual, with viscosity $\varepsilon = 0.1$ in the dual equation (right).

Table 5.5: Effectivity index of the modified and of the formal error estimator

#E	|eff| (modified)	|eff| (formal)
128	2.9584	5.9125
256	5.0346	44.624
512	2.1386	3.126
1024	2.3554	10.977
2048	1.130	1.552

Although further investigation with different parameters is needed, it can be concluded that the modified DWR error estimator proposed in this thesis is also in 2D and with approximated weights a more efficient estimator as the formal approach.

Chapter 6

Conclusions & Outlook

6.1 Conclusions: DWR and shocks

As stated in the objective, the aim of this thesis is to clarify the following questions:

i. What happens, if the dual problem is posed in such a way that the dual solution does not satisfy the necessary regularity conditions for the estimator?

ii. How does a modification of the dual problem by artificial viscosity change the error estimator?

iii. How is the numerical performance of the modified estimator?

These questions were answered by means of an example problem: The solutions of the advection equation and the advection-diffusion equation, as well as their dual equations, all initialized with a step function, were recapitulated to provide necessary definitions for the problem setting. Along this example, it was explained that evaluation of the residuals is a subtle matter in case of coinciding discontinuities. To avoid these difficulties in the continuous problem setting, the dual equation was modified by an artificial viscosity term and the solution of the modified dual does not exhibit discontinuities.

Due to the L^2-convergence of the perturbed solution to the solution of the pure advective problem, the DWR error estimator changes only slightly if the dual of the advection equation is replaced with the dual of the advection-diffusion equation. The advantage of the modification of the dual problem, instead of the primal one, is that the primal problem and the goal functional are unaffected by this change. For this modification, a modified dual weighted residual error representation was derived as

$$J(u_0) - J(u_0^{hk}) = \frac{1}{2}\left[\rho^*(z_\varepsilon^{hk}, u_0 - u_0^{hk}) + \rho(u_0^{hk}, z_\varepsilon - z_\varepsilon^{hk}) \right.$$
$$\left. + \rho^*(z_\varepsilon, u_0 - u_0^{hk})\right] + \tilde{R}.$$

This error estimator has an additional dual residual, $\rho^*(z_\varepsilon, u_0 - u_0^{hk})$, in comparison to the classical setting. Though the direct implementation without the modification showed similar local error indicators, the effectivity of the global error estimator without diffusion in the dual equation was, for the tested parameters, much larger than one and did not exhibit convergence towards one. The effectivity index of the modified problem, on the other hand, converged to one in the 1D test case. In the 2D test case, the effectivity of the modified estimator did not exhibit convergence to one with the tested parameters. However, the effectivity index is much closer to one than the effectivity index of the formal error estimator. Therefore, the modified error estimator is also in 2D a better choice to estimate the actual error in the quantity of interest.

The numerical experiments confirm that the modified adjoint is advantageous compared to the formal DWR method when one wishes to estimate the error, and not only uses the indicators for mesh refinement. To provide a clear separation of difficulties, the section of the 1D test case utilizes the analytic formulas for the primal and dual solution in calculation of the weights rather than applying the otherwise common techniques for the approximation of the weights. With this technique the estimator converges to the error in the quantity of interest. For the 2D test case an approximation of weights was applied. The quality of this approximation could, i.a., be a cause for the non-convergence of the effectivity to one. Furthermore, the numeric solution of the primal advection equation, initialized with a box shaped function, case (B), exhibits large oscillations. Knowing the exact solution to be a shifted box shaped function, the discretization error might still be too large to neglect the remainder term of the error estimation (4.1.9).

Overall, the 1D test case and the 2D test case (B) lead to the conclusion that both approaches, formal and modified, are applicable in practice if the focus is on error indication and local grid refinement. If the aim is to provide a good global error estimator, in terms of effectivity, the modified error estimator is to be preferred.

6.2 Outlook

The outlook splits into two major tasks: Improvement and further testing of the 2D test case and application of the modified error estimator to more complex problems.

While the 1D test case already shows promising results, the 2D test case needs further investigation. For once, the dependency on the diffusion coefficient is assumed to behave similar to the 1D test case, but this has yet to be proven numerically. Additionally, the effectivity of the modified error estimator might further improve with decreasing spatial resolution. As seen in the end of the numerical testing for the 1D case, section 5.1.7, the effectivity is depending on the resolution of the diffusion. This suggests that tests with higher spatial refinement should be executed. Due to stability of the dual diffusion equation a simulation with a 2D uniform gird with the longest edge $h \approx 0.17$ needs the

explicit time step size $k \approx 10^{-5}$. Taking into account the primal and dual computation as well as the evaluation of the residuals, the simulations take some time. However, compared to the 1D test case this is not yet a fine resolution.

Another source of inaccuracy might be the approximation of weights in 2D, see section 5.2.4. Though linear interpolation of quadratic elements and linear interpolation of Euler time step solutions are known to cause only higher order error terms, this should also be tested with the example at hand. [BR03] give a prove of convergence for linear elements and quadratic interpolation but the assumption is a smooth analytic solution in the weight. In the presented test case the primal solution is not smooth and therefore the argument of vanishing impact of the weight approximation on the error estimator might fail. For 2D test case (A) the analytic solution is given and thus it qualifies for testing the impact of the approximation of weights.

A long term goal is the application of the modified error estimator to a hyperbolic system. The shallow water equations can model the fluid dynamic behavior of the atmosphere as well as the ocean. Analogue to the discontinuities in this thesis, shock waves are "steep gradients" of variables. A goal functional as in this thesis, e.g., a potential energy or the average of water hight in a specific area, might cause a shock in the dual solution. Even smoother dual initial conditions might result in shocks due to the hyperbolicity of the problem. Therefore I would like to carry over the modified dual weighted error estimator to grid adaption of a 2D shallow water problem.

Appendices

Appendix A

Appendix

A.1 The error function

Definition:

$$\mathrm{erf}(x) := \frac{1}{\sqrt{\pi}} \int_{-x}^{x} e^{-y^2} \, \mathrm{dy}. \tag{A.1.1}$$

By definition it is obvious that $\mathrm{erf}(x) = -\mathrm{erf}(-x)$, and therefor the error function is an odd function. The error function is monotone increasing because the integrand is always positive.
Also the derivative follows immediately from the definition as

$$\partial_x \mathrm{erf}(x) = \frac{2}{\sqrt{\pi}} e^{-x^2}. \tag{A.1.2}$$

There is no analytical solution to the integration but numerical integration provides function values. For different exponents and the respective multiplication factors of the
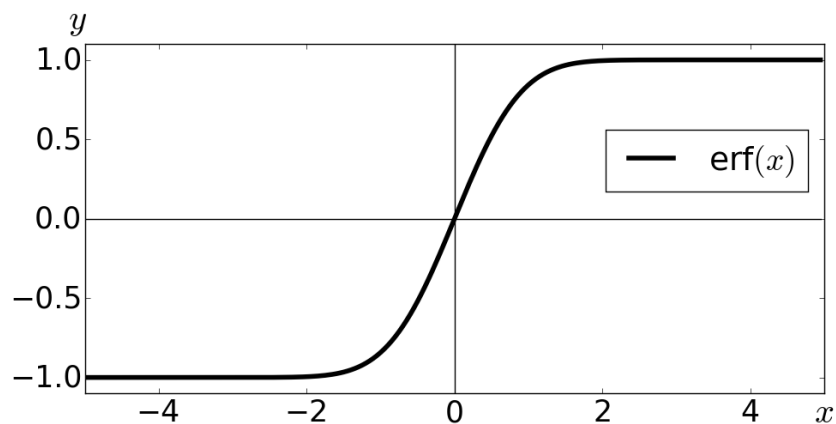

Figure A.1: The error function on the interval $[-5, 5]$

exponential function a transformation reduces the integral back so it is easily recognizable as the error function. For example, it is straight forward to see

$$\int_{\mathbb{R}} \frac{1}{\sqrt{4\pi\varepsilon t}} e^{-\frac{(x+vt)^2}{4\varepsilon t}} \, \mathrm{dx} = \int_{\mathbb{R}} \frac{1}{\sqrt{\pi}} e^{-y^2} \, \mathrm{dy} = \lim_{x\to\infty} \mathrm{erf}(x) = 1. \qquad (\text{A.1.3})$$

Bibliography

[AO97]   M. Ainsworth and J.T. Oden. A posteriori error estimation in finite element analysis. *Computer methods in applied mechanics and engineering*, 142:1–88, 1997.

[Bän91]   E. Bänsch. Local mesh refinement in 2 and 3 dimensions. *IMPACT of computing in science and engineering*, 3(3):181–191, 1991.

[BB09]   J. Behrens and M. Bader. Efficiency considerations in triangular adaptive mesh refinement. *Philosophical transactions of the royal society A*, 367(1907):4577–4589, 2009.

[BBS$^+$14]   W. Bauer, M. Baumann, L. Scheck, A. Gassmann, V. Heuveline, and S.C. Jones. Simulation of tropical-cyclone-like vortices in shallow-water icon-hex using goal-oriented r-adaptivity. *Theoretical and computational fluid dynamics*, 28(1):107–128, 2014.

[BDR92]   I. Babuška, R. Durán, and R. Rodríguez. Analysis of the efficiency of an a posteriori error estimator for linear triangular finite elements. *SIAM Journal on numerical analysis*, 29(4):947–964, 1992.

[BEA91]   J. Baranger and H. El Amri. Estimateurs a posteriori d'erreur pour le calcul adaptatif d'écoulements quasi-newtoniens. *RAIRO-Modélisation mathématique et analyse numérique*, 25(1):31–47, 1991.

[BLN79]   C. Bardos, A.-Y. Leroux, and J.-C. Nédélec. First order quasilinear equations with boundary conditions. *Communications in partial differential equations*, 4(9):1017–1034, 1979.

[BR78a]   I. Babuška and W.C. Rheinboldt. A-posteriori error estimates for the finite element method. *International journal for numerical methods in engineering*, 12(10):1597–1615, 1978.

[BR78b]   I. Babuška and W.C. Rheinboldt. Error estimates for adaptive finite element computations. *SIAM Journal on numerical analysis*, 15(4):736–754, 1978.

[BR81]   I. Babuška and W.C. Rheinboldt. A posteriori error analysis of finite element solutions for one-dimensional problems. *SIAM Journal on numerical analysis*, 18(3):565–589, 1981.

[BR01]   R. Becker and R. Rannacher. An optimal control approach to a posteriori error estimation in finite element methods. *Acta numerica 2001*, 10:1–102, 2001.

[BR03]   W. Bangerth and R. Rannacher. *Adaptive finite element methods for differential equations*. Springer, 2003.

[Bra07]   D. Braess. *Finite Elemente*. Springer, 2007.

[BRH⁺05]   J. Behrens, N. Rakowsky, W. Hiller, D. Handorf, M. Läuter, J. Päpke, and K. Dethloff. amatos: Parallel adaptive mesh generator for atmospheric and oceanic simulation. *Ocean modelling*, 10(1):171–183, 2005.

[But87]   J.C. Butcher. *The numerical analysis of ordinary differential equations: Runge-Kutta and general linear methods*. Wiley-Interscience, 1987.

[BW85]   R.E. Bank and A. Weiser. Some a posteriori error estimators for elliptic partial differential equations. *Mathematics of computation*, 44(170):283–301, 1985.

[CKS00]   B. Cockburn, G.E. Karniadakis, and C. Shu. *The development of discontinuous Galerkin methods*. Springer, 2000.

[CL00]   D. Calhoun and R.J. LeVeque. A cartesian grid finite-volume method for the advection-diffusion equation in irregular geometries. *Journal of computational physics*, 157(1):143–180, 2000.

[CO84]   G.F. Carey and J.T. Oden. *Finite elements: Computational aspects*. Finite elements. Prentice-Hall, 1984.

[Coc99]   B. Cockburn. Discontinuous Galerkin methods for convection-dominated problems. *High-order methods for computational physics*, 9:69–224, 1999.

[DOS84]   L. Demkowicz, J.T. Oden, and T. Strouboulis. Adaptive finite elements for flow problems with moving boundaries I: Variational principles and a posteriori estimates. *Computer methods in applied mechanics and engineering*, 46(2):217–251, 1984.

[DOS85]   L. Demkowicz, J.T. Oden, and T. Strouboulis. An adaptive p-version finite element method for transient flow problems with moving boundaries. *Finite elements in fluids*, 1:291–305, 1985.

[Dö96]   W. Dörfler. A convergent adaptive algorithm for Poisson's equation. *SIAM Journal on numerical analysis*, 33(3):1106–1124, June 1996.

[EEHJ95]   K. Eriksson, D. Estep, P. Hansbo, and C. Johnson. Introduction to adaptive methods for differential equations. *Acta numerica*, 4:105–158, 1995.

[EJ87]   K. Eriksson and C. Johnson. Error estimates and automatic time step control for nonlinear parabolic problems I. *SIAM Journal on numerical analysis*, 24(1):12–23, 1987.

[EJ91]   K. Eriksson and C. Johnson. Adaptive finite element methods for parabolic problems I: A linear model problem. *SIAM Journal on numerical analysis*, 28(1):43–77, 1991.

[EJ95]   K. Eriksson and C. Johnson. Adaptive finite element methods for parabolic problems II: Optimal error estimates in $l_\infty l_2$ and $l_\infty l_\infty$. *SIAM Journal on numerical analysis*, 32(3):706–740, 1995.

[Eva10]   L.C. Evans. *Partial differential equations*. Graduate studies in mathematics. American mathematical society, 2010.

[FŠ04]   M. Feistauer and K. Švadlenka. Discontinuous Galerkin method of lines for solving nonstationary singularly perturbed linear problems. *Journal of numerical mathematics*, 12(2):97–117, 2004.

[GRW15]   C. Goll, R. Rannacher, and W. Wollner. The damped Crank-Nicolson time-marching scheme for the adaptive solution of the Black-Scholes equation. *Journal of computational finance*, 2015.

[GT98]   D. Gilbarg and N.S. Trudinger. *Elliptic partial differential equations of second order*. Grundlehren der mathematischen Wissenschaften. Springer, 1998.

[GU10]   M.B. Giles and S. Ulbrich. Convergence of linearized and adjoint approximations for discontinuous solutions of conservation laws I: Linearized approximations and linearized output functionals. *SIAM Journal on numerical analysis*, 48(3):882–904, 2010.

[Har07]   R. Hartmann. Adjoint consistency analysis of discontinuous Galerkin discretizations. *SIAM Journal on numerical analysis*, 45(6):2671–2696, 2007.

[Kut01]   W. Kutta. Beitrag zur näherungweisen Integration totaler Differentialgleichungen. *Zeitschrift für Mathematik und Physik*, 46:435–453, 1901.

[NG69]   E.W. Ng and M. Geller. A table of integrals of the error functions. *Journal of research of the national bureau of standards - B. Mathematical sciences*, 73B(1):1–20, 1969.

[NVV09]   R. H. Nochetto, A. Veeser, and M. Verani. A safeguarded dual weighted residual method. *IMA journal of numerical analysis*, 29(1):126–140, 2009.

[ODRW89]   J.T. Oden, L. Demkowicz, W. Rachowicz, and T.A. Westermann. Toward a universal hp adaptive finite element strategy II: A posteriori error estimation. *Computer methods in applied mechanics and engineering*, 77(1):113–180, 1989.

[Pat80]   S. Patankar. *Numerical heat transfer and fluid flow*. CRC press, 1980.

[PPF$^+$06]   P.W. Power, M.D. Piggott, F. Fang, G.J. Gorman, C.C. Pain, D.P. Marshall, A.J.H. Goddard, and I.M. Navon. Adjoint goal-based error norms for adaptive mesh ocean modelling. *Ocean modelling*, 15(1):3–38, 2006.

[RH73]   W.H. Reed and T.R. Hill. Triangular mesh methods for the neutron transport equation. *Los Alamos report LA-UR-73-479*, 1973.

[Rit09]   W. Ritz. Über eine neue Methode zur Lösung gewisser Variationsprobleme der mathematischen Physik. *Journal für die reine und angewandte Mathematik*, 135:1–61, 1909.

[Riv08]   B. Rivière. *Discontinuous Galerkin methods for solving elliptic and parabolic equations: Theory and implementation*. Society for industrial and applied mathematics, 2008.

[RKM11]   F. Rauser, P. Korn, and J. Marotzke. Predicting goal error evolution from near-initial-information: A learning algorithm. *Journal of computational physics*, 230(19):7284 – 7299, 2011.

[SH03]   E. Süli and P. Houston. Adaptive finite element approximation of hyperbolic problems. *Error estimation and adaptive discretization methods in computational fluid dynamics*, pages 269–344, 2003.

[SMN11]   J. Schütz, G. May, and S. Noelle. Analytical and numerical investigation of the influence of artificial viscosity in discontinuous Galerkin methods on an adjoint-based error estimator. *Computational fluid dynamics 2010*, pages 203–209, 2011.

[SS98]   T. Sonar and E. Süli. A dual graph-norm refinement indicator for finite volume approximations of the Euler equations. *Numerische Mathematik*, 78(4):619–658, 1998.

[Ulb02]   S. Ulbrich. A sensitivity and adjoint calculus for discontinuous solutions of hyperbolic conservation laws with source terms. *SIAM Journal on control and optimization*, 41(3):740–797, 2002.

[Ulb03]   S. Ulbrich. Adjoint-based derivative computations for the optimal control of discontinuous solutions of hyperbolic conservation laws. *Systems & control letters*, 48(3):313–328, 2003.

[VD00]   D.A. Venditti and D.L. Darmofal. Adjoint error estimation and grid adaptation for functional outputs: Application to quasi-one-dimensional flow. *Journal of computational physics*, 164(1):204–227, 2000.

[Ver94]   R. Verfürth. A posteriori error estimation and adaptive mesh-refinement techniques. *Journal of computational and applied mathematics*, 50(1):67 – 83, 1994.

[Ver96]   R. Verfürth. *A review of a posteriori error estimation and adaptive mesh-refinement techniques.* Wiley-Teubner, 1996.

[Whe78]   M.F. Wheeler. An elliptic collocation-finite element method with interior penalties. *SIAM Journal of numerical analysis*, 15(1):152–161, 1978.

[XTB07]   Z. Xu, J.R. Travis, and W. Breitung. *Green's function method and its application to verification of diffusion models of GASFLOW code.* Forschungszentrum Karlsruhe, 2007.